Towards Novel Effective Combination Therapy for KRAS Mutant Non-Small Cell Lung Cancer

The thesis presented to

The Faculty of Graduate and Post-Doctoral Studies

Of

University of Ottawa

By: Sara Kurim

In partial fulfillment of the requirements for

Master Degree of Science in Biochemistry

University of Ottawa

April 7th 2018

Thesis Advisor

Dr. Christina Addison

ABSTRACT

Non-small-cell lung cancer (NSCLC) accounts for 80–85% of all lung cancers and is associated with significant mortality. As epidermal-growth-factor receptor (EGFR) is over-expressed in 80-90% of NSCLC, its inhibition via EGFR-Tyrosine Kinase inhibitors (EGFR-TKIs) is a main therapeutic strategy. However, patients with mutations in KRAS are resistant to EGFR-TKIs. A study in mutant KRAS-driven lung cancer in transgenic mice showed that tumor growth was dependent on the activity of focal adhesion kinase (FAK). Therefore, we hypothesized that KRAS-mutant NSCLC will be sensitive to FAK-TKIs and, given known FAK-EGFR cross-talk, FAK inhibition will sensitize KRAS-mutant NSCLC to EGFR-TKIs. We performed cell-viability assays of WT versus mutant KRAS NSCLC cell lines following treatment with FAK-TKI alone or in combination with a clinically relevant EGFR-TKI. We found that KRAS-mutant cells were more sensitive to FAK-TKI than KRAS-WT NSCLC. In addition, we found that the combination treatment including FAK and EGFR TKIs resulted in reduced tumor cell viability as compared to treatment with either drug alone. This enhanced anti-tumor response could be due to FAK-TKI's ability to down-regulate EGFR downstream targets. Our preliminary data suggests that in KRAS-mutant cells the drug combination appears to more effectively inhibit Akt activity than single drug treatment alone. This suggests an enhanced ability to impair cell survival following treatment with the drug combination. We also found that treatment with FAK TKI in KRAS mutant NSCLC cells resulted in increased activation of EGFR which was due in part to modulation of EGFR recycling and production of endogenous EGFR ligands. Thus, the combination of FAK- and EGFR-TKIs may be more effective in KRAS

mutant NSCLC as treatment with EGFR-TKI overcomes the unexpected ‘side effect’ of treatment with FAK-TKI, namely activation of the EGFR pathway by this drug. The findings of our study are novel and have uncovered previously unrecognized outcomes of FAK inhibition on EGFR activity. Moreover, our data support the notion that the combination of FAK- and EGFR-TKIs could be an effective treatment for KRAS mutant NSCLC patients.

ACKNOWLEDGMENTS

I would like to first thank my supervisor, Dr. Christina Addison. Since the first day of my journey as a graduate student Dr. Addison has been a great source of knowledge and support. She was patient with me and was always ready to steer me in the right direction. She elevated my confidence by trusting me with this research project and by encouraging me when it came to some of my weakness as a student. I would like to thank her for her continued support and supervision. I would like to thank Dr. Grant Howe, he was there for guidance and support since the beginning of my graduate studies; he always made the time to make sure I was on the right track. Dr. Grant also helped me by providing valuable technical and theoretical advice based on his valuable knowledge and experiences as a previous graduate student in the same program.

I would like to thank the members of my thesis advisory committee, Dr. Jim Dimitroulakos and Dr. Barbara Vanderhyden, for their valuable insights regarding the direction of my thesis. They both acknowledged and encouraged my hard work and provided necessary critical analysis of my research.

I would like to acknowledge my lab members who have also become some of my very good friends. They were all a source of help and support throughout my two years as a graduate student. They made my experience in the lab so much easier by providing a positive work environment. I would like to thank Huijun Zhao for her assistance and for being an amazing technical resource.

Last but not least, I would like to thank my parents, for their support and love. I will forever be thankful and grateful for those two; I would not be where I am today if it

was not for their tremendous sacrifices. They believed in me and my abilities since I was a child and they have continuously been my main source of support and confidence even during the hardest times that we had to go through as a family. They always expected the best from me which was stressful for the most part, but it taught me to go after my goals and to never settle for less. They taught me the hard work ethic by leading with an example and they were always proud of me. I specifically would like to thank my mom as without her I could not pursue this degree. She has been there through it all; through the good and bad days.

TABLE OF CONTENTS

LIST OF ABBREVATION

AFA	Afatinib 2nd generation Epidermal growth factor receptor Tyrosine kinase inhibitors
Akt	Protein Kinase B (PKB)
ATP	Adenosine Tri-Phosphate
BGS	Bovine Growth Serum
BME	Basement membrane extract
BSA	Bovine serum albumin
$C_6H_5O_7Na_3$	Sodium Citrate
ddH_2O	Double distilled water
DMSO	Dimethyl sulfoxide
DPBA	Dulbecco's Phosphate Buffered Saline
EDTA	Ethylenediaminetetraacetic acid
EGF	Epidermal growth factor
EGFR	Epidermal growth factor receptor
EGFR-TKIs	Epidermal growth factor receptor Tyrosine kinase inhibitors
ECM	Extracellular matrix

ERL	Erlotinib 1st generation Epidermal growth factor receptor Tyrosine kinase inhibitors
FACS	Fluorescence Activated Cell Sorting (Flow cytometry)
FAK	Focal adhesion Kinase
FAK-TKIs	Focal adhesion Kinase Tyrosine kinase inhibitors
FBS	Fetal Bovine Serum
GEF	Gefitinib
HRP	Horse radish peroxidase
KCl	potassium chloride
KRAS	KRAS gene
NaCl	Sodium chloride
NaF	Sodium fluoride
$Na_4P_2O_7$	Sodium pyrophosphate
$NaVO_4$	Sodium orthovanadate
NSCLC	Non-small cell lung cancer
M-MLV RT	Moloney Murine Leukemia Virus Reverse Transcriptase
PAGE	Polyacrylamide gel electrophoresis

PBS	Phosphate-buffered saline
Q-RT-PCR	Quantitative Real Time Polymerase Chain Reaction
SDS	Sodium dodecyl sulfate
SDS-PAGE	Sodium dodecyl sulfate polyacrylamide gel electrophoresis
SRC	Src gene
TBS-T	Tris-buffered saline, 0.1% Tween 20
TGFα	Transforming Growth Factor, alpha

LIST OF FIGURES

LIST OF TABLES

CHAPTER 1: INTRODUCTION

1.1 Lung cancer and statistics:

Lung cancer is one of the most common cancers. It is classified into two major types, small cell lung cancer (SCLC) and non-small cell lung cancer (NSCLC). The latter includes squamous-cell (epidermoid) carcinoma, adenocarcinoma, and large-cell carcinoma (1). Approximately 80-85% of all lung cancers are categorized as NSCLC and its detection often occurs at advanced stages (1). A significant number of lung cancer diagnoses are in patients aged 65 and over with a median age at diagnosis of approximately 70 years (2, 3). However, a subset of patients with NSCLC get diagnosed at a younger age (<40 years) (4). Lung cancer is a leading cause of cancer mortality in both men and women (5). In Canada an estimated 26,600 Canadians will be diagnosed with lung cancer and 20,900 will die of it (6). Thus, lung cancer is considered as a major public threat.

The risk of lung cancer development is 20-40 times higher in lifelong smokers compared to non-smokers. Smoking is known to cause 85% of all lung cancers, including NSCLC, and 90% of lung cancer related deaths. Yet, 15% of patients who are diagnosed with lung cancer have never smoked and 35% are former smokers (6, 7).

In Canada, while the incidence rate for lung cancer is higher in men than in women, the death rate of men with lung cancer has begun to drop since the 1980s and it has continued to decline ever since. On the other hand, the death rate for females showed no statistically significant decline between the years of 2006 and 2012 (8). One explanation for this difference could be due to the fact that men's smoking rates

declined earlier than women's smoking rates. Even so, men continue to have a higher rate of lung cancer death than women, so the cause of the effect remains unclear. Regardless, it is estimated that about 1 in 14 Canadian men and 1 in 17 Canadian women will die from lung cancer in their lifetime (8).

Each year, approximately 45,000 Canadians die from smoking related-deaths; which is considered as 1 in 5 deaths in Canada. More specifically, smokers are at 1 in 2 chance of dying from a smoking-related cause, including a 50% chance of death before the age of 70 (6). However, smoking cessation decreases the cumulative death risk from lung cancer. Stopping smoking could contribute to prolonging survival in cancer patients and lowering the risk of recurrent lung cancer. On the other hand, those patients who continue smoking during treatment experience greater difficulties (7). Smoking increases lung cancer risk by: causing genetic changes in the cells of the lung, damaging the lungs' ability to dispose of foreign and harmful particles, and depositing cancer-causing particles in the mucus. All of these events can result in driving normal lung epithelium to develop into cancer tumors (6).

Lung cancer can start in any region of the lungs, invade and destroy nearby tissue then metastasize to other body organs. The most frequent lung cancer metastatic sites are the nervous system, bone, liver, respiratory system, and adrenal gland (9). A study reviewed the records of NSCLC patients with metastasis at the time of diagnosis between 1999 and 2012 and showed that out of 1,542 NSCLC patients diagnosed during the study period, 729 (47.3%) patients presented with distant metastasis. Among those 729 metastatic NSCLC patients, 250 (34.3%), 234 (32.1%), 207 (28.4%), 122 (16.7%), 98 (13.4%) and 69 (9.5%) had bone, contralateral lung, brain, adrenal gland, liver and

extrathoracic lymph node metastasis, respectively (10). Metastasis to these organs causes tissue damage and loss of function precluding the organ from functioning, resulting in the death of cancer patients. Therefore, early detection of lung cancer and undergoing appropriate therapy are both important to increase the chance of survival or the prolongation of life.

The treatment of NSCLC depends on the stage of tumor progression. Patients with early stages are more likely to be advised to undergo surgery, whereas more advanced tumors are more likely to be treated with radiation therapy or chemotherapy (11). Fortunately, our understanding of cancer biology has allowed the development of treatments against specific molecular targets known to promote progression of lung cancers. Certain NSCLCs harbor a mutated oncogene which may be associated with tumor progression and response to therapy. Two of the most common mutated oncogenes in lung cancer encode for the epidermal growth factor receptor (EGFR) and KRAS. EGFR kinase domain mutations are considered a predictor of increased sensitivity to EGFR kinase inhibitors. However, patients with mutant KRAS tumors fail to benefit as they don't respond to EGFR inhibitors (12).

1.2 Lung cancer and the epidermal growth factor receptor (EGFR)

EGFR (aka: ErbB-1 or HER1) is a trans-membrane receptor tyrosine kinase that belongs to the EGFR superfamily along with another three members: HER2 (ErbB-2), HER3 (ErbB-3), and HER4 (ErbB4) (13). EGFR is highly regulated in normal cells as it plays a main role in proliferation, differentiation, survival, angiogenesis, and migration (14). The receptor is composed of an extracellular domain, a transmembrane domain, a

tyrosine kinase domain and a tyrosine-rich intracellular tail (13). Different ligands can bind to the ectodomain of EGFR such as: epidermal growth factor (EGF), transforming growth factor-α (TGFA), heparin-binding EGF-like growth factor (HBEGF), amphiregulin (AREG), betacellulin (BTC), epiregulin (EREG), and epigen (EPGN) (14). As shown in Figure 1A, upon the binding of a soluble ligand, such as EGF, to the ectodomain of the receptor, the EGFR will dimerize with another EGFR molecule or with another member of the EGFR family. Once the two receptors are dimerized, each receptor will use an ATP to phosphorylate the receptor at tyrosine residue sites including Y1068, Y1148, and Y992, which are located on the C-terminal domain (15). These residues, either directly or via adaptor proteins, then activate downstream components of signaling pathways such as the Ras/MAPK, PLCγ1/PKC, PI3kinase/Akt, and STAT pathways (16).

Over-expression of EGFR or mutations in intracellular EGFR have been observed in 80-90% of all NSCLC and as such it is recognized as an important modulator of lung tumorigenesis (17). Studies have shown that EGFR expression in NSCLC is associated with poor outcomes and reduced survival (17). Therefore, EGFR inhibition via EGFR-Tyrosine Kinase Inhibitors (EGFR-TKIs) has become one of the main effective therapeutic strategies.

A)

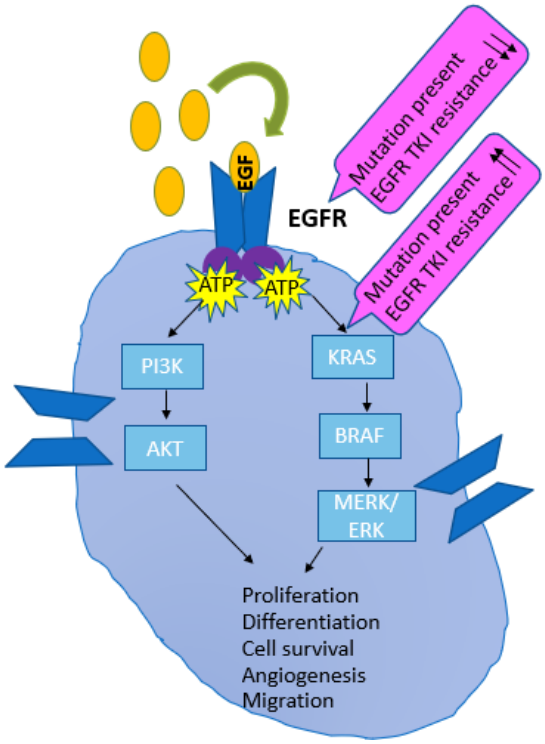
EGF
EGFR
Mutation present
EGFR TKI resistance
Mutation present
EGFR TKI resistance
ATP
ATP
PI3K
AKT
KRAS
BRAF
MERK/
ERK
Proliferation
Differentiation
Cell survival
Angiogenesis
Migration

B)

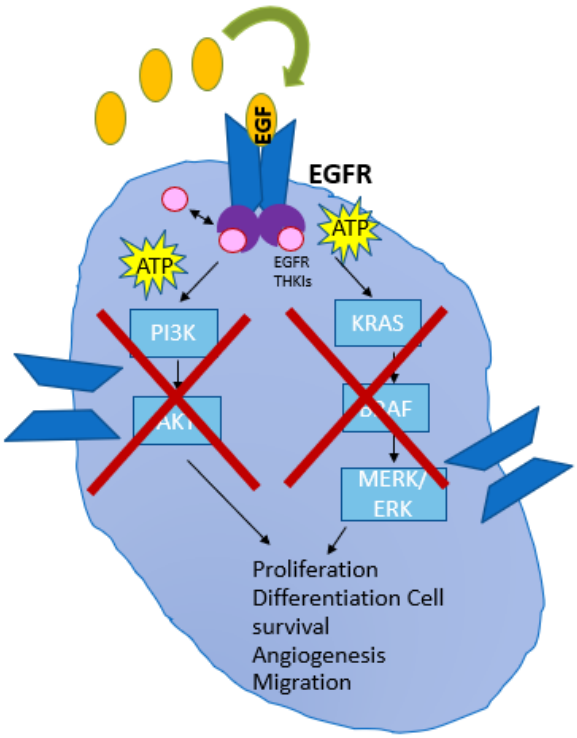
EGF
EGFR
ATP
ATP
EGFR
THKIs
PI3K
KRAS
MERK/
ERK
Proliferation
Differentiation Cell
survival
Angiogenesis
Migration

Figure 1. Schematic representation of EGFR activation and the mechanism of blockade by EGFR-TKIs. A) The activation of the epidermal growth factor receptor (EGFR). EGFR is activated by binding to its ligands; in this case it is epidermal growth factor (EGF) molecule. Upon activation, the EGFR receptors either homodimerize with another EGFR receptor or heterodimerize with another member of the EGFR family. Once the two receptors are dimerized, an intrinsic intracellular protein-tyrosine kinase activity gets stimulated. Each receptor will then use an ATP to phosphorylate each other at a tyrosine residue site, such as Y1068, which are located within the C-terminal domain of EGFR. B) EGFR Tyrosine Kinase inhibitors, including small-molecule tyrosine kinase inhibitors, ERL, GEF or AFA. Both of ERL and GEF are first generation TKIs that act as reversible competitive inhibitors of ATP. They block EGFR activity by competing with ATP for the binding pocket of the kinase domain. This hinders receptor autophosphorylation, thus blocking activation of downstream signals. Conversely, AFA binds to the ATP pocket and competes with ATP binding in an irreversible manner.

1.3 First and second generation EGFR-TKIs

Cancer studies have provided major breakthroughs in the understanding, diagnosis and management of lung cancer, especially for the more common NSCLC. Several drugs have been created to interfere with the activation of EGFR, including small-molecule tyrosine kinase inhibitors, Erlotinib (Tarceva) and Gefitinib (Iressa) (18, 19). Both Erlotinib (ERL) and Gefitinib (GEF) are first generation TKIs that act as reversible competitive inhibitors of ATP. They inhibit EGFR activity by competing with ATP for the binding pocket of the kinase domain. This hinders receptor autophosphorylation, thus blocking activation of downstream signals (20) (Figure 1B). In fact, a double-blinded phase III trial performed by Dr. Shepherd *et. al* in 2005, randomly assigned 731 patients to ERL daily or placebo and showed that ERL can prolong survival (Average survival with ERL: 6.7 months, placebo: 4.7 months) (21). Also, a phase II study demonstrated that GEF showed clinically meaningful antitumor activity and provided symptom relief in NSCLC patients (19).

Treatment with EGFR-TKIs is especially effective in patients with EGFR mutations. They are highly sensitive to the treatment and have shown large progression-free survival benefit with negligible toxicity when treated with these drugs (12, 22). However, EGFR-TKIs are not as efficacious in patients with wild type (WT) EGFR as these patients rarely show any benefits from clinical treatment with EGFR inhibitors (23). It is important to note that inhibiting a specific kinase that plays a main role in the survival of cancer cells via kinase inhibitors can lead to the emergence of resistance mechanisms to allow tumor cells continued survival. Clinically, it has been shown that patients who respond to ERL or GEF gain resistance to these drugs, in part due to

mutations such as T790M mutation in EGFR (24). This mutation prevents the drug from binding to the ATP pocket of the receptor by causing an increase in ATP affinity (24). This however, could be avoided to some extent via treatment with irreversible drugs like Afatinib. Afatinib (AFA) is a second generation EGFR-TKI. It is an irreversible EGFR-TKI unlike ERL and GEF, which both are reversible EGFR-TKIs. Studies have shown that AFA treatment was associated with significant improvements in progression-free survival and overall survival compared to treatment with ERL (25). However, some NSCLC patients still show some resistance to AFA; specifically those patients with WT EGFR NSCLC (26, 27). The reasons for the innate resistance to EGFR-TKIs in WT EGFR NSCLC tumors have not yet been investigated in depth. However, it has been suggested that the ability to trigger autophagy may be a key determinant of resistance to EGFR-TKIs in WT EGFR NSCLC (28).

1.4 Lung cancer and KRAS mutations

In spite of this, recent studies indicate that NSCLC patients with KRAS mutant tumors gain less benefit from chemotherapy and are also resistant to EGFR-TKIs (12). EGFR is among the many diverse cell receptors that have been shown to play a role in regulating KRAS (29); a G-protein that regulates cell growth, differentiation and apoptosis (30). Mutations in KRAS in NSCLC cause loss of GTPase function which causes the protein to be locked in the active form (29).

KRAS mutations are associated with smoking and are present in 20-30% of all NSCLCs (31). However, KRAS mutations only occur in EGFR-WT patients (31). Those mutations most commonly found in NSCLC are caused by an amino acid

replacement in codon 12, 13 or 61. This results in forms of RAS with impaired GTPase activity, causing a constitutive activation of RAS signalling pathway (32). KRAS mutation frequency varies among different ethnic groups. They are very common in Western countries with lower frequency observed among Asians and higher frequency among African Americans as compared to Caucasians (33). Furthermore, KRAS mutation is predictive of poor prognosis and strong resistance to treatment with EGFR-TKIs, ERL or GEF (34). Despite knowing KRAS is an important therapeutic target in lung cancer, current agents targeting KRAS activity have been ineffective due to difficulties in drug design. These difficulties are caused by the high binding affinity between KRAS and GDP/GTP as well as the relatively flat surface without deep hydrophobic pockets in the KRAS protein. As such, one should investigate downstream targets in order to block KRAS activity (35, 36).

In NSCLC cells, focal adhesion kinase (FAK) plays a critical role in downstream activities modulated by mutant KRAS (37). Specifically, a recent study in mutant KRAS-driven lung cancer (KRAS-G12D) in transgenic mice showed abnormal up-regulation of RhoA activity (37), a GTPase that controls cytoskeleton, cell migration, proliferation and survival (38). Data has also shown that the silencing of FAK alone, which is activated downstream of RhoA, was able to inhibit tumor cell growth and viability in KRAS G12D NSCLC (37). The fact that FAK is one of the downstream RhoA targets supported the idea that KRAS G12D promotes the progression of lung cancer through a mechanism that involves sustained activation of RhoA-FAK signaling (37).

1.5 Additional therapeutic targets in NSCLC

Numerous cellular functions can be regulated by interactions between the cell and its extracellular microenvironment, including components of the extracellular matrix (ECM). Unregulated synthesis of certain ECM components contributes to creating the perfect microenvironment for cancer development and spread (39). This means that the resistance or sensitization to the various therapies can depend on the specific microenvironmental context of the ECM and their interactions (40). The ECM binds integrins to generate intracellular signals by activating cellular kinases such as the cytoplasmic FAK protein and this activation is important to regulate cell survival, proliferation and migration (41).

Activated FAK in turn cross-talks with growth factor receptors, including EGFR, which can be activated by FAK-Src complexes in a ligand independent manner (42) (43) (Figure 2). PAK-1 phosphorylates Src which then enables Src localization to the plasma membrane allowing it to interact with both EGFR and FAK (44). Phosphorylated Src interacts with EGFR through its N-terminus, which is mediated by T56 phosphorylation, and FAK binds to the SH2 domain of Src. Thus, Src mediates the interaction between EGFR and FAK (44, 45).

It is important to note that high expression of FAK is associated with more aggressive NSCLC and worse prognosis (46). Therefore, in addition to its inherent ability to regulate tumor phenotypes, its ability to regulate EGFR activity makes FAK an interesting therapeutic target in NSCLC.

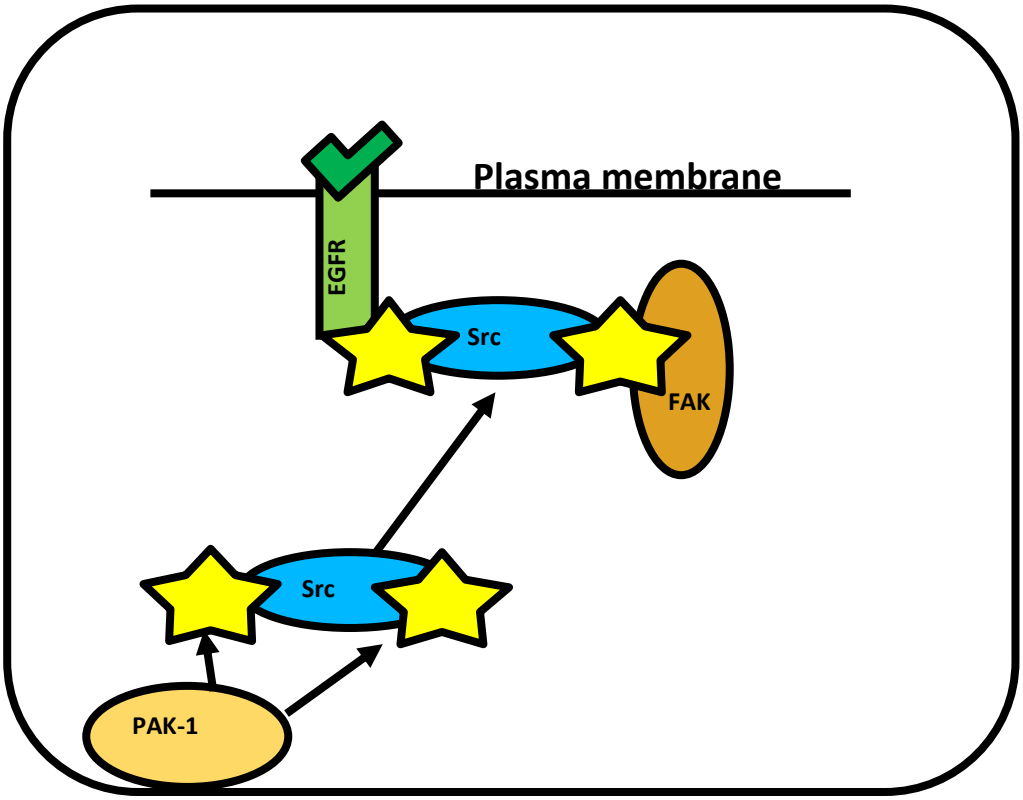

Figure 2. Schematic representation of EGFR activation through the FAK-Src complex in a ligand independent manner. PAK1 phosphorylates Src promoting Src localization to the plasma membrane where it interacts and mediates the interaction between EGFR and FAK.

FAK is also known to promote cell survival through enhancing the activity of Akt (49). PI3K/Akt pathway is a signal transduction pathway that regulates multiple cellular functions including cell proliferation, survival, differentiation, adhesion, motility and invasion and is deregulated in many cancers, including NSCLC (50). Upon Phosphoinositide 3-kinase (PI3K) activation after growth factor activation of EGFR, a second messenger phosphatidylinositol (3,4,5)-trisphosphate (PIP3) is generated. PIP3 localizes both Akt and PDK1 to the membrane, where PDK1 activates Akt by phosphorylating it at the T308 and S473 sites (51, 52). The activated Akt then regulates the phosphorylation of additional downstream targets leading to changes in gene expression and cell behaviour. Multiple NSCLC cell lines show persistent Akt activation in serum starved conditions, thus supporting the notion of Akt as a central regulator of cell proliferation and survival (53). In vivo, mice with genetically modified Akt status have shown that irregular Akt signaling can contribute to malignancy (54). Further, persistent Akt activation is associated with a lack of response to EGFR-TKIs in NSCLC patients (55, 56).

The fact that the Akt signaling cascade is frequently deregulated in many types of cancer potentially makes targeting the Akt pathway an important key in cancer therapy studies. Moreover, the association of Akt activation with poorer prognosis is possibly due its association with disease progression and metastasis (57). While it has been shown that Akt activation promotes metastasis, under certain conditions, it also inhibits metastasis (58). The reason behind these contradictory results is as yet undetermined (59). Furthermore, a study showed that Akt1 is an important regulator of metastasis and down-regulation of its activity is associated with increased metastatic

potential of A549 cells (59). They showed that the inhibition of Akt1 using MK-2206 enhanced migration and invasion in KRAS- or EGFR-mutant NSCLC cells. Specifically, it promoted metastasis of KRAS-mutated A549 cells in vivo (59). The uncertainty about inhibiting Akt directly for NSCLC treatment gives another reason for the need of finding alternative effective therapy. Moreover, in a phase II study they investigated the combination of an Akt inhibitor, MK-2206, and ERL in NSCLC patients who had previously progressed on ERL alone. The combination trial met the pre-specified cut-off of a 40% clinical benefit rate in the WT EGFR patients but did not meet the pre-specified cut-off of a 20% objective response rate for EGFR mutant patients (the observed response rate was only 9%) (60). The moderate benefits seen in this trial allows us to predict that there are additional targets that still need to be investigated for more effective patient responses.

Data recently published from our lab suggests that in KRAS mutant cells, the combination of FAK-TKI and ERL appears to be more effective in inhibiting Akt activity, as evidenced by significantly reduced levels of Akt phosphorylation at S473 site, than does treatment with either drug alone (61). This suggests an enhanced ability to impair cell survival following treatment with the drug combination (61). These results were not observed in WT KRAS NSCLC where levels of p-Akt (S473) were not significantly reduced by the combination treatment compared to treatment with either drug alone (61). Taken together these data suggest that KRAS mutant NSCLC may be more sensitive to FAK-TKIs, and, given known cross-talk of FAK with the EGFR signaling pathway, that FAK inhibition will sensitize KRAS mutant NSCLC cells to EGFR-TKIs.

1.6 Additional Preliminary Data Supporting Rationale of Drug Combination Study

Published data from Dr. Addison's lab shows that NSCLC growth was more significantly inhibited by FAK-TKIs PF-573,228 and PF-562,271 (a precursor of defactinib) alone or in combination with ERL (61). Experiments were initially performed in EGFR-WT cells that are inherently EGFR-TKI resistant (A549, H1734) or with H1975 cells (61). H1975 cells have both the L858R mutation, which results in increased sensitivity to EGFR-TKIs, in addition to the T790M mutation, which is responsible for acquired resistance to EGFR-TKIs in most patients (Table 1) (62, 63). Treatment with FAK-TKI alone showed moderate growth inhibition. However, the treatment combination with ERL resulted in enhanced inhibition in KRAS mutant A549 and H1734 cells as compared to either drug treatment alone in both 3D and 2D culture (61). Given recent clinical trial results suggesting AFA is a more potent EGFR inhibitor than ERL, we decided to continue our studies with this more clinically relevant agent (AFA) and further test whether increased sensitivity was due to the presence of KRAS mutations, and by what mechanism sensitivity to the combination treatment might be conferred.

Table 1. Known KRAS and EGFR status of NSCLC cell lines used in this study.

Mutant KRAS NSCLC Cell Line	Wild Type KRAS NSCLC Cell Line
A549 **WT EGFR**	**NCI-H1299** **WT EGFR**
NCI-H460 **WT EGFR**	**H1975 * resistant to 1st generation EGFR-TKIs** **Mutant EGFR**
A427 **WT EGFR**	**H4006** **Mutant EGFR**
	H827 **Mutant EGFR**
	H1666 **WT EGFR**
	H1563 **WT EGFR**
	Calu-3 **WT EGFR**

1.7 Hypothesis and Objectives:

1.7.1 Hypothesis

KRAS mutant NSCLC is dependent on FAK activity, thus dual blockade of FAK and EGFR will be a more effective combination therapy in KRAS mutant versus wild type NSCLC compared to inhibition of either target alone.

1.7.1 Objectives

1) Assess sensitivity of mutant or WT KRAS NSCLC cells to EGFR-TKIs with or without FAK-TKIs.

2) Investigate the mechanism by which FAK inhibition may sensitize NSCLC cells to EGFR-TKIs.
   a- Determine if FAK inhibition is blocking FAK-EGFR cross talk and downstream signaling
   b- Examine whether FAK inhibition alters cell survival or induces cell apoptosis
   c- Test if FAK is causing a defect in EGFR recycling

CHAPTER 2: MATERIALS AND METHODS

2.1 Antibodies, Growth Factors and Inhibitors

Primary antibodies used were: EGFR, Phospho-EGFR (Y1068) (P-EGFR), Phospho-Akt (S473) #9271 (P-Akt) and Akt #9272 all from Cell Signalling Technology (Danvers, MA). Monoclonal anti-β-Actin antibody (clone AC-74) was purchased from Sigma-Aldrich (St. Louis, MO). Secondary antibodies used were: goat anti-mouse IgG horse radish peroxidase (HRP) conjugate and goat anti-rabbit IgG HRP conjugate, both from Calbiochem EMD Biosciences (San Diego, CA).

Afatinib (AFA) was purchased from Cayman Chemical (Burlington, NC, USA). Erlotinib (ERL) was purchased from Shanghai Biochempartner Co. Ltd. (Shanghai, China). FAK-TKI PF-562,271 (PF-271) was purchased from two different companies Shanghai Biochempartner Co. Ltd. (Shanghai, China) and from Cayman Chemical (Burlington, NC, USA). Stock solutions for AFA, ERL, and PF-271 were prepared in dimethyl sulfoxide (DMSO) at 10μM and stored at -20^{o}C.

2.2 Cell Culture

Lung adenocarcinoma cell lines, A549, H522, H460, H1563, Calu3, A427 and H1299, were purchased from ATCC (Manassas, VA). The lung adenocarcinoma cell lines H1975 (EGFR L858R and T790M mutations), HCC827 (EGFR ΔE746-E750) and HCC4006 (EGFR ΔL747-E749) cell lines were a generous gift of Dr. Ming Tsao (Princess Margaret Hospital, Toronto, ON). A549 cells were maintained in DMEM (Mediatech, Manassas, VA) supplemented with 10% Fetal Bovine Serum (FBS) (Medicorp, Montreal, QC), or with Bovine Growth Serum (BGS) (HyClone Laboratories, Waltham, MA). H1299, H1975, HCC827, H460, H1563 and HCC4006

cells were all maintained in RPMI-1640 (Mediatech, Manassas, VA) with 10% FBS or BGS. The cell lines Calu3 and A427, were grown in EMEM medium (ATCC, Manassas, VA) with 10% FBS or BGS.

Cells were routinely passaged at 80-90% confluence through cell dissociation with 0.05% Trypsin-EDTA from (Mediatech, Manassas VA), after washing with Dulbecco's Phosphate Buffered Saline (DPBA 1X) (Mediatech, Manassas, VA) to detach cells before re-plating in fresh medium. Cells were maintained at 37 °C in 5% CO_2 humidified atmosphere.

2.3 MTT Cell Viability Assay

The assay was initiated by seeding NSCLC cells onto 96-well plates at a density of 5000 cells per well and incubating overnight. Cells were then treated with several concentrations of AFA, PF-271 or with a combination of both drugs for 48 hours in growth media with 10% FBS or BGS. Cell viability was measured with MTT reagent (3-(4,5-dimethyl-thiazol-2-yl) 2,5-diphenyltetrazolium bromide) (Sigma, Oakville, ON). At 24 hours intervals, 42 µL of MTT reagent was added to wells for 3–4 hours, and subsequently 0.01 N HCl in 10% Sodium Dodecyl Sulfate (SDS) lysis solution was added. The plate was then incubated overnight, and absorbance was read at 570 nm in a Multiskan Ascent plate reader (Thermo Scientific, Rockford, IL). For each drug treatment, every biological replicate was performed in eight technical replicate wells with the mean values calculated as the percent viability relative to the DMSO treated control.

2.4 Protein Extraction and Western blotting

For protein extraction, cells were seeded in 60 mm dishes and were left to attach overnight. The next day, cells were serum starved overnight then drug treated for various times based on the requirement of the performed experiment. At the time of collection, the cells were washed once with phosphate-buffered saline (PBS), then were lysed by adding 100 µL of Frack's lysis buffer (10 mM Tris-HCl pH7.4, 150 mM Sodium chloride (NaCl), ethylenediaminetetraacetic acid (EDTA), 1% Triton X-100) supplemented with 500 µM sodium orthovanadate ($NaVO_4$), 2 mM Sodium fluoride (NaF), 2 mM sodium pyrophosphate ($Na_4P_2O_7$) and SigmaFAST™ Protease Inhibitor Cocktail (Sigma-Aldrich, St. Louis, MO).

The lysate from each sample was collected in 1.5 mL microcentrifuge tubes after scraping each dish with a rubber cell scraper and then centrifuged at 18000 xg for 25 minutes. Cleared lysates were then stored at -80 °C. Protein concentration was measured using Bio-Rad Protein Assay Dye Reagent Concentrate from (Bio-Rad, Hercules, CA) and the absorbance was recorded at 595 nm using a Thermo Scientific Evolution™ 60S UV-visible spectrophotometer (Thermo Fisher Scientific, Burlington, ON). The concentrations were determined by comparing to a standard curve generated by known quantities of protein. Equal amounts of total protein per sample were diluted with 5X sample buffer (15 g tris base, 72 g glycine, 5 g SDS, and 1 L ddH_2O) prior to being subjected to polyacrylamide gel electrophoresis (PAGE).

Extracted protein was then used to perform western blot analysis. Samples were denatured at 100°C for 5 minutes and centrifuged briefly, and then were separated on a

10% sodium dodecyl sulfate polyacrylamide gel electrophoresis (SDS-PAGE gel) at 120V in 1x running buffer (30.0 g tris base, 144.0 g glycine, 10.0 g SDS, 1000 mL H_2O) for approximately 90 minutes. Following that, the protein was transferred onto a methanol activated 0.45 μM Polyvinylidene fluoride (PVDF) transfer membrane Immobilon-P (MilliporeSigma, St. Louis, MS) in tris-glycine transfer buffer 1x Transfer Buffer (6.04 g tris base, 28.2 g glycine, and 1.6 L ddH_2O) with 20% methanol at 100V for approximately 90 minutes on ice.

Membranes were then blocked for 1 hour at room temperature in 5% powdered skim milk in TBS-T (tris-buffered saline, 0.1% Tween 20). All primary antibodies were incubated overnight at 4°C at a concentration of 1:1000 - with the exception of the β-actin antibody which was used at the concentration of 1:2000 - in 5% powdered skim milk in TBS-T or 5% bovine serum albumin (BSA) in TBS-T for western blot detection using antibodies against phosphorylated proteins.

Following incubation with primary antibody overnight, membranes were washed three times for 5 minutes each with TBS-T then incubated in HRP conjugated goat anti-mouse or goat anti-rabbit secondary antibody (1:2000) in 5% powdered skim milk in TBS-T for 1 hour at room temperature. Following that, membranes were washed five times for 5 minutes each in TBS-T. Clarity Western ECL substrate (Bio-Rad, Hercules, CA) was then applied before image development using the GeneGnome Syngene Bio Imaging Chemiluminescence System and GeneSnap software Syngene (Frederick, MD). Before re-probing blots, the membranes were stripped at room temperature using stripping buffer (1% SDS, 1.7% NaCl, 1.5% Glycine, pH 2) by

washing three times for 5 minutes per wash, followed by five 5 minutes washes with TBS-T.

2.5 3D Colony growth assay

The reduced growth factor basement membrane extract (BME) (Trevigen, Gaithersburg, MD) was thawed overnight at 4°C before use. Lab-Tek II 4-well chamber slides (Nalge Nunc International, Naperville, IL) were coated with 100 µL BME which was spread evenly with a pipette tip, avoiding bubbles and meniscus formation. The chamber slides were kept on ice during coating then the gel coats were allowed to solidify for 120 minutes at 37°C in a 5% CO_2 containing humidified environment.

Cells were seeded onto the solidified BME layer at a density of 5,000 cells/well in 500 µL medium containing 10% FBS or BGS and 2.5% BME (25 µL BME). The cells were allowed to seed overnight and were treated the next day with solvent control (DMSO), AFA, PF-271, or both AFA and PF-271 in medium containing 10% FBS or BGS. Medium supplemented with the respective drug treatments was changed every three days. Colonies were allowed to form over a period of 14 days. Colonies were documented by taking six images at 40x magnification using a Nikon Eclipse TE2000-U microscope and camera (Melville, NY). Cell colony number and area sizes were determined with ImageJ software from the images of each well from each experiment (https://imagej.net/Welcome); Only colonies >0.000015 μm^2 were considered in the measurements.

2.6 Flow cytometry

For the EGFR surface staining experiment, cells were seeded at $5x10^5$ cells per 10 cm dish and were left to settle overnight. Next day the cells were serum starved and pre-treated with solvent control (DMSO) or with different concentrations of PF-271 overnight. The following day, internalization of EGFR receptors was initiated by adding 100 ng/ml of Recombinant Human EGF Invitrogen (Burlington, ON) 15 minutes or 2 hours before the collection of cells using 1 X citric saline (1.35 M potassium chloride (KCl), 0.15 M sodium citrate ($C_6H_5O_7Na_3$)).

Cell suspensions were blocked with 1% BSA in PBS for 30 minutes then were stained for 30 minutes at 4^{o}C with Alexa Fluor 488 conjugated anti-EGFR antibodies (clone 528, designed to specifically recognize extracellular EGFR) or with mouse IgG, both from Santa Cruz Biotechnology (Dallas, Texas). Cell suspensions were washed once and $5x10^5$ cells were re-suspended in 500 µL of 1% BSA in PBS prior to being evaluated using the Beckman Coulter Epics XL flow cytometer (Beckman-Coulter, Brea, CA). The median peak value was calculated using FCS CXP Software flow cytometry analysis software version 2.0 (Beckman-Coulter, Brea, CA). Optical filter was set up such that green fluorescence was measured at 520 nm (FL1). The fluorescence of samples stained for extracellular EGFR were acquired using a forward scatter (FSC) and side scatter (SSC) gate around the appropriate cell population excluding most cell debris or aggregated cells.

For the detection of apoptosis, we used propidium iodide (PI) staining and FACS analysis of cells. For this experiment, cells were seeded at a confluency of $5x10^5$

cells per 10 cm dish and were left to settle overnight. Next day the cells were serum starved and treated with solvent control (DMSO), various concentrations of AFA, various concentrations of PF-271, or both AFA and PF-271, in medium containing 10% FBS or BGS for 24 hours before collection. Media containing non-adherent cells was collected in 15 mL conical tubes. The remaining adherent cells from the dishes were trypsinized and were added to the collected media to pool adherent and non-adherent cells. The cells were then centrifuged at 1000 xg for 5 minutes. The media was aspirated, and the cells pellets were washed two times with PBS containing 0.02% BSA. After the second wash, the wash was carefully removed so as to not disturb cell pellets. The cells were then permeabilized by adding 500 µL of ice cold 70% ethanol to each cell pellet sample. The samples were kept at -20^{o}C for minimum of 24 hours prior to staining with PI.

On the day of analysis by FACS, 1 mL of PBS with 0.02% BSA was added to each sample and cells were centrifuged at 1000 xg twice. The cell pellet was stained by adding 1 mL of propidium iodide (PI) solution (48 mg/mL PI, 40 mg/mL RNase A in PBS) which was then allowed to incubate in the dark at room temperature for 30 minutes prior to reading on the flow cytometer. Finally, stained cells were evaluated by measuring PI fluorescence at 585 nm (FL2) using the Beckman Coulter Epics XL flow cytometer (Beckman-Coulter, Brea, CA). The PI stained samples were acquired using a FSC/SSC gate to exclude debris, and a second gate indicating the subG1 (i.e. <2N) cells was used to determine apoptotic cell number. The percentage of apoptotic cells was calculated using FCS CXP Software flow cytometry analysis software version 2.0 (Beckman-Coulter, Brea, CA).

2.7 RNA extraction, cDNA synthesis and q-RT-PCR Array plates

Cells were seeded at a confluency of $8x10^5$ cells per 60 mm dish and left to settle overnight. Next day cells were serum starved and were treated with DMSO or with various concentrations of PF-271 for 24 hours. Following treatment, cells were lysed and RNA was harvested using the RNeasy Mini Kit from Qiagen (Redwood City, CA) as per manufacturer's instructions. Total RNA concentration was determined with a NanoDrop 1000 Spectrophotometer (Thermo Fisher Scientific, Waltham, MA) with 260/280 absorbance ratio between 1.9 and 2.1.

cDNA synthesis was carried out using the Moloney Murine Leukemia Virus Reverse Transcriptase (M-MLV RT) reagent. Either 0.5 µg or 1 µg total RNA was combined with 1 µL dNTP's and 1µL 10 mM random hexamers (Invitrogen, Burlington, ON) and made to a final volume of 12 µL with RNAse free H_2O which was then incubated in the thermocycler for 5 minutes at 65°C. Following the 5 minutes incubation, a mixture of 4 µL 5x First Strand Buffer, 2 µL DTT and 1 µL RNAse Out, all from Invitrogen (Burlington, ON), was added and samples were incubated for 2 minutes at 37°C and then placed at 4°C for at least 1 minute. In the final step 1 µL of M-MLV RT (Invitrogen, Burlington, ON) was added to the tube and the tube was placed in the thermocycler with the following sequence, 27°C for 10 minutes, 37°C for 50 minutes and 70°C for 15 minutes followed by an indefinite 4°C incubation until the tubes were retrieved.

The generated cDNA was then diluted 1:10 or 1:5 in sterile ddH_2O and 1 µL of this mixture was added to each well of a 96-well PCR plate which contained a total of

10 µL of final reaction mixture (5 µL SYBR-Green 2x Master Mix, 1 µL 1:10 cDNA, 1 µL 10 µM primer pair (forward and reverse) and 3 µL ddH2O). The primers used recognized MMP9, TGFα, and β-actin (Invitrogen, Burlington, ON) with sequences as shown in Table 2. Prepared reaction mixtures for each sample were loaded in triplicate onto the 96-well array plate (10 µL in each well). Plates were run in the 7500 Fast Real-Time PCR System (Applied Biosciences, Carlsbad, CA) according to manufacturer's protocol using the ΔΔCt analysis with melt curve setting. The reaction was completed with the following steps: hold at 50°C for 20 seconds, then another hold at 95°C for 10 minutes, followed by 40 cycles of 95°C for 15 seconds and 60°C for 1 minute for each cycle. Analysis was performed with the Applied Biosciences Software version 2.3 designed specifically for the 7500 FAST machines. Relative expression was determined via ΔΔCt method whereby the amount of RNA in each sample was normalized to β-actin levels within that sample and was then compared to the levels of the control DMSO treated sample.

Table 2: Forward and Reverse Primer sequences used in this study.

Primer	Forward sequence	Reverse sequence
MMP9	**GAACCAATCTCACCGACAGG**	**GCCACCCGAGTGTAACCATA**
TGFα	**GCTGCCACTCAGAAACAGTG**	**ATCTGCCACAGTCCACCTG**
βactin	**CCAACCGCGAGAAGATGA**	**CCAGAGGCGTACAGGGATAG**

2.8 Statistical Analysis

Statistical analyses were calculated using the statistic analysis program Prism 5 (La Jolla, CA, USA). Multiple comparisons were performed by ANOVA and single comparisons were performed by unpaired Student's t tests with a 95% confidence interval. Statistically significant differences were determined as $P < 0.05$ from a minimum of two independent experiments.

CHAPTER 3: RESULTS

3.1 The assessment of KRAS mutant or WT NSCLC cell sensitivity to EGFR-TKIs with or without FAK-TKIs

3.1.1 Assessment of Cell Viability in 2D Assays

A previous study in the Addison lab evaluated whether EGFR WT NSCLC have differential sensitivity to treatment with an FAK-TKI alone, ERL alone or with both drugs in combination (61). As the original study was simply to evaluate the efficacy of this drug treatment in EGFR WT NSCLC cells, the data was obtained from only two cell lines, one with KRAS mutant status and one with KRAS WT status. From this initial study, it appeared that the KRAS mutant EGFR WT cell line was more sensitive to the FAK-TKI and ERL combination treatment than the KRAS WT EGFR WT NSCLC cell line. So, this project took the study a step further and expanded the study to confirm the possibly increased sensitivity of KRAS mutant EGFR WT NSCLC to this drug combination. We achieved this by using additional mutant and WT KRAS cell lines and a more clinically relevant EGFR-TKI, AFA. Initially, I performed cell viability assays to confirm that the cell lines treated with AFA behave similarly to when they are treated with ERL, which was used in the previous Addison study. Two cell lines with known EGFR mutations that make them sensitive to EGFR-TKIs, H4006 and H827, were initially tested. Both cell lines showed significant sensitivity to AFA (IC_{50} (μM) of H4006: **0.004229**, H827: **0.01756**) compared to ERL (IC_{50} (μM) of H4006: **0.01910**, H827: **0.004528**) (Figure 3A & B respectively).

A) B)

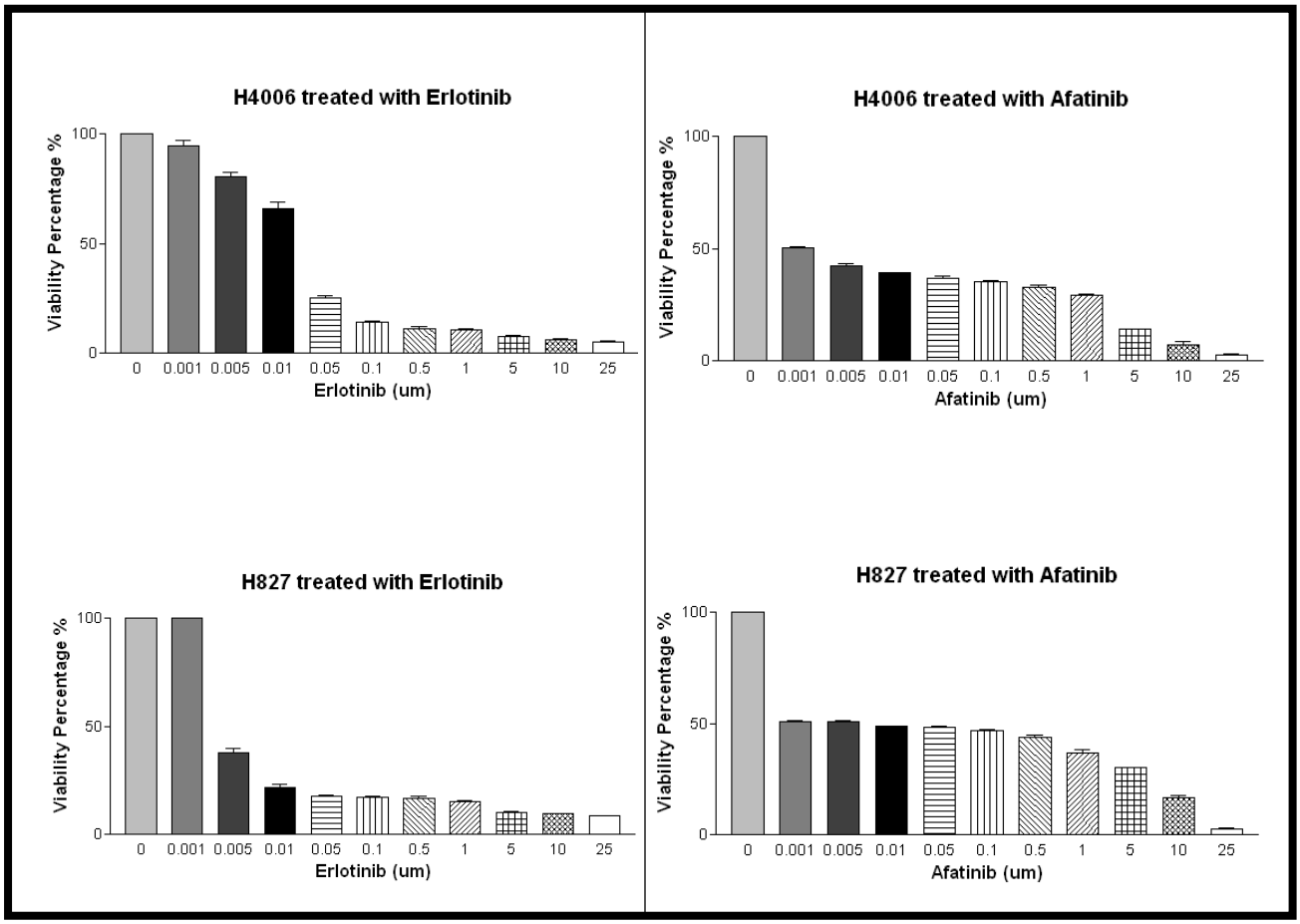

Figure 3. **Cell viability assays to confirm the similar effect of AFA compared to ERL treatments.** Cells were plated in 96-well microtiter plates, and subsequently treated with increasing concentrations of A) ERL or B) AFA. Cell viability was measured using MTT 48 hours post-drug treatment. NSCLC cells H4006 and H827, both of which have the deletion amplification mutation of EGF known to confer EGFR-TKI sensitivity, show significant inhibition of viability and sensitivity to A) ERL, and B) AFA drug. The data was obtained from three independent biological replicates with 8 technical replicates each.

The next step was to perform cell viability assays using KRAS mutant (A549, H460, A427) compared to KRAS wild type (H1299, H1563, Calu3) NSCLC cell lines following treatment with FAK-TKI or AFA alone (Figures 4 & 5, Table 1). The data from viability assays 48 hours post treatment with AFA alone were visualized and the IC_{50} was calculated from log (inhibitor) *vs* normalized response graph with variable slope. The obtained IC_{50} values (μM) suggest that KRAS mutant cells (A549: **21.96**, H460: **13.48**, A427: **13.07,** Overall IC_{50} average: **16.17**) are generally slightly more resistant to AFA drug treatment compared to KRAS WT cells (H1299: **11.44**, H1563: **12.43**, Calu3: **0.0695**, Overall IC_{50} average: **7.98**) (Figure 4). Additionally, the data from viability assays 48 hours post treatment with FAK-TKI alone were visualized and the IC_{50} were again calculated from log (inhibitor) *vs* normalized response graph with fixed slope. The obtained IC_{50} values (μM) show that, as predicted, KRAS mutant cells (A549: **2.55**, H460: **1.93**, A427: **1.66,** Overall IC_{50} average: **2.04**) were generally more sensitive to FAK-TKI than KRAS wild-type NSCLC (H1299: **3.67**, H1563: **5.59**, Calu3: **5.71**, Overall IC_{50} average: **4.98**) (Figure 5). Following confirmation of sensitivity to each drug alone, we wanted to determine whether the addition of PF-271 could further sensitize cells to AFA or, at the very least, result in an additive reduction in cell viability beyond that of treatment with either AFA or PF-271 alone. Cells were then treated with various concentrations of AFA (1–20 μM) or PF-271 (1–20 μM), alone or in combination, and cell viability was assessed by MTT assay (Figure 6). As shown in Figure 6, we found that the use of FAK-TKI and AFA in combination resulted in a statistically significant enhanced reduction in tumor cell viability in the KRAS mutant NSCLC tumor cell lines (A549, H460, A427) compared to the single drug

treatment with most effective inhibition in each cell line. In KRAS WT NSCLC tumor cell lines (H1299, H1563, Calu3) (Figure 6), although a trend for enhanced inhibition of cell viability was generally observed with the drug combination, this did not reach statistical significance as compared to the most effective single drug treatment with AFA (Figure 6C & D).

A generalized statement that could be concluded from this data is that KRAS mutant NSCLC cells seem to show enhanced inhibition of tumor viability when treated with the drug combination. Conversely, the WT KRAS cells seem to respond similarly to both the single drug treatment with AFA and to the treatment with the combination with AFA and FAK-TKI. Studies have shown that higher concentrations of FAK-TKI PF-271 can be associated with off target effects (64). Therefore, the statistical analysis was done based on those samples treated with 5 µM PF-271 or less. In Figure 6B, data are shown for both mutant and WT KRAS cell lines treated with each of 5 µM AFA and 5 µM PF-271 alone or in combination. The fold difference between mutant KRAS cells treated with the most effective single drug and those treated with drug combination (A549: **28**, H460: **23**, A427: **49**) is higher than the difference observed in similarly treated WT KRAS cells (H1299: **9**; Calu3: **4**; H1563: **8**). A similar trend was observed when both mutant and WT KRAS cell lines were each treated with 10 µM AFA and 5µM PF-271 alone or in combination (Figure 6D). The fold difference between mutant KRAS cells treated alone or in combination at these doses (A549: **25**, H460: **27**, A427: **52**) was again higher than the difference observed in similarly treated WT KRAS cells (H1299: **7**, Calu3: **6**, H1563: **4**).

KRAS WT

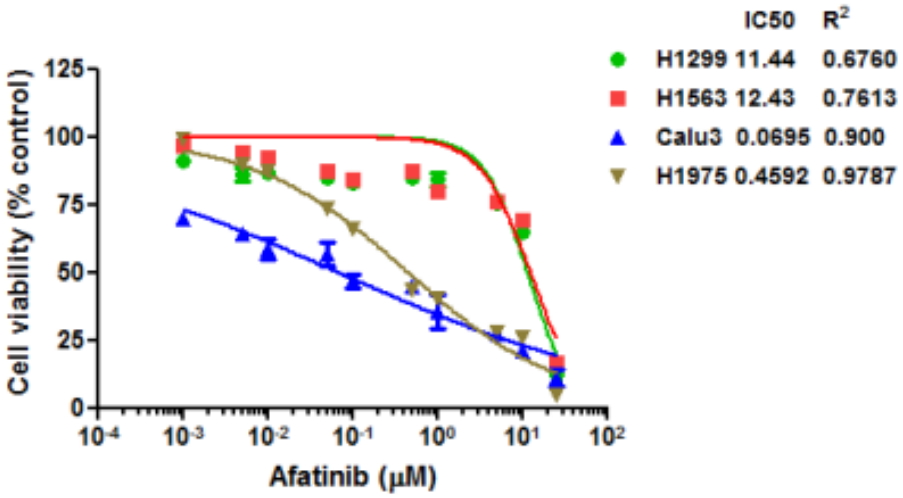

KRAS mutant

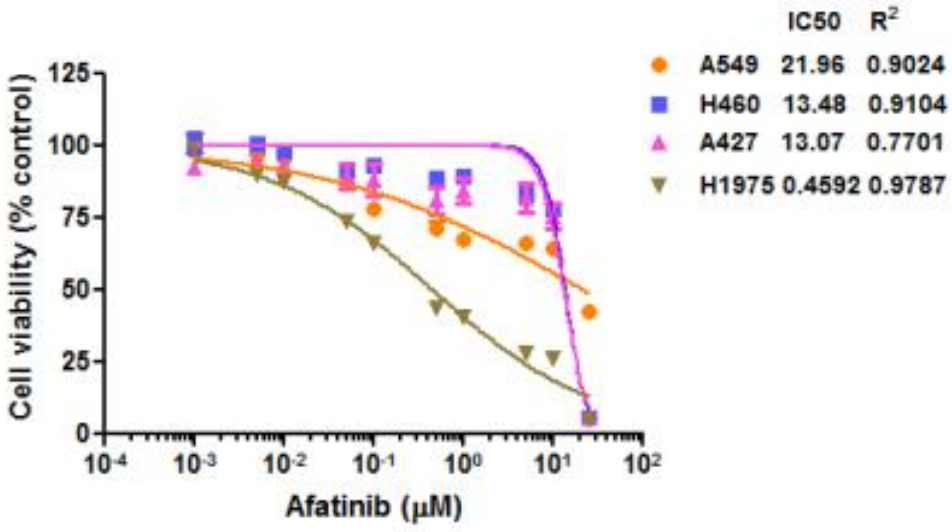

Figure 4. **Cell viability assays of WT and mutant KRAS NSCLC cells treated with increased concentrations of AFA**. Cells were plated in 96-well microtitre plates, and were treated the next day with concentrations of AFA ranging from 0.001 - 25 μM. Cell viability was assessed using MTT assays 48 hours post-drug treatment. KRAS mutant cells (Avg IC_{50}: 16.17 μM) show increased resistance to AFA following 48 hours drug treatment as compared to KRAS WT cells (Avg IC_{50}: 7.98 μM) treated for the same length of time. The data presented is an average of 3 separate biological replicates with 8 technical replicates each.

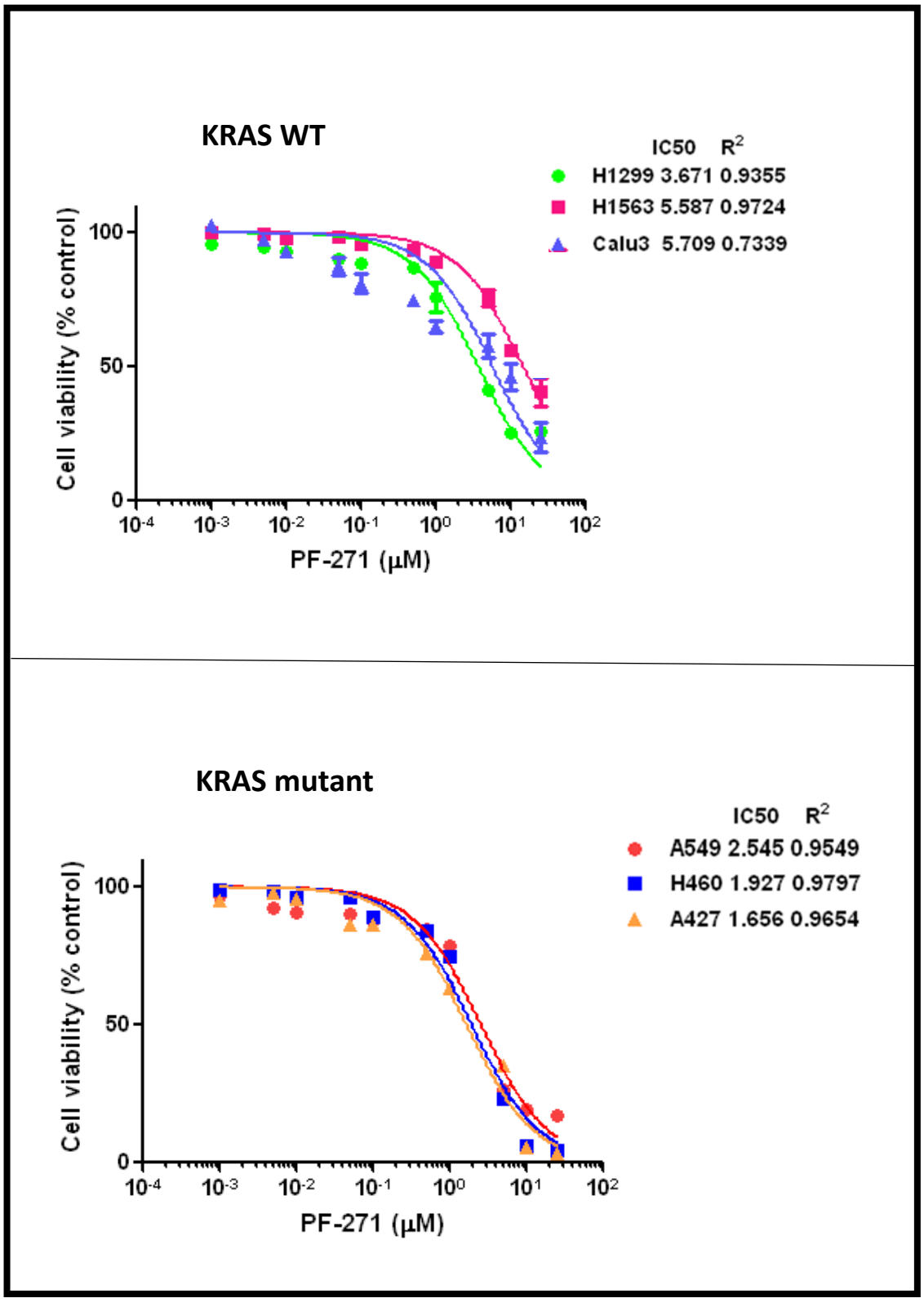
KRAS WT
IC50 R2
H1299 3.671 0.9355
H1563 5.587 0.9724
Calu3 5.709 0.7339
Cell viability (% control)
100
50
0
10-4 10-3 10-2 10-1 100 101 102
PF-271 (μM)
KRAS mutant
IC50 R2
A549 2.545 0.9549
H460 1.927 0.9797
A427 1.656 0.9654
Cell viability (% control)
100
50
0
10-4 10-3 10-2 10-1 100 101 102
PF-271 (μM)

Figure 5.**Cell viability assays of WT and mutant KRAS NSCLC cells treated with increased concentrations of PF-271.** Cells were plated in 96-well microtitre plates, and next day were treated with concentrations of PF-271 ranging from 0.001 - 25 μM. Cell viability was assessed using MTT assays 48 hours post-drug treatment. KRAS mutant cells (Avg IC_{50}: 2.04 μM) show increased sensitivity to PF-271 following 48 hours of treatment as compared to KRAS WT cells (Avg IC_{50}: 4.98 μM) treated for the same length of time. The data presented is an average of 3 separate biological replicates, each with 8 technical replicates.

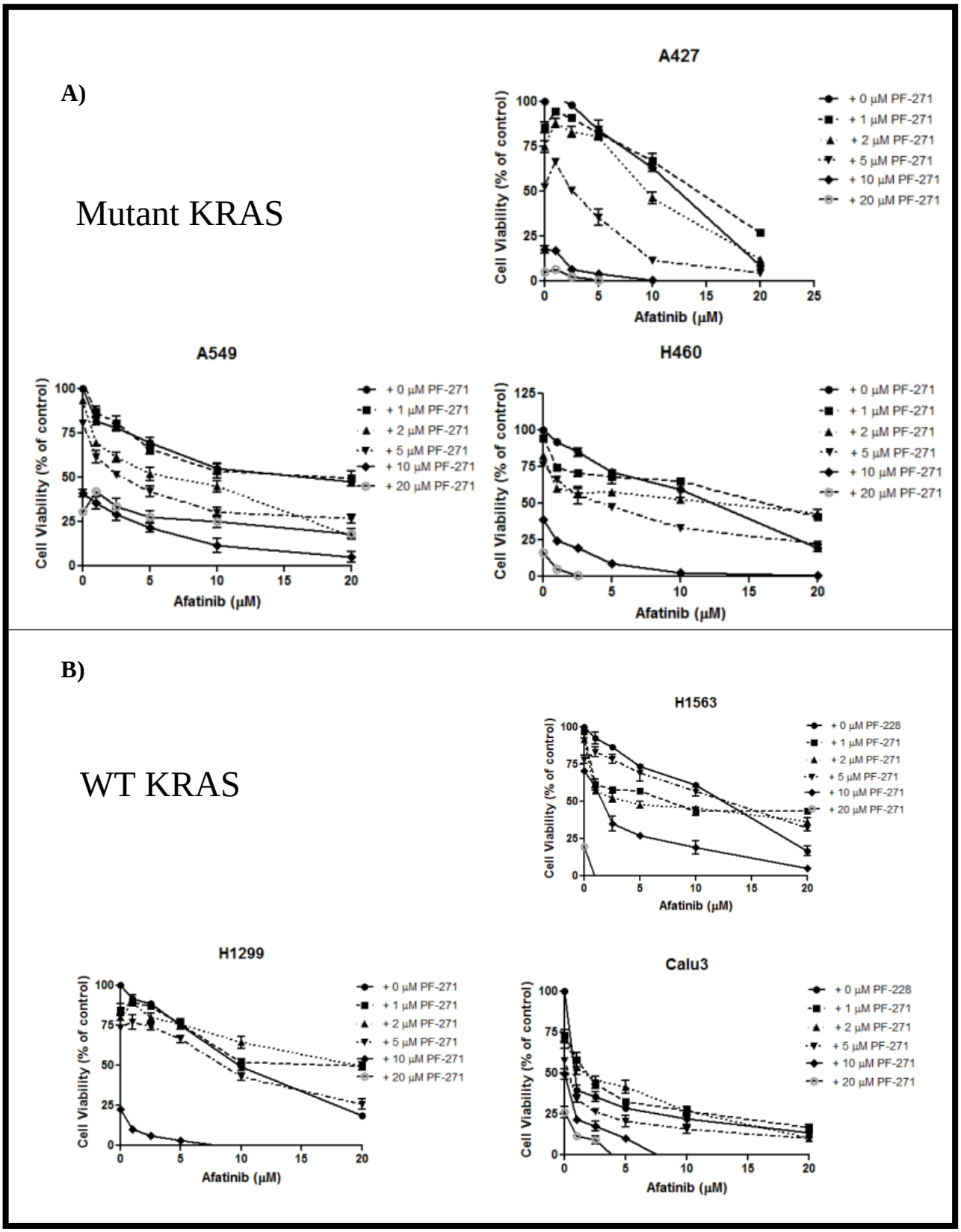
A)
Mutant KRAS
A427
A549
H460
B)
WT KRAS
H1563
H1299
Calu3
Cell Viability (% of control)
Afatinib (μM)
+ 0 μM PF-271
+ 1 μM PF-271
+ 2 μM PF-271
+ 5 μM PF-271
+ 10 μM PF-271
+ 20 μM PF-271
+ 0 μM PF-228

C)

Mutant KRAS

5μM AFA+ 5μM PF-271

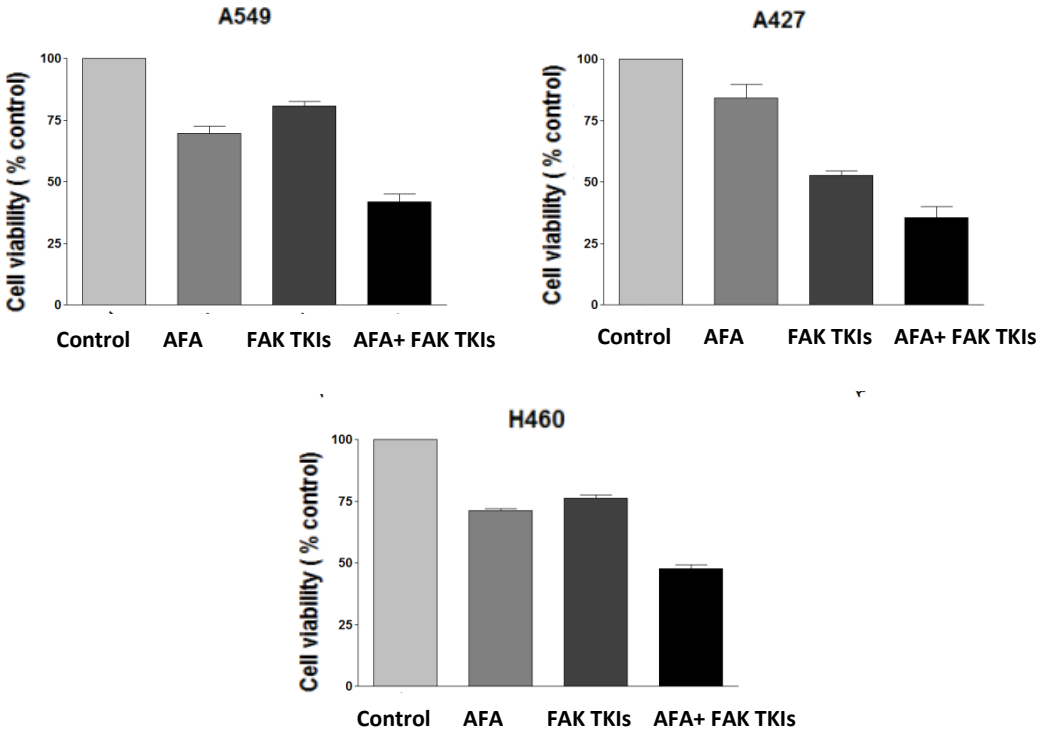

WT KRAS

5μM AFA+ 5μM PF-271

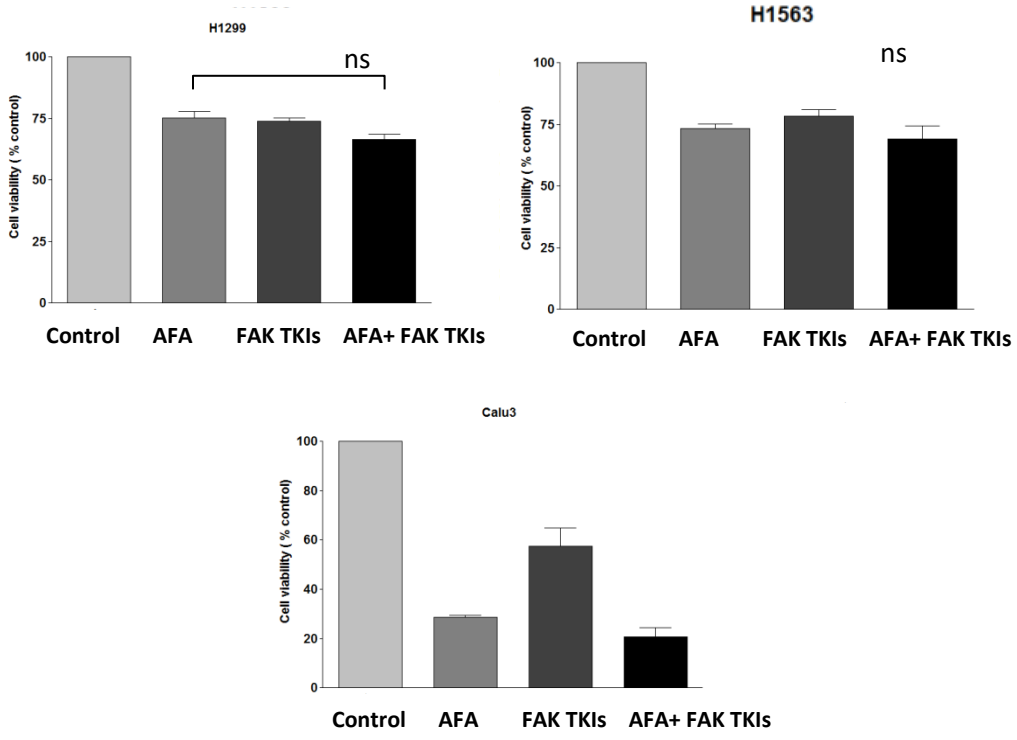

D)

Mutant KRAS

10μM AFA+ 5μM PF-271

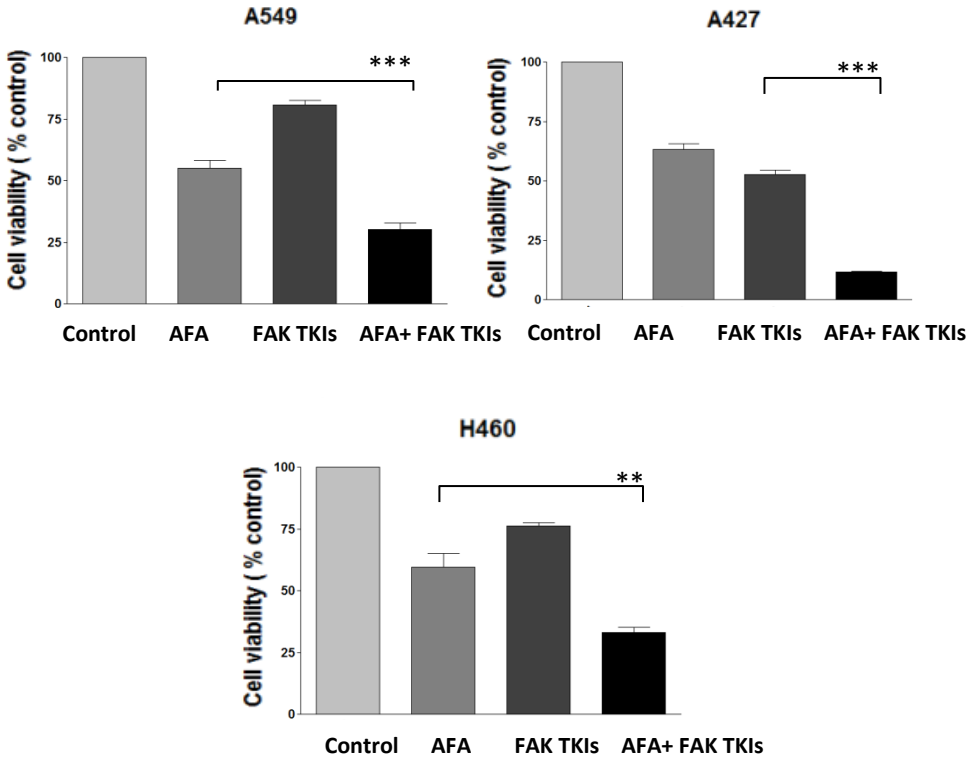

WT KRAS

10 μM AFA+ 5μM PF-271

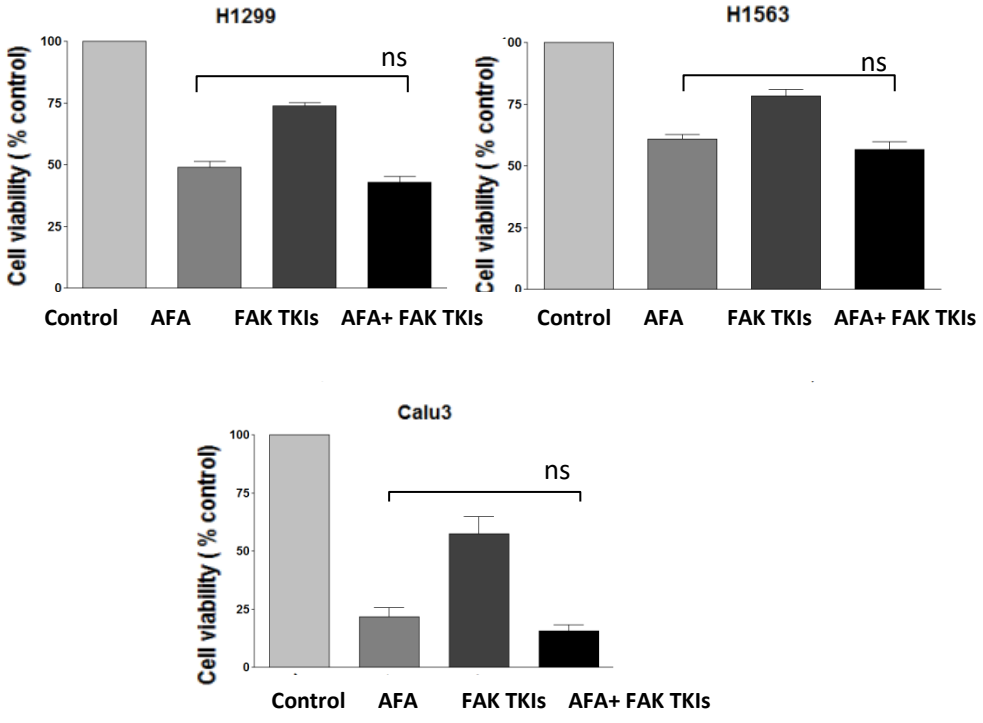

Figure 6. KRAS mutant NSCLC cells show significantly enhanced reduction in cell viabilty post treatment with combination of AFA and PF-271 compared to WT KRAS cells. Cells were plated in 96-well microtitre plates, and were treated the next day with various concentrations of AFA or PF-271 alone or in combination ranging from 0.001 – 20 µM for each drug. Cell viability was assessed using MTT assays 48 hours post-drug treatment. A) Cell viability at all concentrations. Graphical representation of cell viability for mutant and WT KRAS NSCLC cells treated with B) 5 µM AFA and 5 µM PF-271 alone or in combination or with C) 10 µM AFA and 5µM PF-271alone or in combination. All data was collected from 3 independent biological replicates and 8 wells of technical replicates within each experiment. The statistically significant differences were determined by ANOVA. Asterisks denote statistically significant differences compared to single drug treated cells with most effect (* = $p<0.05$,** = $p<0.01$, *** = $p<0.001$). (ns) denotes statistically insignificant difference compared to single drug treated cells with most effect.

3.1.2 Assessment of Cell Colonies in 3D Assays.

Given that the integrin-FAK signaling axis is differentially activated when cells are grown in 3-dimensions (3D) compared to 2-dimensions (2D), we repeated similar drug combination experiments to those described in Section 3.1.1 in 3D, a setting that better mimics the potential growth of these cells in vivo (65). NSCLC cells were embedded in growth factor-reduced BME in complete growth medium and treated with AFA, PF-271, or the combination of both drugs. Colony formation by A549, H460, H1299 and Calu3 cells was assessed from three independently performed experiments. An evident difference in colony size between treatment groups was seen after 14 days in all cell lines tested. Images of H460, A549, and Calu3 cells were taken after 14 days. Due to the branching style of growth of the cell line, H1299 images shown are taken 8 days post seeding (Figures 7 & 8).

In the KRAS mutant cell lines A549 and H460, the number of colonies appeared to not have significantly changed as compared to the single drug treatment with the most effect. However, a shift in the distribution of colony size towards smaller colonies was observed for both AFA and PF-271 treated cells (Figure 7 A& B). On the other hand, in the KRAS WT cell lines H1299 and Calu3, AFA was effective on its own at decreasing colony growth of the treated cells (as measured by colony size) in a similar manner to those treated with the combination of both drugs with no statically significant difference (Figure 8A). Like mutant KRAS, KRAS WT NSCLC cells did not show significant differences in colony number for cells treated with the drug combination as compared to those cells treated with the single drug with most effect (Figure 8B). It is important to recognize the increase of colony number post-single or

combination drug treatment when compared to DMSO control in both mutant and WT NSCLC. This observation could be explained by the fact that control colonies were fusing together as they got larger in size.

Together, the 3D data matches the results obtained in 2D assays and supports the notion that the combination treatment is more effective at blocking 3D growth and proliferation of KRAS mutant NSCLC cells compared to KRAS WT NSCLC cells which, in turn, suggests that this combination treatment could also be effective in vivo.

A) A549 KRAS mutant

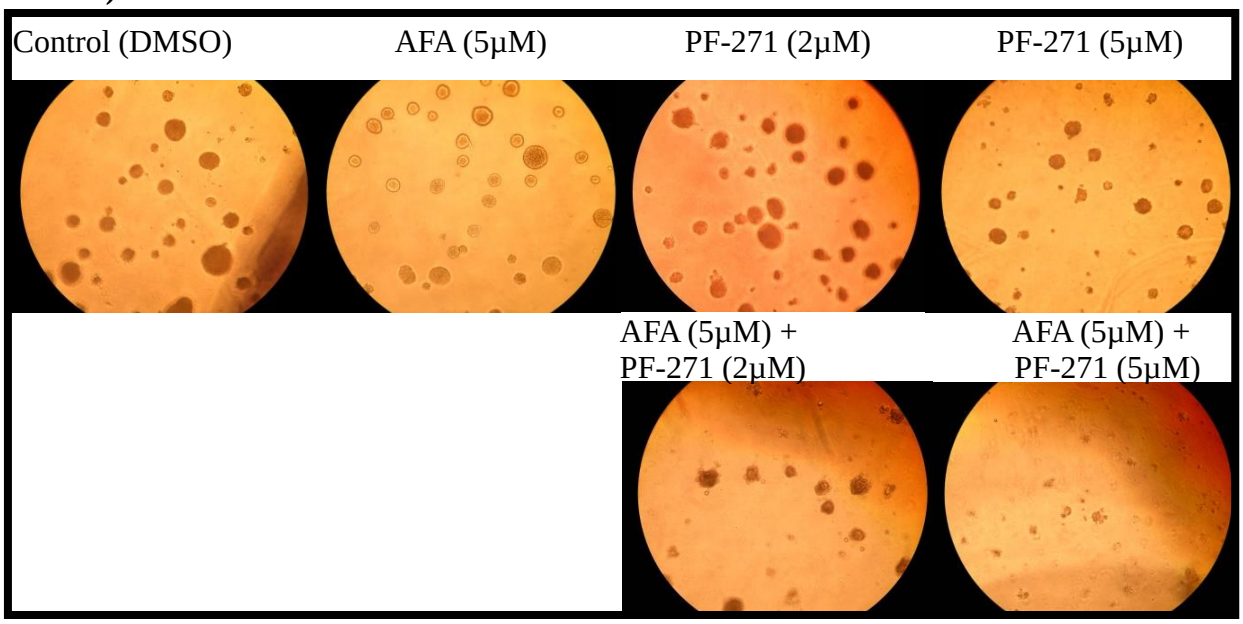

H460 KRAS mutant

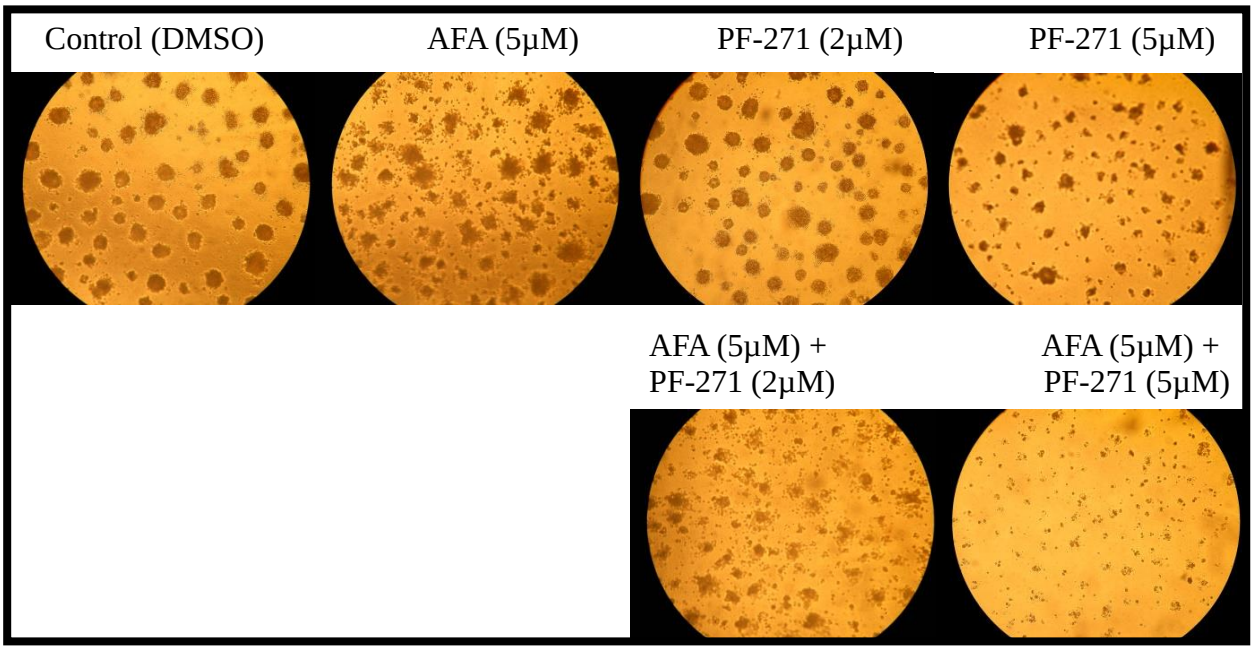

B)

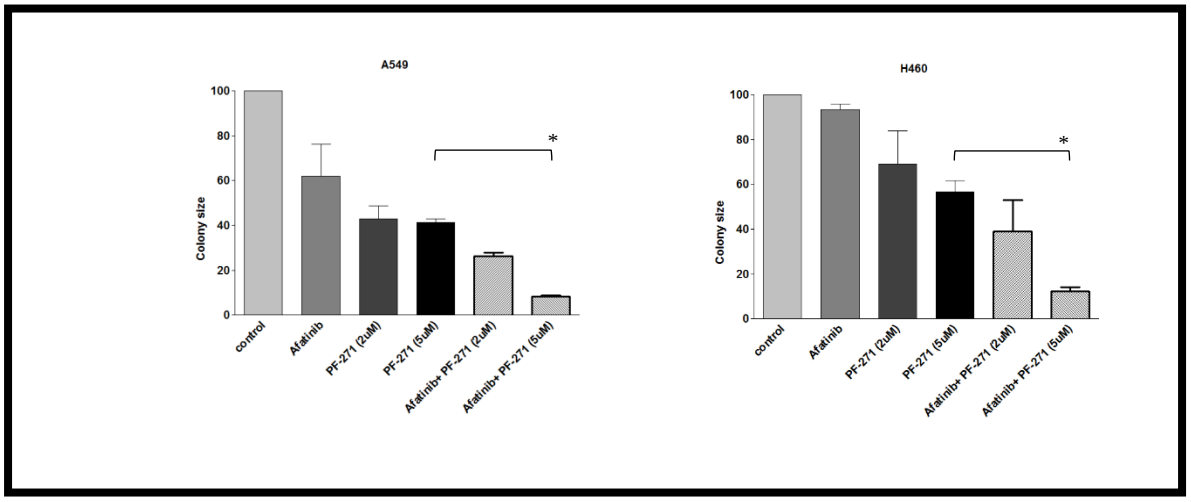
A549
Colony size
100
80
60
40
20
0
*
control
Afatinib
PF-271 (2uM)
PF-271 (5uM)
Afatinib+ PF-271 (2uM)
Afatinib+ PF-271 (5uM)
H460
Colony size
100
80
60
40
20
0
*
control
Afatinib
PF-271 (2uM)
PF-271 (5uM)
Afatinib+ PF-271 (2uM)
Afatinib+ PF-271 (5uM)

C)

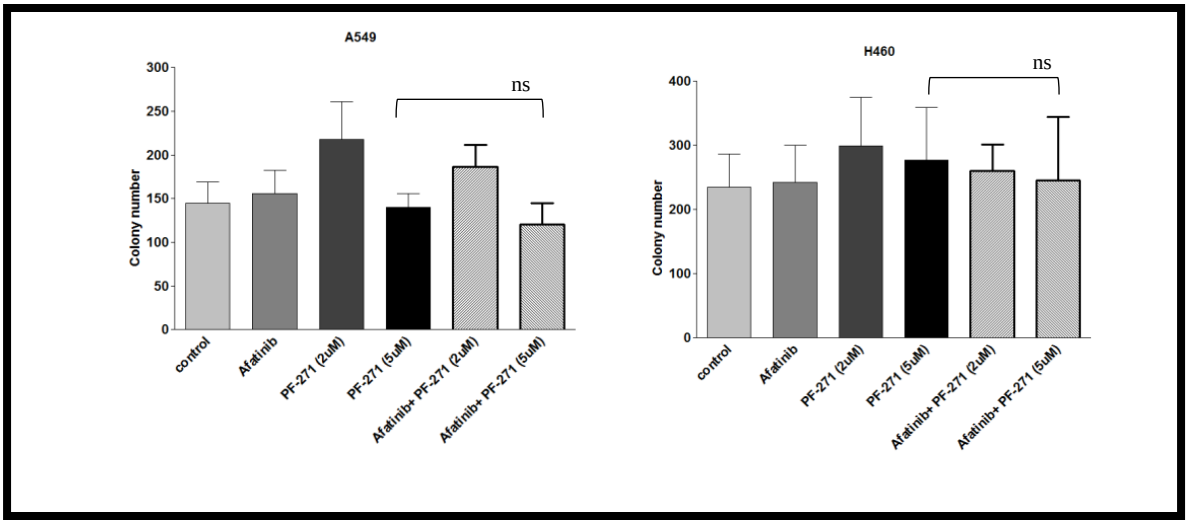
A549
Colony number
300
250
200
150
100
50
0
ns
control
Afatinib
PF-271 (2uM)
PF-271 (5uM)
Afatinib+ PF-271 (2uM)
Afatinib+ PF-271 (5uM)
H460
Colony number
400
300
200
100
0
ns
control
Afatinib
PF-271 (2uM)
PF-271 (5uM)
Afatinib+ PF-271 (2uM)
Afatinib+ PF-271 (5uM)

Figure 7. Combination treatment with AFA and PF-271 is more effective in reducing 3-dimensional colony formation in KRAS mutant NSCLC (A549 & H460). A) 3D colony formation was assessed from NSCLC cells embedded in growth factor reduced BME in 4-well chamber slides in the presence of either vehicle control (DMSO), AFA (5 μM), PF-271 (2 μM or 5 μM), or with combinations of AFA and PF-271 in complete media. Media with fresh drug was replenished every 3 days and colony size was assessed after 14 days. Images representative of three independently performed experiments are shown. B) Graphical representation of 3D cell colony viability for mean colony area. All drug treatments were normalized based on the value obtained from the control sample (DMSO). C) Graphical representation of 3D cell colony viability for mean colony number for treated NSCLC cell lines. Measurements for B) and C) were performed using ImageJ, using a colony threshold size of >0.000015 μm^2. The data were collected from three independently performed experiments with one biological replicate each. The statistically significant differences were determined by ANOVA. Asterisks denote statistically significant differences compared to single drug treated cells with most effect (* = $p < 0.05$). (ns) denotes statistically insignificant difference compared to single drug treated cells with most effect.

A) H1299 KRAS WT

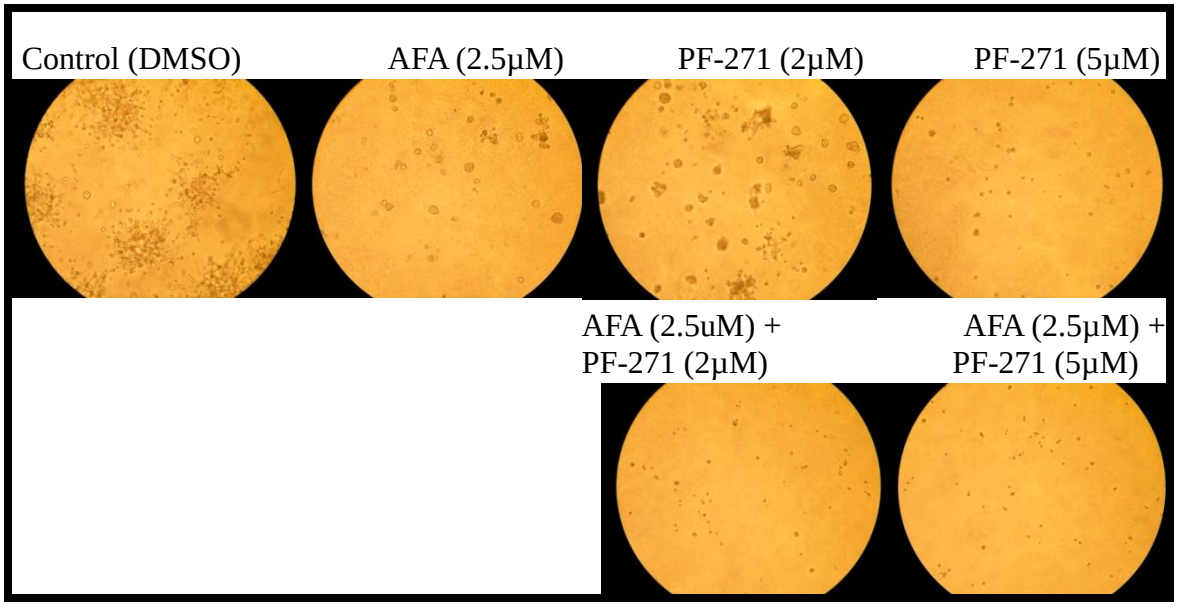

Calu3 KRAS WT

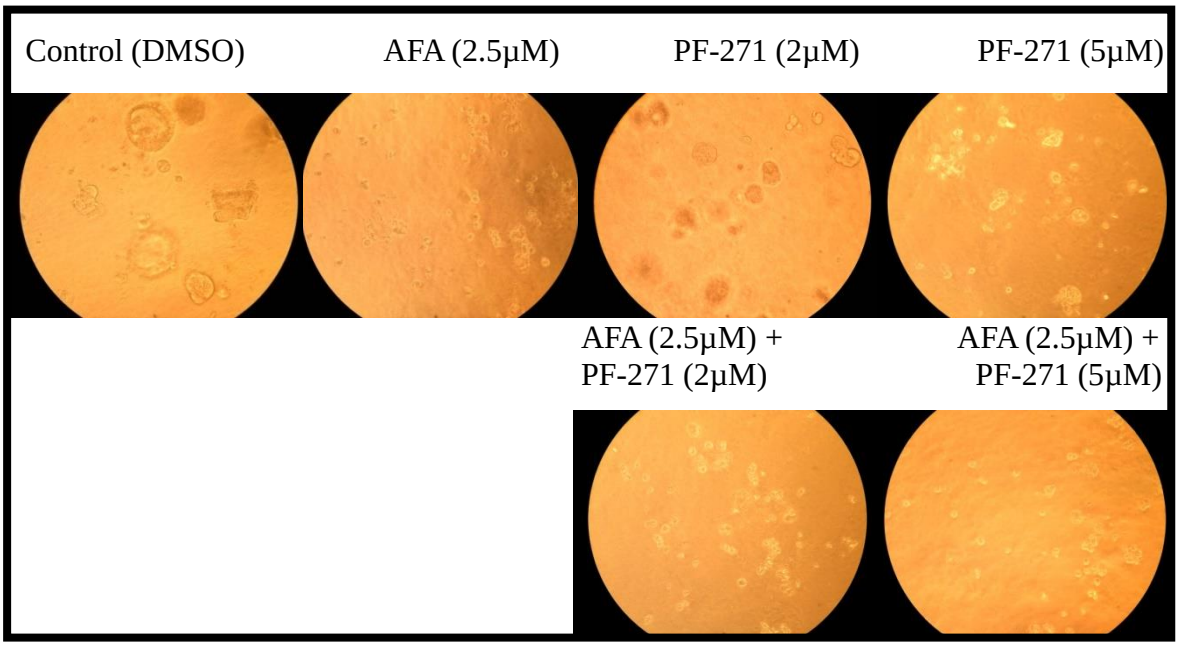

B)

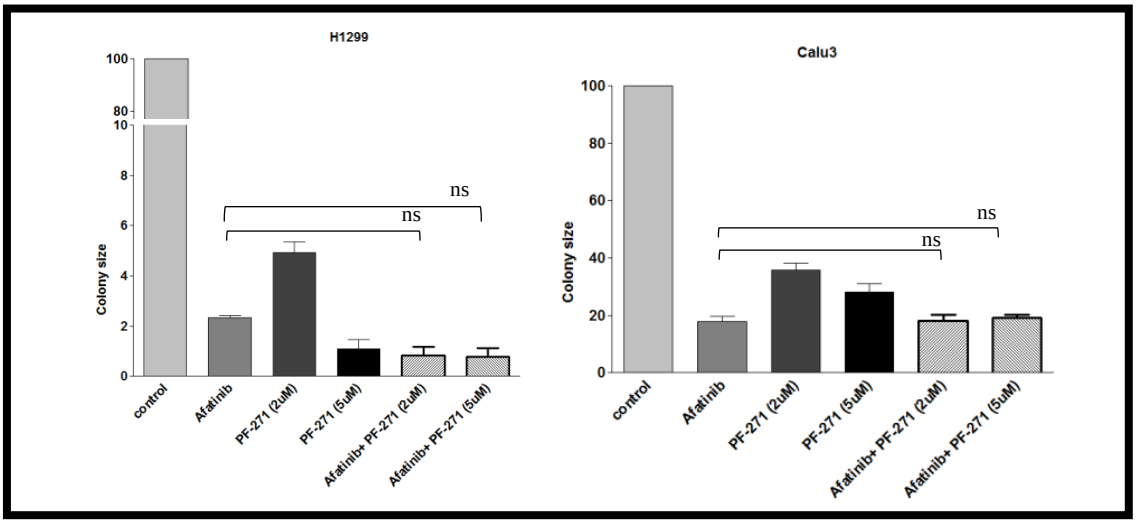
H1299
Colony size
100
80
10
8
6
4
2
0
ns
ns
control
Afatinib
PF-271 (2uM)
PF-271 (5uM)
Afatinib+ PF-271 (2uM)
Afatinib+ PF-271 (5uM)
Calu3
Colony size
100
80
60
40
20
0
ns
ns
control
Afatinib
PF-271 (2uM)
PF-271 (5uM)
Afatinib+ PF-271 (2uM)
Afatinib+ PF-271 (5uM)

C)

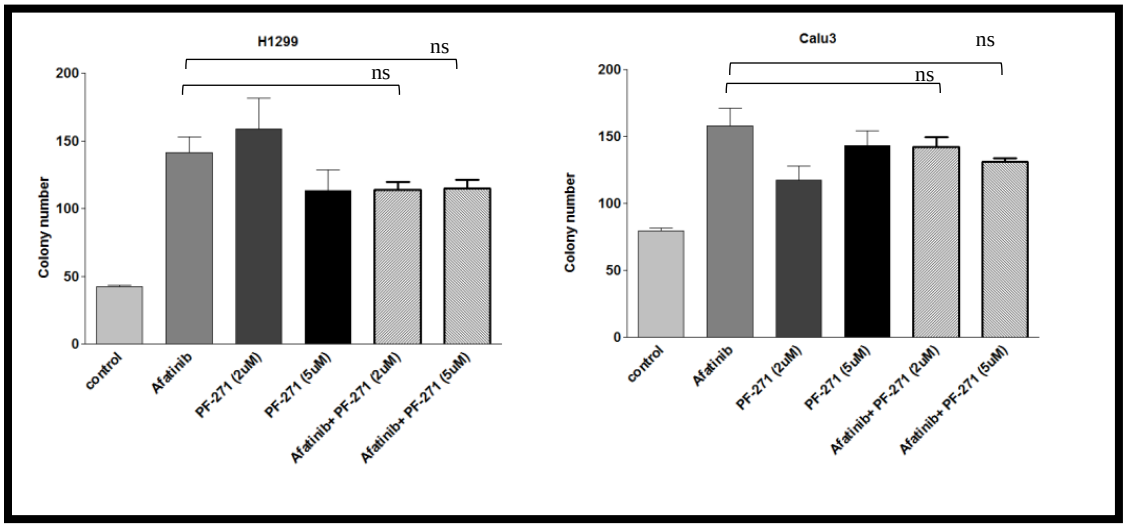
H1299
Colony number
200
150
100
50
0
ns
ns
control
Afatinib
PF-271 (2uM)
PF-271 (5uM)
Afatinib+ PF-271 (2uM)
Afatinib+ PF-271 (5uM)
Calu3
Colony number
200
150
100
50
0
ns
ns
control
Afatinib
PF-271 (2uM)
PF-271 (5uM)
Afatinib+ PF-271 (2uM)
Afatinib+ PF-271 (5uM)

Figure 8. Combination treatment with AFA and PF-271 reduces 3-dimensional colony formation similar to treatment with either drug alone in KRAS WT NSCLC cells. A) 3D colony formation was assessed in KRAS WT H1299 & Calu3 NSCLC cells embedded in growth factor reduced BME in 4-well chamber slides in the presence of either vehicle control (DMSO), AFA (2.5 μM), PF-271 (2 μM or 5 μM), or with combinations of both AFA and PF-271 in complete media. Media with fresh drug was replenished every 3 days and colony size was assessed after 14 days for Calu3 and after 8 days for H1299. Images shown are representative of three independently performed experiments. B) Graphical representation of 3D cell colony viability for mean colony area. All drug treatments were normalized based on the value obtained from the control sample (DMSO). C) Graphical representation of 3D cell colony viability for mean colony number for treated NSCLC cell lines. Measurements were performed using ImageJ, using a colony threshold size of >0.000015 μm^2. The data were collected from three independently performed experiments with one biological replicate. The statistically significant differences were determined by ANOVA. Asterisks denote statistically significant differences compared to single drug treated cells with most effect (* = $p < 0.05$). (ns) denotes statistically insignificant difference compared to single drug treated cells with most effect.

3.2 The mechanism by which FAK inhibition may sensitize NSCLC cells to EGFR-TKIs

To better understand how FAK and EGFR-TKIs in combination may be more effective at inhibiting NSCLC tumor growth that either drug in isolation, we speculated that FAK inhibition might sensitize cells to EGFR-TKIs via putative inhibition of receptor cross-talk ability. This could further inhibit cell proliferation, induce apoptosis or possibly even alter EGFR signaling through effects on receptor recycling. We therefore performed experiments designed to evaluate the possibility of FAK blockade working through each of these possible mechanisms.

3.2.1 Effect of FAK inhibition on FAK- EGFR cross talk

To understand underlying mechanisms of sensitivity, the activity of important downstream signaling proteins such as Akt were examined. Akt is a downstream target of activated EGFR and persistent Akt activity was reported to be associated with a lack of response to EGFR-TKIs (66). In NSCLC cells it is possible that Akt is getting phosphorylated through two different pathways. The first pathway of Akt activation downstream of EGFR binding to receptor ligands occurs following autophosphorylation of EGFR Y1068 site which then results in EGFR-mediated Y1101 phosphorylation. This creates a binding site for Phosphoinositide 3-kinase (PI3K) which becomes activated as a result and which in turn activates Akt (Figure 9A).

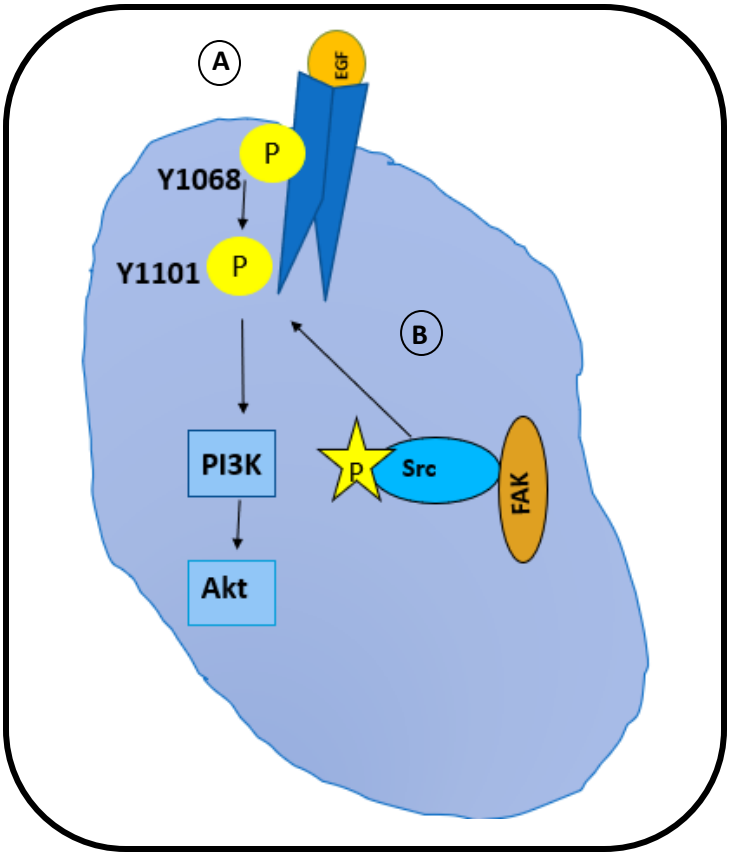

Figure 9: Schematic representation of Akt activation. A) Akt is activated downstream of PI3K activation post growth factor activation of EGFR. B) Akt is activated downstream of EGFR in an EGFR ligand independent manner via the FAK-Src complex which phosphorylates EGFR at Y1101 and recruits and activates PI3K, which in turn activates Akt.

The second pathway by which Akt may be activated is following phosphorylation of EGFR on Y1101 by the activated FAK-Src complex. This site again serves to recruit and activate PI3K which then activates Akt (Figure 9B). This means that blocking EGFR signaling using EGFR-TKIs alone may not be sufficient to block the activation of Akt signaling completely, as it still could be getting activated though the FAK–Src complex. Therefore, we speculated that using the combination of two inhibitors may be important in KRAS mutant cells to completely block Akt phosphorylation and thereby inhibit NSCLC tumor cell survival.

Our previous preliminary data suggested that in KRAS mutant A549 cells, the combination of FAK-TKI and ERL appeared to be more effective in inhibiting Akt activity. This was evidenced by the ability of the combination treatment to more significantly reduce levels of Akt phosphorylation at S473, than did treatment with either drug alone. This suggests an enhanced ability to impair cell survival following treatment with the drug combination as we predicted (61). These results were not observed in WT KRAS H1299 NSCLC cells where the levels of p-Akt S473 were not significantly more reduced in the combination treatment as compared to treatment with either drug alone (61). As such, we investigated whether the effect of AFA alone or in combination with FAK-TKIs had similar effects on active Akt in the context of our expanded analysis of KRAS mutant vs WT NSCLC cell lines (Figure 10 A & B). In all cases, protein levels are normalized to levels of total specific protein, and β-actin.

A)

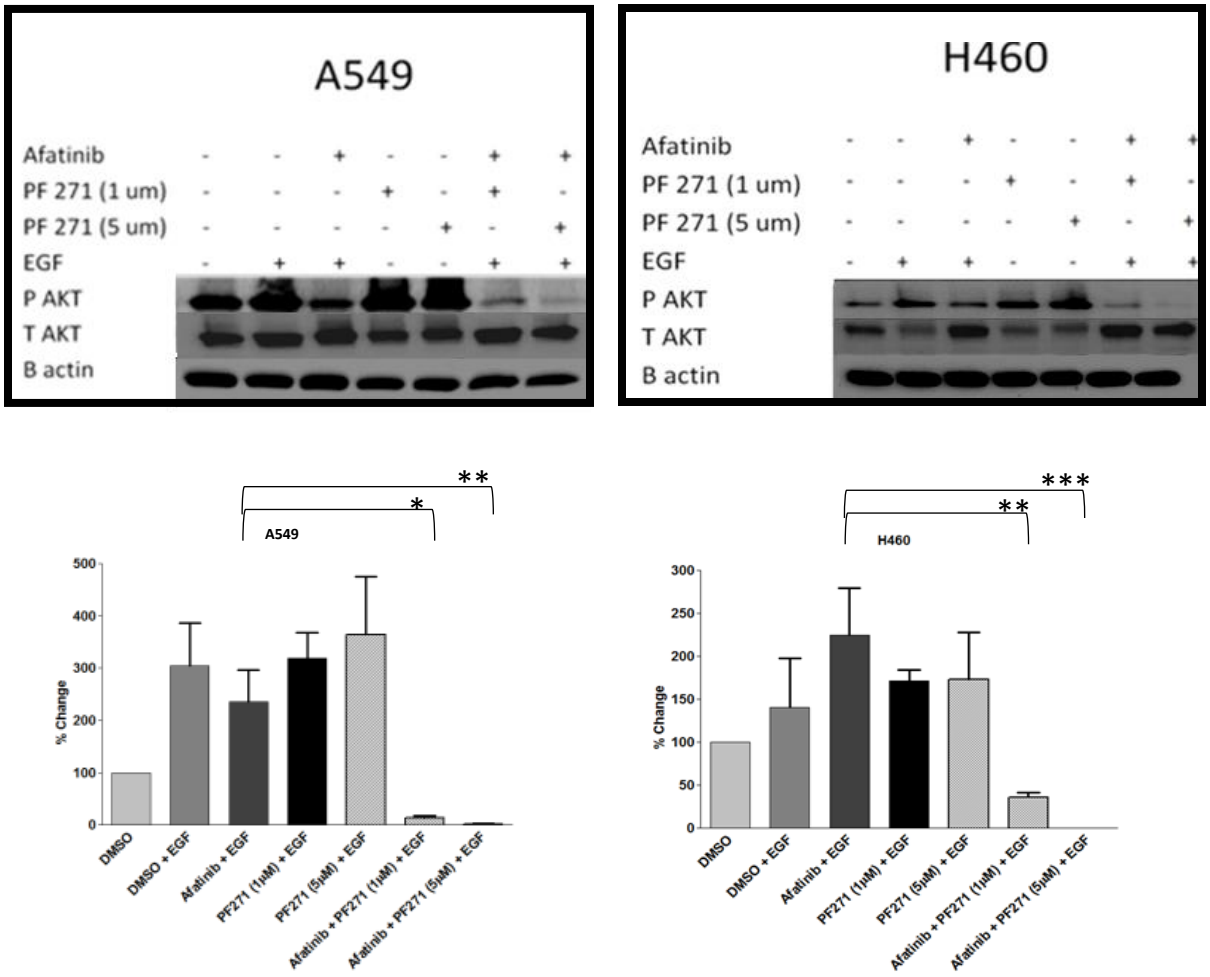
A549
Afatinib
PF 271 (1 um)
PF 271 (5 um)
EGF
P AKT
T AKT
B actin
H460
Afatinib
PF 271 (1 um)
PF 271 (5 um)
EGF
P AKT
T AKT
B actin
**
*
A549
% Change
500
400
300
200
100
0
DMSO
DMSO + EGF
Afatinib + EGF
PF271 (1μM) + EGF
PF271 (5μM) + EGF
Afatinib + PF271 (1μM) + EGF
Afatinib + PF271 (5μM) + EGF
***
**
H460
% Change
300
250
200
150
100
50
0
DMSO
DMSO + EGF
Afatinib + EGF
PF271 (1μM) + EGF
PF271 (5μM) + EGF
Afatinib + PF271 (1μM) + EGF
Afatinib + PF271 (5μM) + EGF

B)

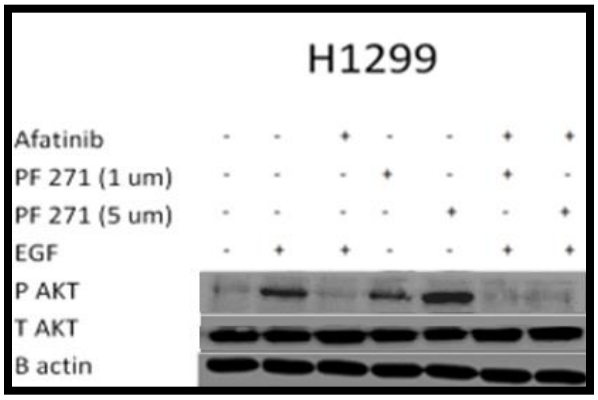
H1299
Afatinib
PF 271 (1 um)
PF 271 (5 um)
EGF
P AKT
T AKT
B actin

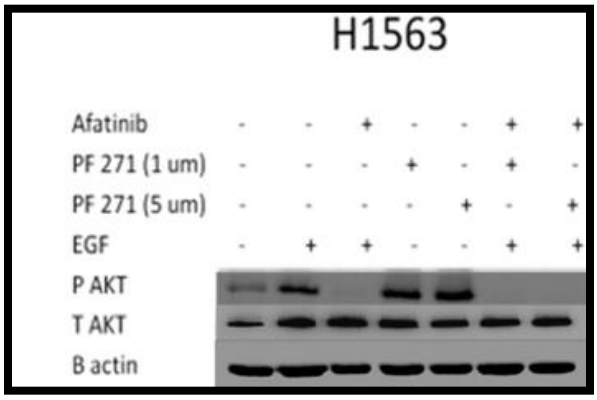
H1563
Afatinib
PF 271 (1 um)
PF 271 (5 um)
EGF
P AKT
T AKT
B actin

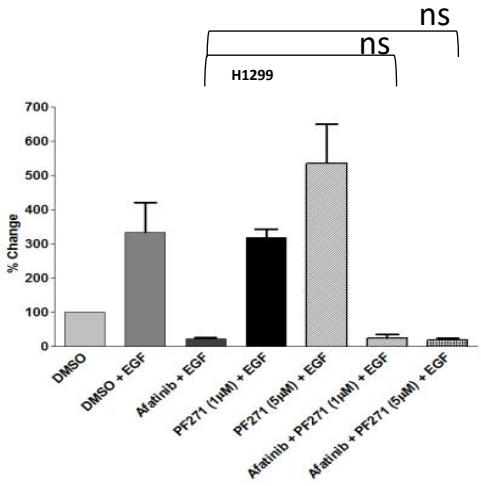
ns
ns
H1299
% Change
DMSO
DMSO + EGF
Afatinib + EGF
PF271 (1uM) + EGF
PF271 (5uM) + EGF
Afatinib + PF271 (1uM) + EGF
Afatinib + PF271 (5uM) + EGF

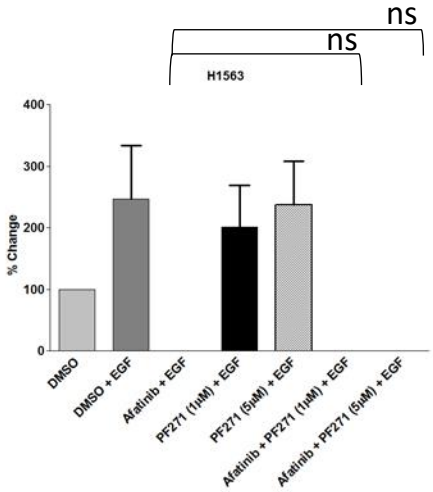
ns
ns
H1563
% Change
DMSO
DMSO + EGF
Afatinib + EGF
PF271 (1uM) + EGF
PF271 (5uM) + EGF
Afatinib + PF271 (1uM) + EGF
Afatinib + PF271 (5uM) + EGF

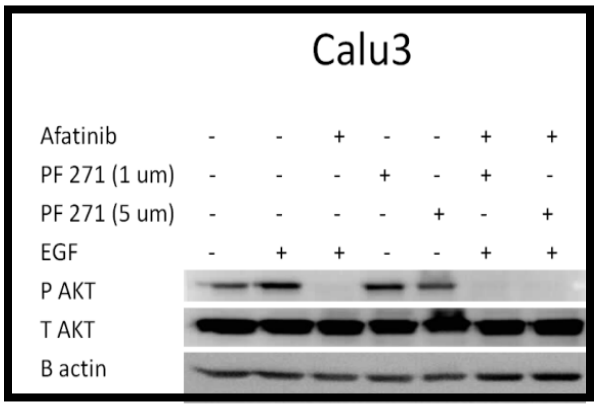
Calu3
Afatinib
PF 271 (1 um)
PF 271 (5 um)
EGF
P AKT
T AKT
B actin

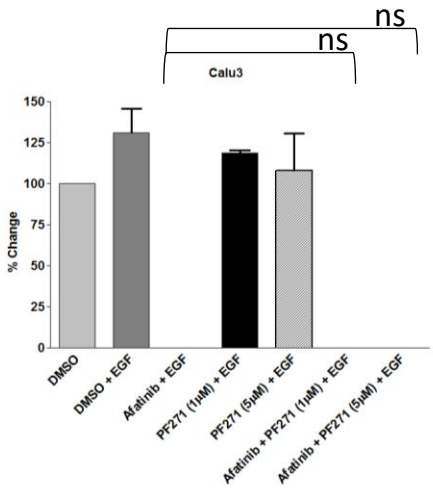
ns
ns
Calu3
% Change
DMSO
DMSO + EGF
Afatinib + EGF
PF271 (1uM) + EGF
PF271 (5uM) + EGF
Afatinib + PF271 (1uM) + EGF
Afatinib + PF271 (5uM) + EGF

Figure 10. Akt phosphorylation at (S473) is significantly more reduced following treatment with both AFA and PF-271 in combination in KRAS mutant but not in KRAS WT NSCLC cell lines as compared to treatment with each drug alone. Western blot and densitometry analysis of A) KRAS mutant NSCLC B) KRAS WT NSCLC. All cell lines were serum starved and were treated with either vehicle control (DMSO), AFA (10 μM), PF-271 (1 μM or 5 μM), or with a combination of both AFA and PF-271 for 30 minutes prior to stimulation of cells with 100 ng/mL EGF. After 30 minutes of EGF stimulation, total cellular protein was isolated. Phosphorylated and total Akt were detected by western blotting. β-actin was used as loading control. Blots presented are representative of results obtained from three independent experiments. Densitometry analysis of p-Akt normalized to total Akt is expressed as the average from three independent experiments. The statistically significant differences of the p-Akt: T-Akt ratio were determined by ANOVA. Asterisks denote statistically significant differences compared to single drug treated cells with most effect (* = $p<0.05$, ** = $p<0.01$, *** = $p<0.001$). (ns) denotes statistically insignificant difference compared to single drug treated cells with the most effect.

The combination of FAK-TKI and AFA appears to be more effective in inhibiting Akt activity, as evidenced by significantly reduced levels of phospho-Akt S473, as compared to treatment with either drug alone in the KRAS mutant NSCLC cell lines. This suggests an enhanced ability to impair cell survival following treatment with the drug combination (Figure 10A). However, similar results were not observed in WT KRAS NSCLC (Figure 10B), where we observed that the combination did not reduce phospho-Akt S473 levels further than the levels achieved with AFA alone, as was previously observed in the context of treatment with ERL. These results suggest that the use of FAK- and EGFR-TKIs in combination has an enhanced ability to inhibit KRAS mutant NSCLC cell survival in part due to an increased capacity to block downstream signaling proteins such as Akt.

3.2.2 Effect of FAK inhibition on altering cell survival or inducing cell apoptosis.

We demonstrated that combination treatment with FAK-TKIs and EGFR-TKIs in combination showed a higher reduction in cell viability as compared to treatment with each of the drugs alone in KRAS mutant NSCLC cells (Figure 6). However, as these assays assessed cell viability using MTT assays, it is possible that results could be due to either inhibition of cell growth, induction of cell death, or a combination of both. There is precedence for FAK inhibition enhancing apoptotic responses induced by the DNA damaging agent doxorubicin (67) and as such we were interested in assessing NSCLC cell apoptosis following treatment with FAK- and EGFR-TKIs.

In addition to effects on Akt activity, which can also contribute to survival/ apoptosis in cells, we assessed the ability of the drug combination to induce increased

apoptosis in treated cells as compared to treatment with either drug alone using propidium iodide staining and detection of the percentage of cells in subG1 by flow cytometry (Figure 11 A & B). For this, the KRAS mutant cell line A549 and the KRAS WT H1299 cell lines were analyzed as representative NSCLC lines 24 hours post-treatment with either AFA (10 uM) or PF-271 (1 µM or 5 uM) alone. These conditions resulted in relatively low apoptotic rates in the treated cells. The drug AFA showed less apoptotic effect on KRAS mutant A549 cells (avg 6% apoptotic cells) compared to WT KRAS H1299 cells (avg 15.8% apoptotic cells) (Figure 12 A & B). The number of apoptotic cells was found to increase dose-dependently following treatment with PF-271. Mutant and WT KRAS cells treated with 1 µM PF-271 had 5% and 7% of apoptotic cells respectively; those treated with 5 µM PF-271 had 40% and 32.4% of apoptotic cells, respectively. Even so, the number of total apoptotic cells was increased further upon treatment with the combination of AFA and PF-271 in both NSCLC lines tested.

Interestingly, the apoptotic difference between the two cell lines following treatment with the combination versus single drugs is more prominent at lower concentrations of FAK-TKI (i.e. 1 µM) in mutant KRAS cells. A549 mutant KRAS cell treated with 1 µM AFA and 1 µM PF-271 showed statistically significant differences in apoptotic cells when compared to A549 cells treated with 1 µM AFA alone ($p<0.05$) or 1 µM PF-271 ($p<0.01$) alone (Figure 12A). However, H1299 WT KRAS cells treated with the same concentrations of AFA and PF-271 showed no significant difference compared to those cells treated with AFA or PF-271 alone (Figure 12B).

A)

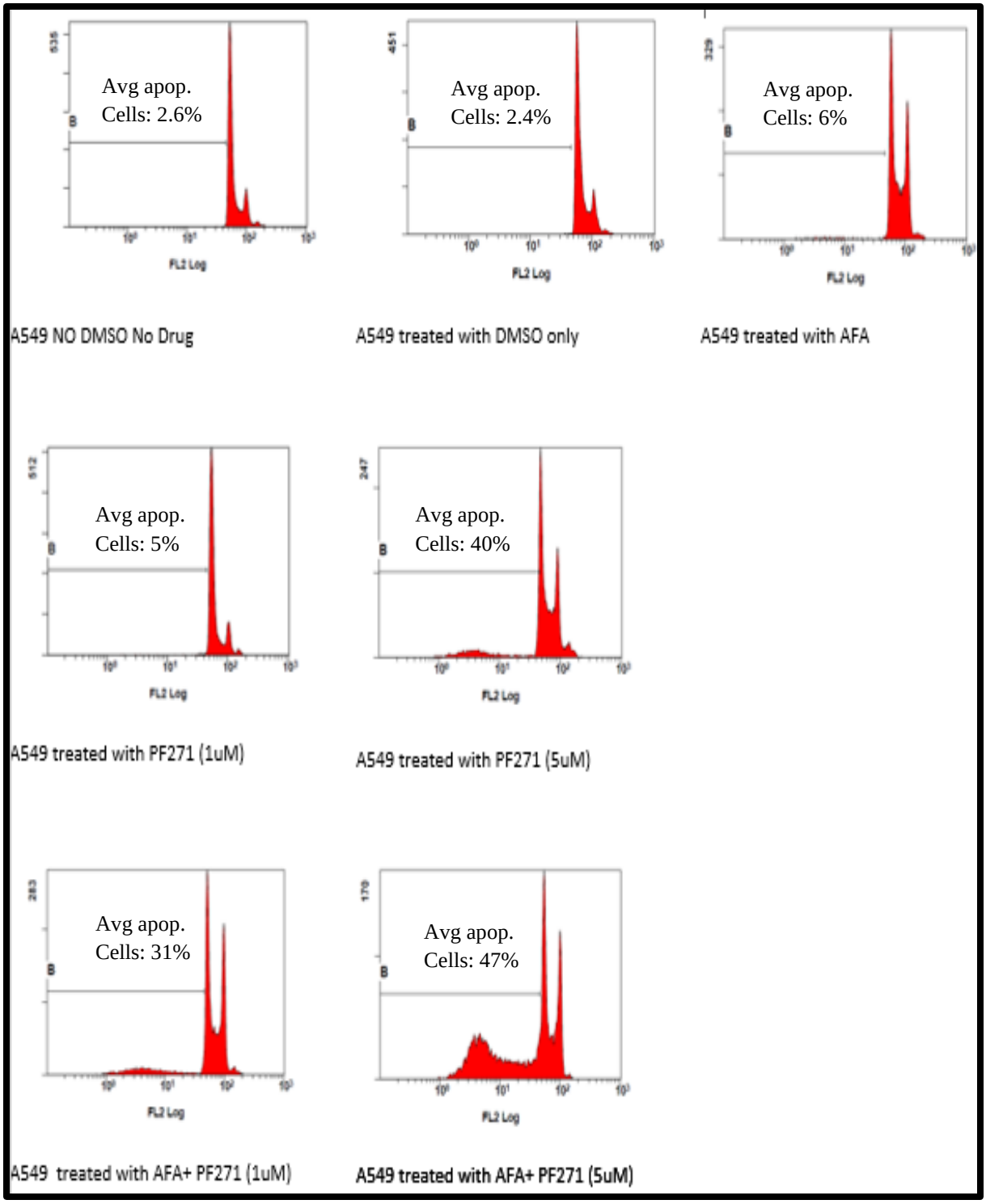
Avg apop.
Cells: 2.6%
FL2 Log
A549 NO DMSO No Drug
Avg apop.
Cells: 2.4%
FL2 Log
A549 treated with DMSO only
Avg apop.
Cells: 6%
FL2 Log
A549 treated with AFA
Avg apop.
Cells: 5%
FL2 Log
A549 treated with PF271 (1uM)
Avg apop.
Cells: 40%
FL2 Log
A549 treated with PF271 (5uM)
Avg apop.
Cells: 31%
FL2 Log
A549 treated with AFA+ PF271 (1uM)
Avg apop.
Cells: 47%
FL2 Log
A549 treated with AFA+ PF271 (5uM)

B)

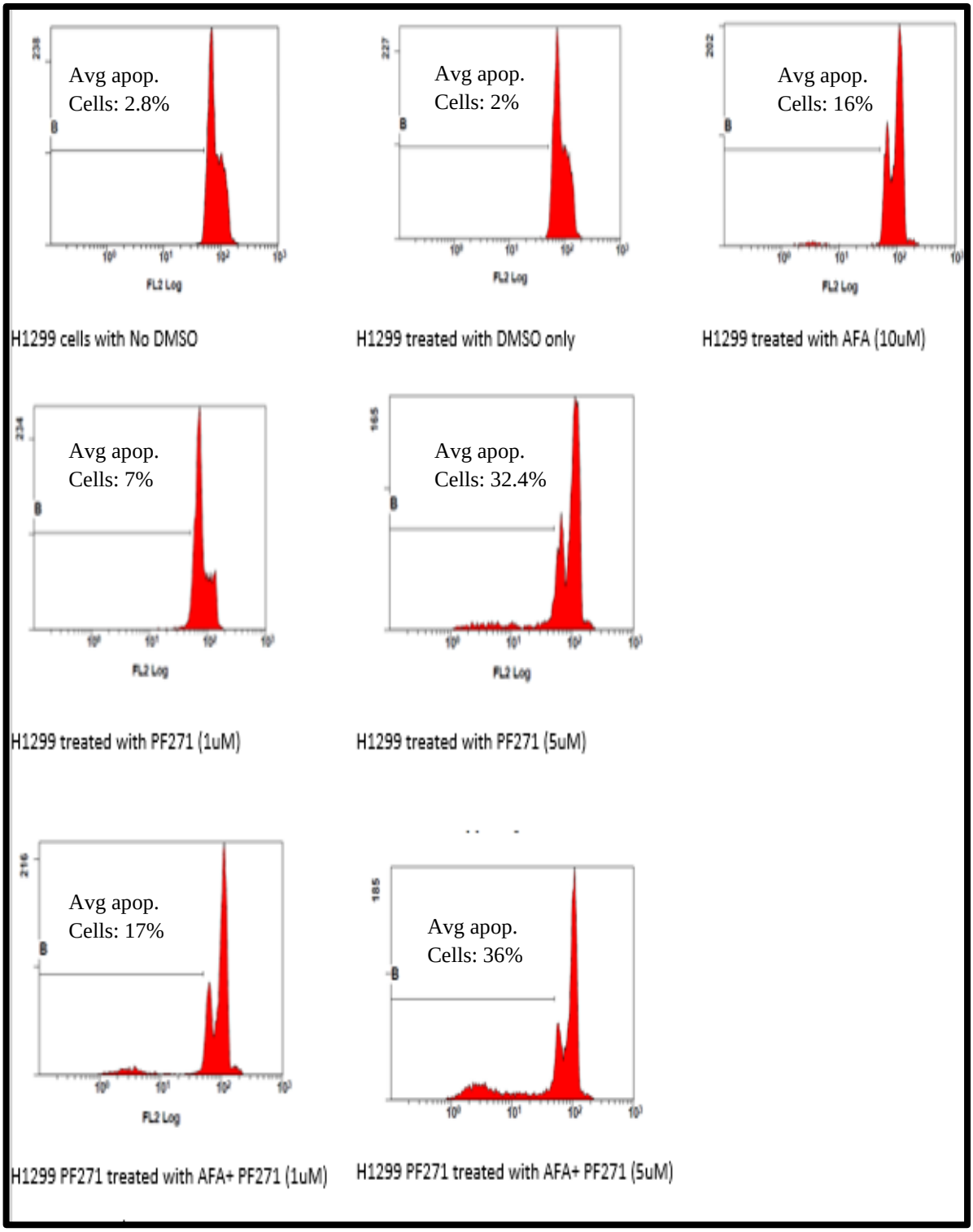
Avg apop.
Cells: 2.8%
FL2 Log
H1299 cells with No DMSO
Avg apop.
Cells: 2%
FL2 Log
H1299 treated with DMSO only
Avg apop.
Cells: 16%
FL2 Log
H1299 treated with AFA (10uM)
Avg apop.
Cells: 7%
FL2 Log
H1299 treated with PF271 (1uM)
Avg apop.
Cells: 32.4%
FL2 Log
H1299 treated with PF271 (5uM)
Avg apop.
Cells: 17%
FL2 Log
H1299 PF271 treated with AFA+ PF271 (1uM)
Avg apop.
Cells: 36%
H1299 PF271 treated with AFA+ PF271 (5uM)

Figure 11. Flow cytometric analysis of cell cycle parameters following treatment of NSCLC cells with EGFR and/or FAK-TKIs. Representative histograms of drug treated NSCLC cells harvested 24 hours post-drug treatment. A) KRAS mutant A549 or B) KRAS WT H1299. Cells were incubated for 24 hours in the presence of DMSO as a control, AFA, PF-271 (1 µM or 5 µM), or with the combination of both drugs. Cells were harvested, fixed, and stained with propidium iodide for analysis by flow cytometry. Apoptotic cells were gated as sub-G1 cells to the left of the G1 peak in each of the histograms. Average percentages of apoptotic cells were calculated from three independent biological replicates are shown.

A)

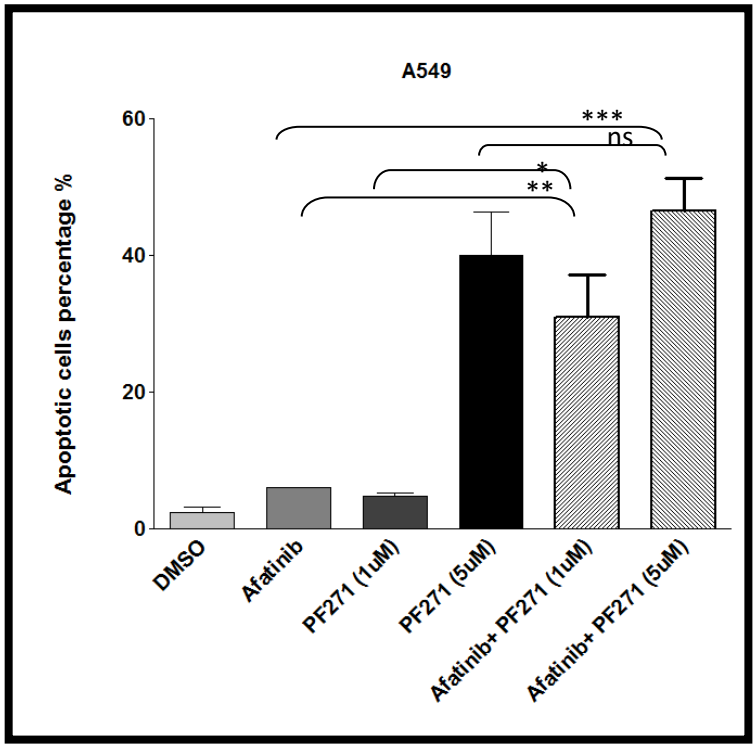
A549
Apoptotic cells percentage %
60
40
20
0
***
ns
*
**
DMSO
Afatinib
PF271 (1uM)
PF271 (5uM)
Afatinib+ PF271 (1uM)
Afatinib+ PF271 (5uM)

B)

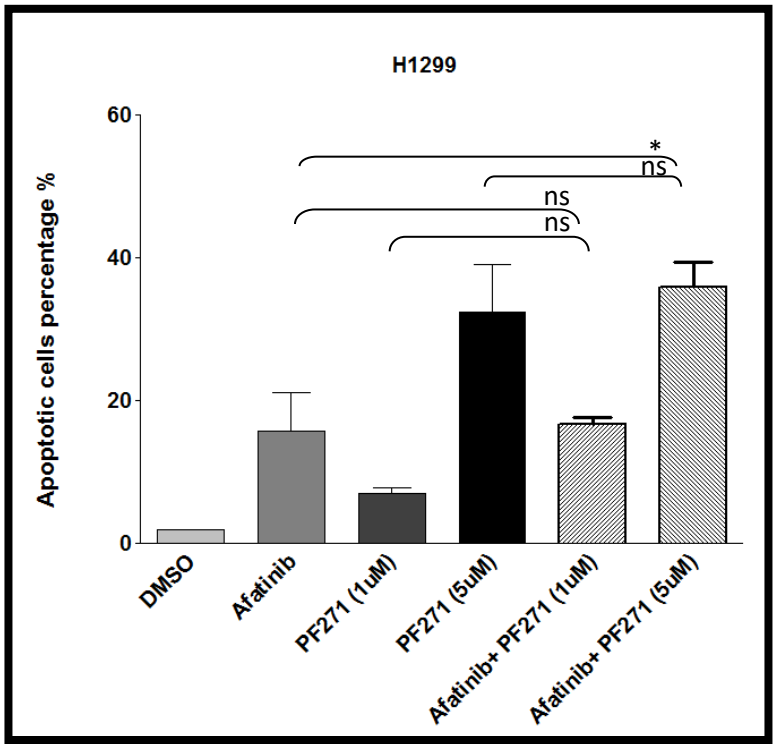
H1299
Apoptotic cells percentage %
60
40
20
0
*
ns
ns
ns
DMSO
Afatinib
PF271 (1uM)
PF271 (5uM)
Afatinib+ PF271 (1uM)
Afatinib+ PF271 (5uM)

Figure 12. Average percentage of apoptotic NSCLC cells of post treatment with AFA or PF-271 alone or in combination. The graphs represent the average percentage of apoptotic cells as determined by subG1 analysis of PI stained cells obtained from three replicates for A) KRAS mutant A549 and B) KRAS WT H1299. Cells were incubated for 24 hours in the presence of DMSO as a control, AFA, PF-271, or with the combination of both drugs. Cells were then harvested, fixed, permeabilized then stained with PI for analysis by flow cytometry. Apoptotic cells were gated in each of the histograms. The statistically significant differences were determined by ANOVA. Asterisks denote statistically significant differences (* = $p<0.05$, ** = $p<0.01$, *** = $p<0.001$). (ns) denotes statistically insignificant difference compared to single drug treated cells with most effect.

Furthermore, in KRAS mutant cells, it is noteworthy that, while the drug combination (PF-271 5 µM + AFA 10 µM) effect is significantly more effective than the single drug treatment AFA ($p<0.001$) at increasing apoptosis, the combination was not significantly more effective than the single drug treatment with 5 µM PF-271 in KRAS WT cells (Figure 12). Also, KRAS WT showed no significant difference in increased apoptosis when cells were treated with the combination of 10 µM AFA and 5 µM PF-271 compared to cells treated with the most effective single drug alone, in this case 5µM PF-271. Additionally, it was observed that in both of mutant and WT NSCLC cells the combination of two drugs resulted in a G2/M arrest as seen by increase in the number of cells in that peak.

3.2.3 Effect of FAK inhibition on EGFR recycling

As part of our study investigating the effects of drug treatment on various signaling pathways and on activity of the drug protein targets of interest, we also confirmed altered phosphorylation of FAK (via p-Y397) and EGFR (via p-Y1068) following drug treatment as a marker of drug efficacy. Preliminary data from the lab in A549 KRAS mutant cells showed a lack of response to EGF stimulation, as measured by autophosphorylation of EGFR (Y1068) (Figure 13). This suggests a possible lack of surface EGFR as has been previously shown in KRAS mutant colon cancer cells (68). However, in the presence of FAK-TKI, EGF-induced EGFR phosphorylation was also significantly enhanced, and this phosphorylation was effectively diminished by the addition of EGFR-TKI in combination. This suggests that in KRAS mutant cells, EGFR signaling is suppressed by active FAK, and that by blocking FAK the reactivation of EGFR signaling will occur, potentially promoting tumor cell growth and survival.

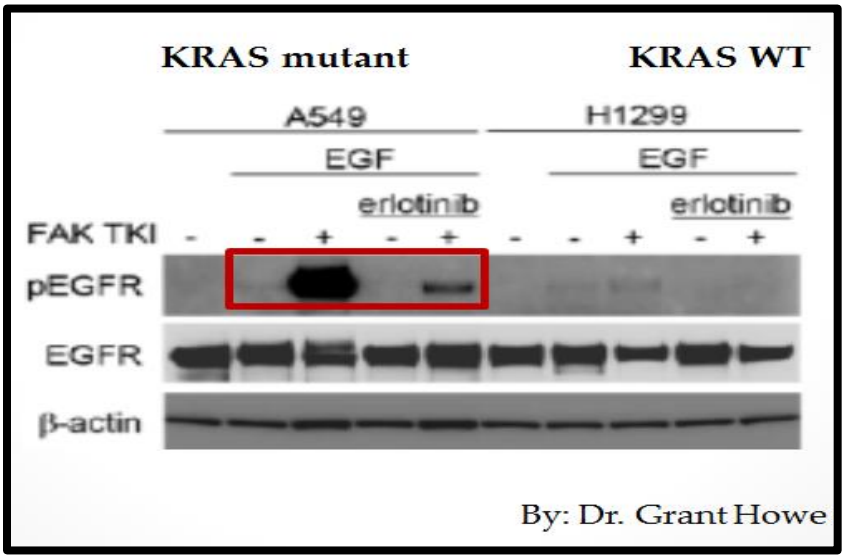

Figure 13. FAK-TKI treatment restores EGF-induced EGFR signaling in KRAS mutant but not KRAS WT NSCLC, which is subsequently blocked by EGFR-TKI. Mutant and WT KRAS NSCLC were serum starved overnight. The next day cells were treated with DMSO as a control, PF-271 (5 μM), EGFR TKI (ERL) (10 μM), or with both of PF-271 and ERL followed by 30 minutes EGF stimulation with 100 ng/mL EGF, as stated in the figure image. Total cellular protein was isolated, and phosphorylated and total EGFR were detected by western blotting. β-actin was used as loading control. Data presented is representative of results obtained from three independent experiments which were done by Dr. Grant Howe.

Thus, EGFR blockade is required to see more effective tumor inhibition. Moreover, when we serum starved and treated KRAS mutant NSCLC cells with PF-271 overnight we unexpectedly observed increased phosphorylation of EGFR at a high dosage of FAK-TKI (5 μM) in the absence of exogenous EGFR ligands (Figure 14). This increase in p-EGFR was not observed in KRAS WT cells (Figure 14). These findings also highlight unexpected signaling cross-regulation that is dependent on KRAS mutations. We speculated two possible reasons for the high expression of p-EGFR in the absence of ligand in KRAS mutant cells post PF-271 treatment.

First, we speculated that inhibiting FAK increases the expression of EGFR on the cell surface. It has been shown in KRAS mutant colorectal tumors that surface EGFR expression is down regulated and is a main factor impairing response to EGFR-TKIs drugs (68). It is also known that FAK signaling plays a role in vesicle trafficking, including endocytosis of integrin complexes (69). These two findings led us to hypothesize that FAK activation downstream of mutant KRAS induces EGFR endocytosis and blocks recycling, hence the impairing EGFR signaling (Figure 15 A & B).

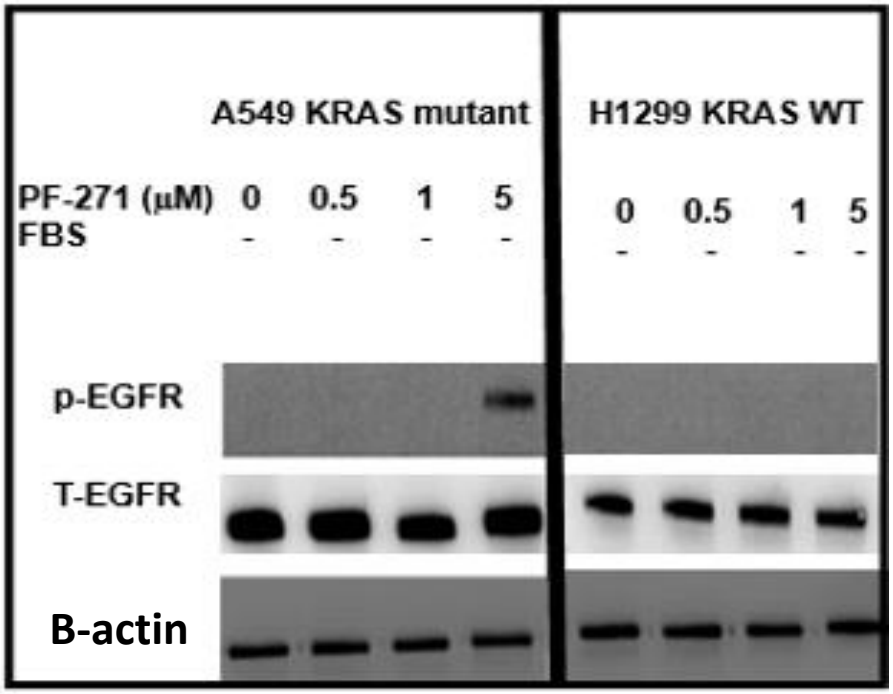

By: Zenab Moazin

Figure 14. Levels of p-EGFR are increased in KRAS mutant A549 but not KRAS WT H1299 following overnight treatment with different conctrations of PF-271. KRAS mutant A549 or WT H1299 cells were serum starved and were treated with different concentrations of PF-271 (0.5, 1, 5 μM) in the absence of serum overnight. The next day, total protein lysates were generated and levels of p-EGFR, total EGFR and β-actin were assessed by western blot analysis. Figure shown is a representation of three experimental replicates which were done by Zenab Moazin.

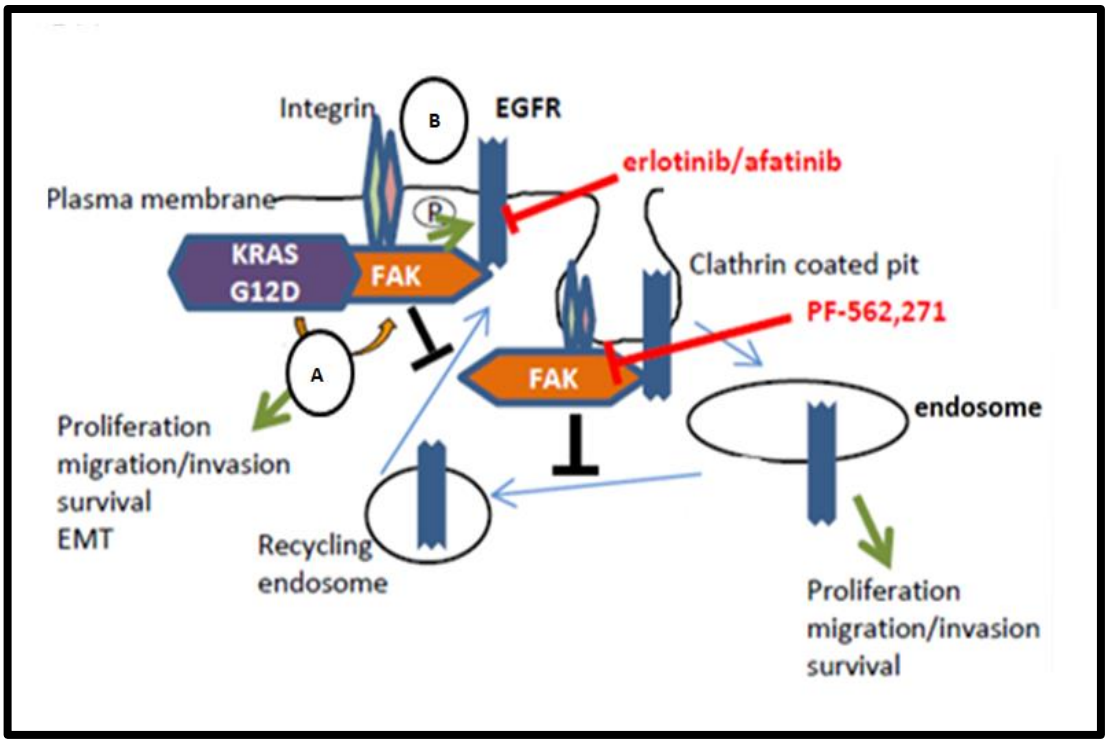

Figure 15. Schematic representation showing the putative mechanisms of FAK inhibition of EGFR signaling or trafficking. In KRAS mutant cells, FAK blockade may **(A)** alter KRAS induced inhibition of EGFR recycling or **(B)** prevent FAK-EGFR crosstalk and downstream signaling.

To address these possibilities, we investigated alterations in ligand induced EGFR internalization and recycling by measuring EGFR surface expression using FACS analysis of non-permeabilized cells. It has been previously shown in a study looking at EGFR through pulse-chase experiments that EGFR undergoes endocytosis within 15 minutes following stimulation with EGF and close to 100% of the receptor is recycled back to the surface within 2 hours (70). We therefore chose to analyze our samples by FACS at these two time points post stimulation with EGF. KRAS mutant A549 and KRAS WT H1299 cells were pre-treated with FAK-TKI or DMSO as a vehicle control. Cells were then stimulated with EGF ligand for 15 minutes or 2 hours prior to collection of cells (Figure 16 &17). Cells were then stained with an Alexa488-conjugated anti-EGFR antibody or with mouse IgG post-harvesting while keeping cells ice cold to prevent receptor internalization following antibody binding.

In Figures 16A and 17A, the control conditions are shown. The fluorescent histogram shows a shift to the right when incubated with anti-EGFR antibodies as compared to control antibodies. Cells treated with EGF and then stained with the anti-EGFR antibodies show a histogram shift to the left indicative of EGFR receptor being internalized following ligand binding. A shift back towards the right was expected when EGFR is back on the surface and subsequently stained with antibodies. In Figure 16B & 17B, when cells were treated with the FAK-TKI PF-271 in the absence of EGF ligand stimulation, EGFR stayed on surface of cells as evidenced by the lack of a histogram shift to the left.

A)

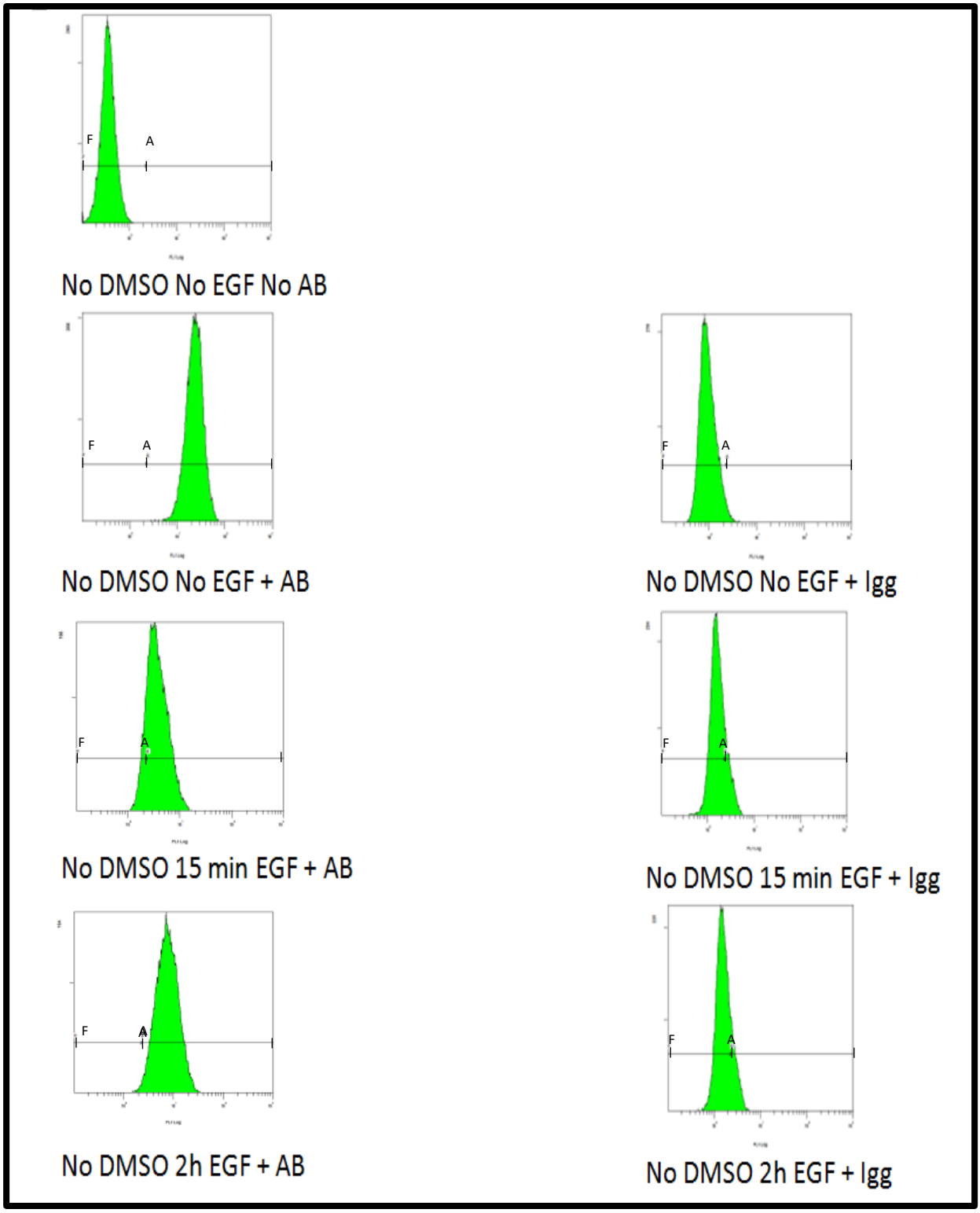
F
A
No DMSO No EGF No AB
No DMSO No EGF + AB
No DMSO No EGF + Igg
No DMSO 15 min EGF + AB
No DMSO 15 min EGF + Igg
No DMSO 2h EGF + AB
No DMSO 2h EGF + Igg

Sample	Average median histogram peak intensity		Average percent of cells with externalized EGFR - Bounded to antibody		Average percent of cells (including cells with internalized EGFR) -Unbounded to antibody	
	Mean	SE	Mean	SE	Mean	SE
No DMSO No EGF No AB	0.359	0.003	N/A	N/A	N/A	N/A
No DMSO No EGF + AB	21.45	0.855	99.27	0.3360	0.730	0.335
No DMSO No EGF + IgG	1.044	0.083	5.770	2.110	94.02	1.931
No DMSO 15 min EGF + AB	3.088	0.218	71.04	8.002	28.34	7.943
No DMSO 15 min EGF + IgG	1.210	0.182	9.608	4.387	90.12	21.58
No DMSO 2h EGF + AB	7.5	0.204	98.16	0.507	1.775	0.495
No DMSO 2h EGF + IgG	1.071	0.191	7.753	4.047	92.02	4.155

B)

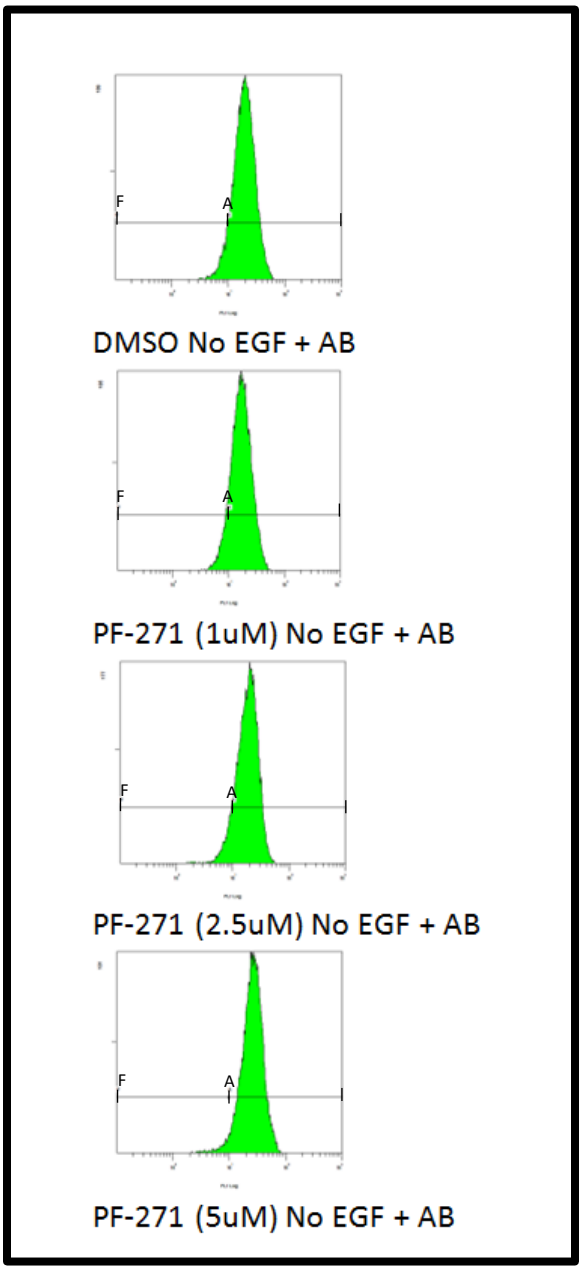
F
A
DMSO No EGF + AB
F
A
PF-271 (1uM) No EGF + AB
F
A
PF-271 (2.5uM) No EGF + AB
F
A
PF-271 (5uM) No EGF + AB

Sample	Average median histogram peak intensity		Average percent of cells with externalized EGFR - Bounded to antibody		Average percent of cells (including cells with internalized EGFR) -Unbounded to antibody	
	Mean	SE	Mean	SE	Mean	SE
DMSO No EGF + AB	20.45	0.819	90.97	0.479	9.123	0.536
PF-271 (1µM) No EGF + AB	17.1	0.314	85.11	3.276	15.05	3.155
PF-271 (2.5µM) No EGF + AB	17.85	0.698	85.00	3.507	15.08	3.365
PF-271 (5µM) No EGF + AB	21.60	2.517	87.71	6.945	12.24	6.748

C)

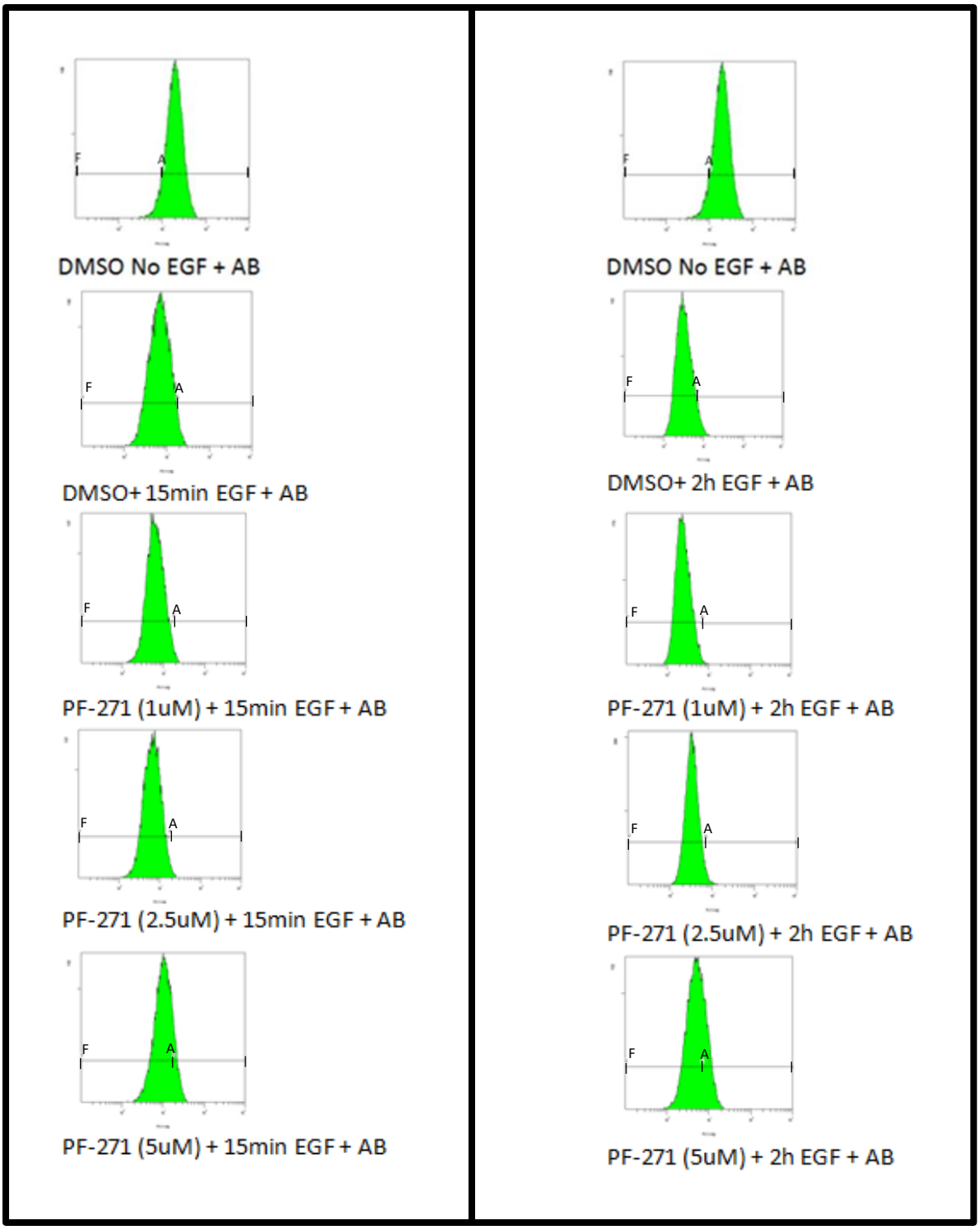
DMSO No EGF + AB
DMSO+ 15min EGF + AB
PF-271 (1uM) + 15min EGF + AB
PF-271 (2.5uM) + 15min EGF + AB
PF-271 (5uM) + 15min EGF + AB
DMSO No EGF + AB
DMSO+ 2h EGF + AB
PF-271 (1uM) + 2h EGF + AB
PF-271 (2.5uM) + 2h EGF + AB
PF-271 (5uM) + 2h EGF + AB

Sample	Average median histogram peak intensity		Average percent of cells with externalized EGFR - Bounded to antibody		Average percent of cells (including cells with internalized EGFR) -Unbounded to antibody	
	Mean	SE	Mean	SE	Mean	SE
DMSO No EGF + AB	20.45	0.819	90.97	0.479	9.123	0.536
DMSO 15min + AB	6.465	0.391	4.593	0.194	95.45	0.162
PF-271 (1µM) 15min + AB	6.100	0.188	3.543	1.194	96.44	1.295
PF-271 (2.5µM) 15min + AB	5.755	0.308	2.050	0.246	97.96	0.285
PF-271 (5µM) 15min + AB	8.005	1.476	10.78	3.034	89.42	2.876
DMSO 2h + AB	2.75	0.127	6.360	0.39	93.48	0.333
PF-271 (1µM) 2h + AB	2.898	0.315	8.373	2.922	91.33	3.098
PF-271 (2.5µM) 2h + AB	2.463	0.267	2.293	0.441	97.69	0.390
PF-271 (5µM) 2h + AB	4.615	0.925	32.92	10.39	66.72	10.66

Figure 16. EGFR surface expression analyses by fluorescence activated cell sorting (FACS) in mutant KRAS cell line A549. A549 mutant KRAS NSCLC cells were treated with DMSO as a vehicle control or with PF-271 (1, 2.5, 5 μM) overnight in a serum starved medium and were then EGF stimulated for 15 minutes or 2 hours before harvesting and staining with Alexa488-conjugated anti-EGFR antibody or IgG at a dilution of 1:50 while kept cold. A non-treated cell sample was used to gate the appropriate population of cells based on FSC/SSC. Gate A represents EGFR bounded to antibody on the cell surface and gate F represents EGFR not present on surface (unbounded to antibody). Histograms shown are a representation of two biological replicates with two experimental replicates each. The average median shift, average number of cells with EGFR on surface, and average number of cells with no surface EGFR bounded to antibody are all shown in tables under the respective histogram. A) Representative histograms for appropriate experimental controls. B) Representative histograms for A549 cells treated with FAK-TKI (PF-271) in the absence of EGF ligand. C) Representative histograms for A549 cells treated with FAK-TKI (PF-271) while being stimulated with EGF at two different time points: 15 minutes and 2 hours.

A)

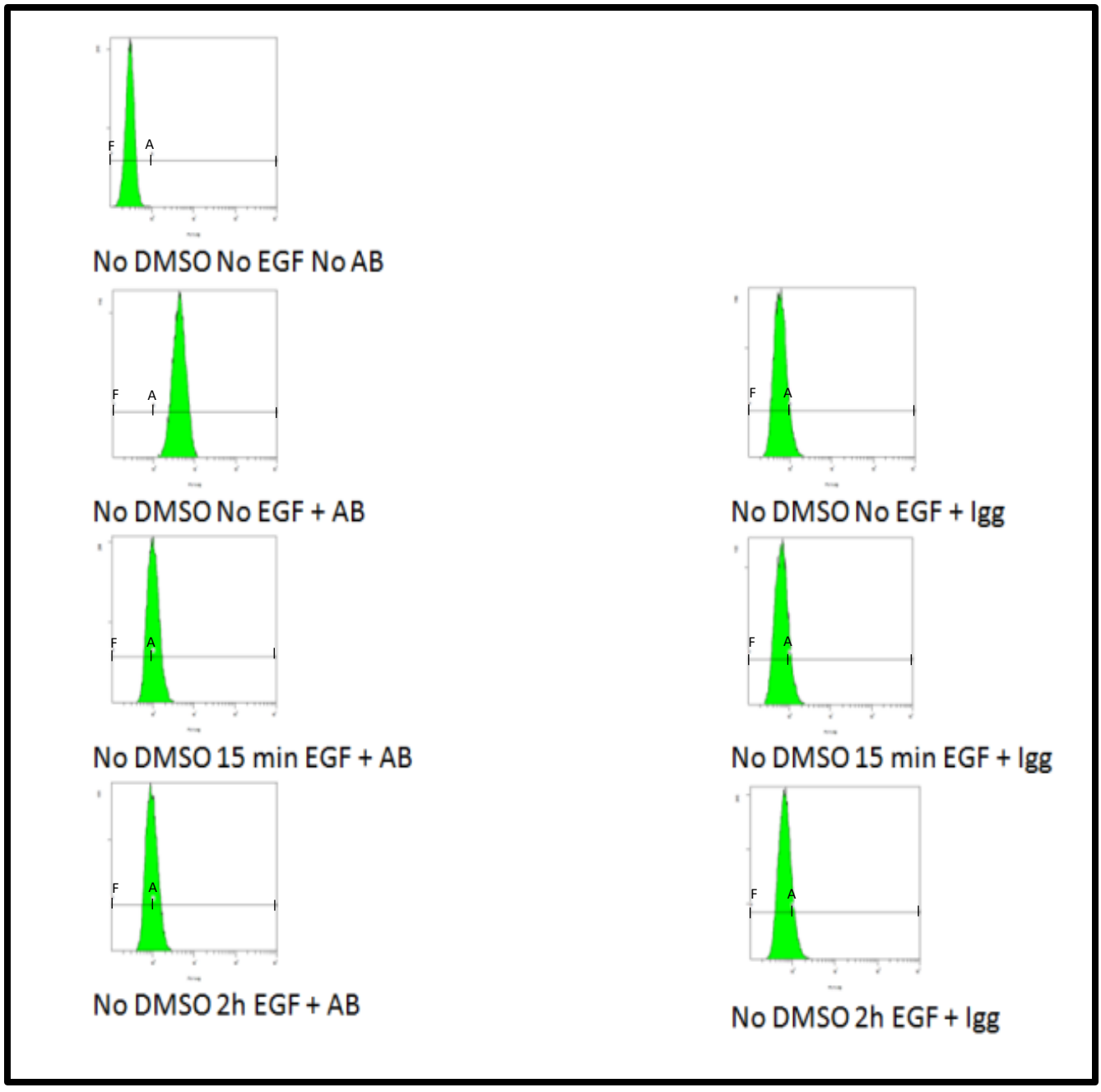
F
A
No DMSO No EGF No AB
No DMSO No EGF + AB
No DMSO No EGF + Igg
No DMSO 15 min EGF + AB
No DMSO 15 min EGF + Igg
No DMSO 2h EGF + AB
No DMSO 2h EGF + Igg

Sample	Average median histogram peak intensity		Average percent of cells with externalized EGFR - Bounded to antibody		Average percent of cells (including cells with internalized EGFR) -Unbounded to antibody	
	Mean	SE	Mean	SE	Mean	SE
No DMSO No EGF No AB	0.212	0.047	N/A	N/A	N/A	N/A
No DMSO No EGF + AB	3.492	0.455	99.55	0.303	0.525	0.373
No DMSO No EGF + IgG	0.472	0.109	12.29	4.045	88.41	4.042
No DMSO 15 min EGF + AB	0.977	0.107	76.72	6.861	25.01	6.640
No DMSO 15 min EGF + IgG	0.603	0.179	26.79	13.52	74.27	13.54
No DMSO 2h EGF + AB	0.892	0.078	64.40	9.965	37.52	9.540
No DMSO 2h EGF + IgG	0.462	0.101	10.04	2.441	90.63	2.513

B)

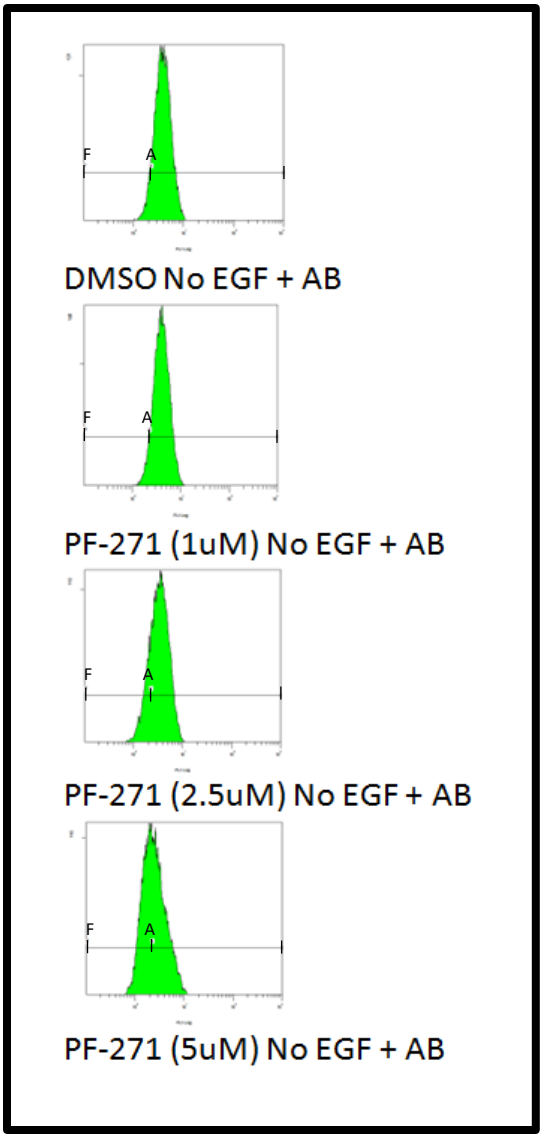
F
A
DMSO No EGF + AB
F
A
PF-271 (1uM) No EGF + AB
F
A
PF-271 (2.5uM) No EGF + AB
F
A
PF-271 (5uM) No EGF + AB

Sample	Average median histogram peak intensity		Average percent of cells with externalized EGFR - Bounded to antibody		Average percent of cells (including cells with internalized EGFR) -Unbounded to antibody	
	Mean	SE	Mean	SE	Mean	SE
DMSO No EGF + AB	3.537	0.138	93.47	0.447	6.573	0.579
PF-271 (1µM) No EGF + AB	3.375	0.310	90.31	2.852	9.585	2.684
PF-271 (2.5µM) No EGF + AB	2.496	0.340	67.09	7.981	32.88	7.714
PF-271 (5µM) No EGF + AB	1.689	0.267	37.26	8.565	62.83	8.253

C)

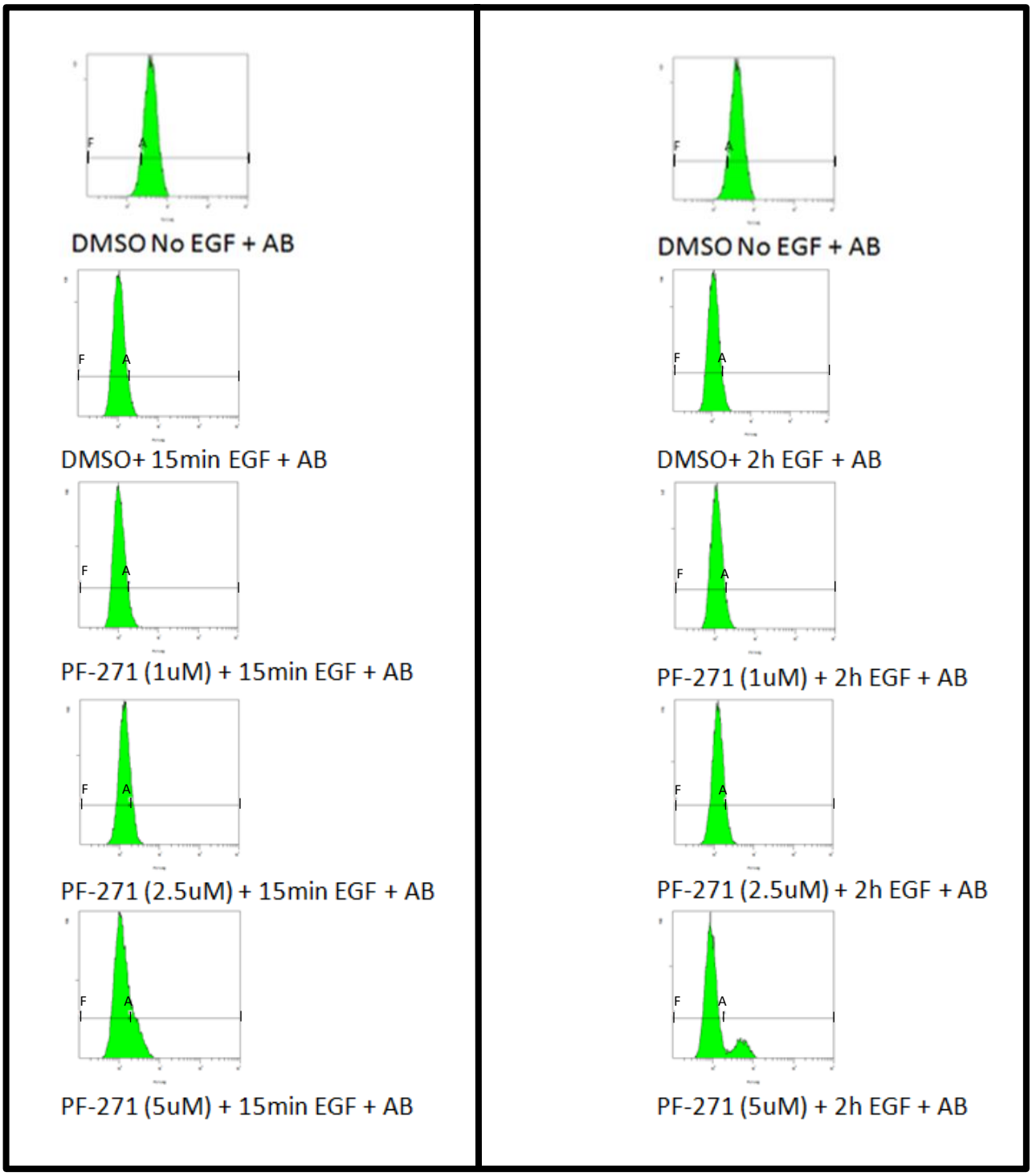
DMSO No EGF + AB
DMSO+ 15min EGF + AB
PF-271 (1uM) + 15min EGF + AB
PF-271 (2.5uM) + 15min EGF + AB
PF-271 (5uM) + 15min EGF + AB
DMSO No EGF + AB
DMSO+ 2h EGF + AB
PF-271 (1uM) + 2h EGF + AB
PF-271 (2.5uM) + 2h EGF + AB
PF-271 (5uM) + 2h EGF + AB

Sample	Average median histogram peak intensity		Average percent of cells with externalized EGFR - Bounded to antibody		Average percent of cells (including cells with internalized EGFR) -Unbounded to antibody	
	Mean	SE	Mean	SE	Mean	SE
DMSO No EGF + AB	3.537	0.138	93.47	0.447	6.573	0.579
DMSO 15min + AB	0.979	0.994	6.728	0.474	93.48	0.444
PF-271 (1µM) 15min + AB	1.011	0.859	6.953	1.260	93.23	1.395
PF-271 (2.5µM) 15min + AB	1.164	0.599	13.64	4.948	86.57	5.150
PF-271 (5µM) 15min + AB	0.956	0.695	12.5375	5.482	87.71	5.354
DMSO 2h + AB	0.871	0.355	5.985	0.423	93.48	0.523
PF-271 (1µM) 2h + AB	0.998	0.463	11.32	2.769	87.81	2.996
PF-271 (2.5µM) 2h + AB	1.172	0.649	21.73	11.60	77.16	11.98
PF-271 (5µM) 2h + AB	0.801	0.337	11.86	2.074	87.84	2.043

Figure 17. EGFR surface expression analyses by fluorescence activated cell sorting (FACS) in WT KRAS cell line H1299. H1299 WT KRAS NSCLC cells were treated with DMSO as a vehicle control or with PF-271 (1, 2.5, 5 μM) overnight in a serum starved medium. The cells were then EGF stimulated for 15 minutes or 2 hours before harvesting and staining with an Alexa488-conjugated anti-EGFR antibody or IgG at a dilution of 1:50 while kept cold. A non-treated cell sample was used to gate the appropriate population of cells based on FSC/SSC. Gate A represents EGFR bounded to antibody on the cell surface and gate F represents EGFR not present on surface (unbounded to antibody). Histograms shown are a representation of two biological replicates with two experimental replicates each. The average median shift, average number of cells with EGFR on surface, and average number of cells with no surface EGFR bounded to antibody are all shown in tables under the respective histogram. A) Representative histograms for appropriate experimental controls. B) Representative histograms for H1299 cells treated with FAK-TKI (PF-271) in the absence of EGF ligand. C) Representative histograms for H1299 cells treated with FAK-TKI (PF-271) while being stimulated with EGF at two different time points: 15 minutes and 2 hours.

In Figure 16C, as we hypothesized, treatment with increasing concentrations of FAK-TKI (1-5 µM) showed no significant effect on EGF-induced internalization of EGFR at 15 minutes post-stimulation. However, a noticeable 2-fold increase in surface EGFR at 2 hours post-stimulation with EGF was observed at the highest dose of PF-271 (5 µM) compared to control treated A549 cells (Figure 16C). Conversely, as shown in Figure 17C, KRAS WT cell line H1299 did not show any effect of PF-271 treatment on surface EGFR levels at either the 15 minutes or 2 hours time points at similar concentrations of PF-271.

To determine statistical significance, the median peak differences of samples treated with PF-271 (5 µM) was calculated and plotted (Figure 18). As expected, significant differences were confirmed between the median shift from the replicates of mutant KRAS A549 treated with higher concentration of PF-271 (5µM) post stimulation with EGF at 2 hours. There was no significant difference observed with PF-271 (5µM) stimulated with EGF ligands for 15 minutes (Figure 18A). No significant difference was confirmed between the median shift from the replicates of WT KRAS H1299 treated with higher concertation of PF-271 (5µM) post stimulation with EGF at 15 minutes or 2 hours (Figure 18B). This confirms that inhibiting FAK in KRAS mutant cells allows EGFR recycling to the surface which may allow its subsequent activation to facilitate tumor cell growth and survival. As such, this could be contributing to the increased sensitivity of those cells to EGFR-TKIs.

A)

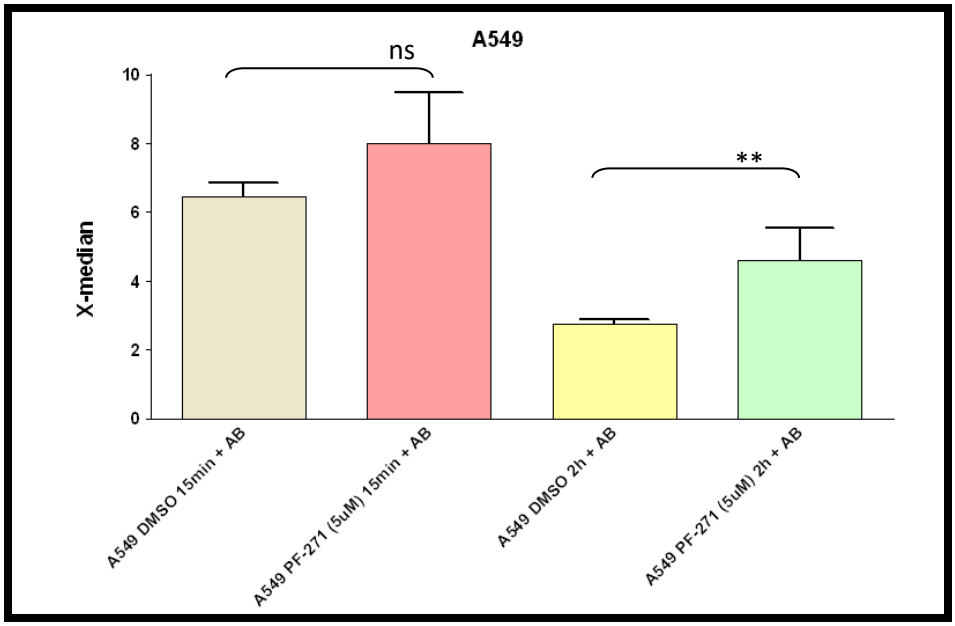
A549
ns
**
X-median
10
8
6
4
2
0
A549 DMSO 15min + AB
A549 PF-271 (5uM) 15min + AB
A549 DMSO 2h + AB
A549 PF-271 (5uM) 2h + AB

B)

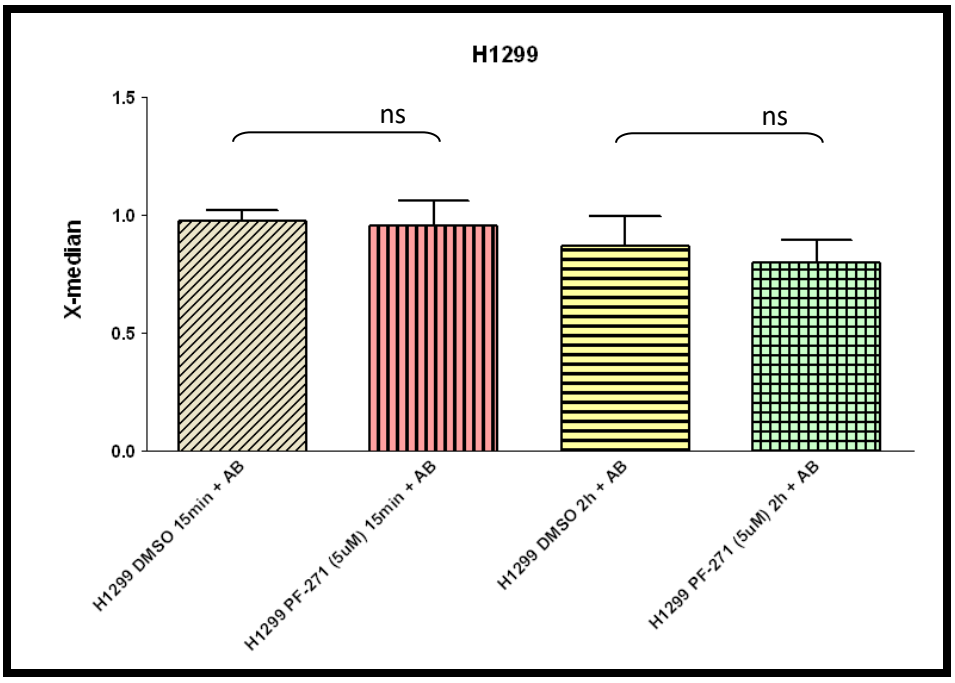
H1299
ns
ns
X-median
1.5
1.0
0.5
0.0
H1299 DMSO 15min + AB
H1299 PF-271 (5uM) 15min + AB
H1299 DMSO 2h + AB
H1299 PF-271 (5uM) 2h + AB

Figure 18. FAK-TKI treatment of KRAS mutant NSCLC increases cell surface EGFR post ligand stimulation. A) KRAS mutant A549 and B) KRAS WT H1299 NSCLC cells were assessed for EGFR surface expression by fluorescence activated cell sorting (FACS) using fluorescently-conjugated anti-EGFR extracellular domain recognizing antibodies. Cells were treated with DMSO as a vehicle control or PF-271 FAK-TKI overnight in a serum starved medium. This was followed by stimulation with EGF ligand for 15 minutes or 2 hours. Cells were then harvested with citric saline to maintain surface protein expression, and stained with an Alexa488-conjugated anti-EGFR antibody or IgG at a dilution of 1:50 and kept cold. The average median shift was derived from two biological replicates with two experimental replicates each. The statistically significant differences were determined by two tailed T-test. Asterisks denote statistically significant differences (** = $p<0.01$). (ns) denotes statistically insignificant difference compared to single drug treated cells with most effect.

While our data suggested that FAK-TKI treatment could alter EGFR receptor recycling in KRAS mutant cells, we also observed increased EGFR phosphorylation in serum free conditions following FAK-TKI treatment, suggesting the possibility that inhibiting FAK may increase the autocrine production of EGFR ligands by the cells.

In a review study, it was mentioned that EGFR signaling is activated following the matrix metalloproteinase-mediated (MMP) release of soluble EGFR ligands such as TGFα. TGFα binds EGFR and causes EGFR phosphorylation (71). Given previous studies (72) suggesting FAK regulates MMP9 expression, we speculated that the increased phosphorylation of EGFR following FAK drug treatment could be due to increased production or release of autocrine endogenous TGFα.

As such, using qRT-PCR we evaluated the message level of TGFα in KRAS mutant NSCLC (A549, A427, H460) and KRAS WT NSCLC (H1299, H1563, Calu3) cells 24 hours post serum starvation and treatment with increasing concentrations of PF-271 as compared to DMSO control (Figure 19A & B). In KRAS mutant A549, H460 and A427 NSCLC cells it was evident that FAK inhibition via PF-271 caused a significant increase in TGFα mRNA post treatment with 5 μM PF-271. On the other hand, as we expected, similar increases in TGFα mRNA levels were not observed in KRAS WT H1299 NSCLC cells. We looked at additional KRAS WT cell lines (H1563, Calu3) and we saw a trend of dose-dependent increase in TGFα mRNA level that did not reach a significant difference in H1563 but was significant in the Calu3 cell line post treatment with 5 μM PF-271 similar to what we observed in KRAS mutant cells. Moreover, we looked at other targets such as MMP9 which also showed increased

levels of expression post-treatment with PF-271 in both of KRAS mutant and WT NSCLC (Figure 19C).

To confirm the findings of elevated levels of mRNA, we also ran ELISA analysis of cell supernatant treated with FAK-TKI to assess levels of TGFα protein (Figure 20). We confirmed dosage dependent elevated TGFα protein following FAK-TKI treatment in A549 KRAS mutant cells. Unfortunately, attempts to detect TGFα protein in other cell lines failed as levels were below the threshold of detection of the ELISA assay. Despite this, together these findings suggest that the increased p-EGFR detected as a result of FAK-TKI treatment could be as a result of increased EGFR recycling to the cell surface in combination with increased production of autocrine EGFR ligands such as TGFα.

A)

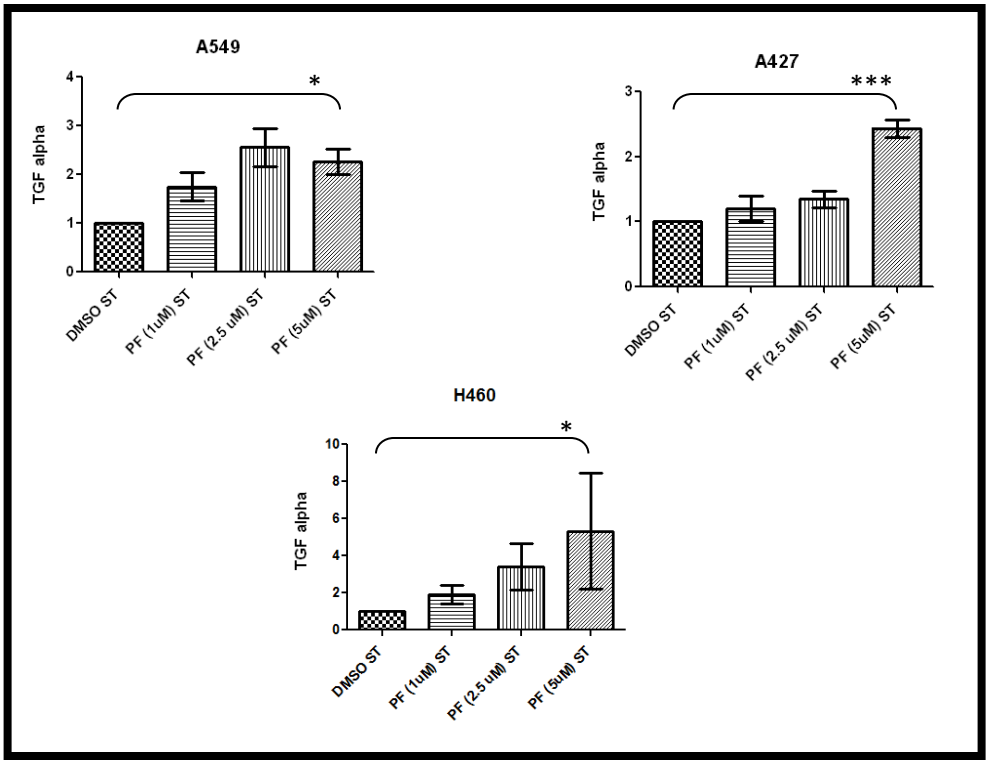
A549
*
TGF alpha
DMSO ST
PF (1uM) ST
PF (2.5 uM) ST
PF (5uM) ST
A427
***
H460
*

B)

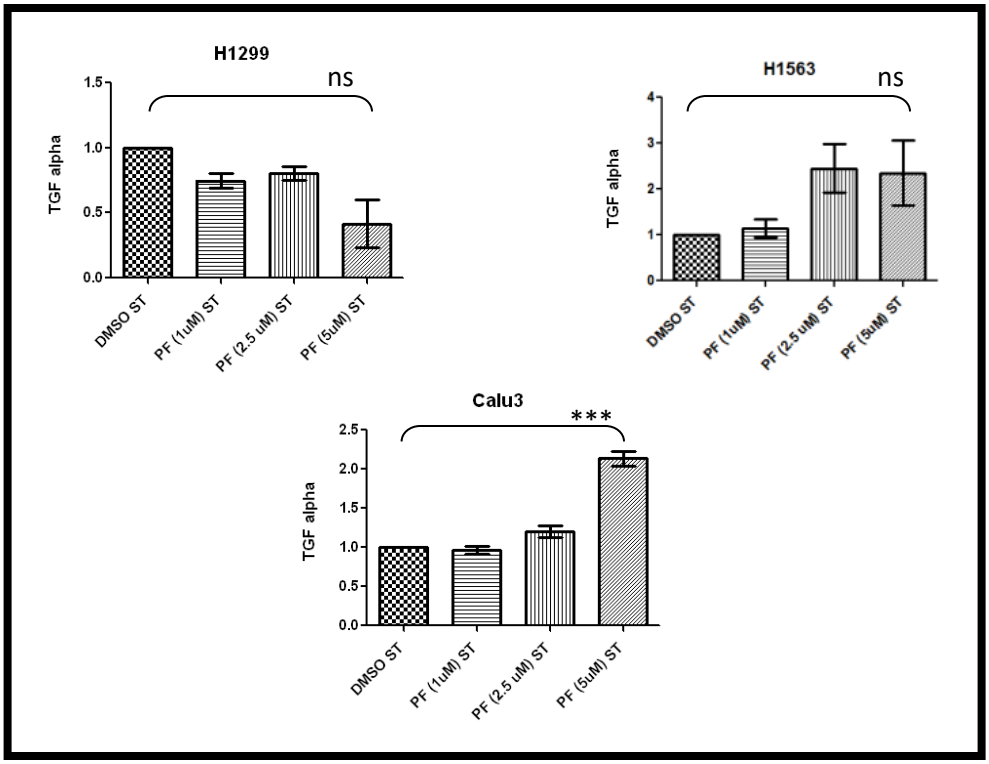
H1299
ns
TGF alpha
DMSO ST
PF (1uM) ST
PF (2.5 uM) ST
PF (5uM) ST
H1563
ns
Calu3
***

C)

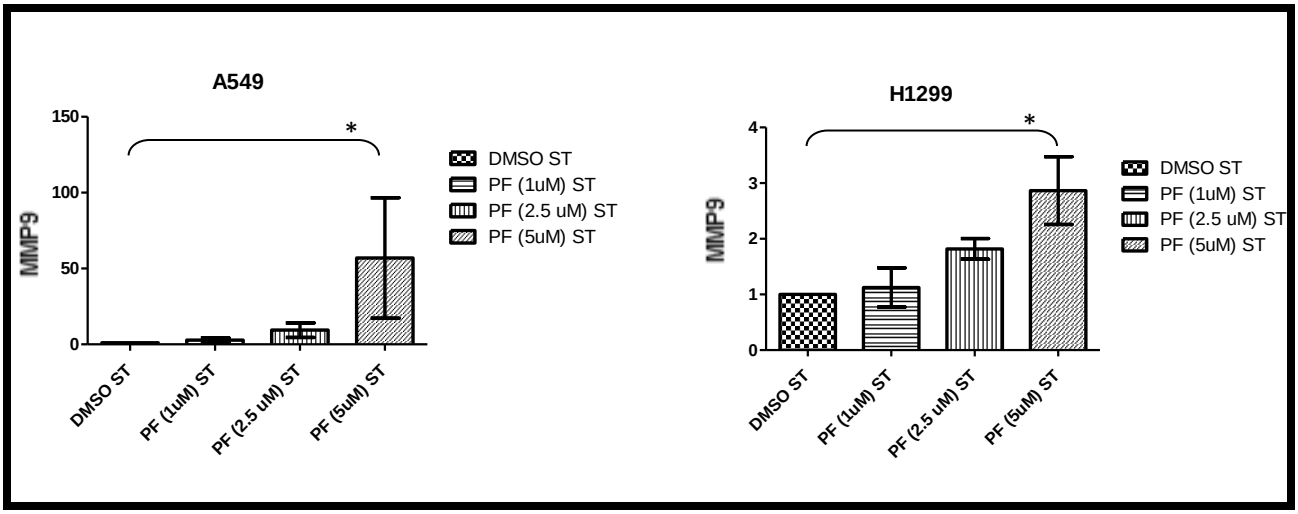

Figure 19. Assessment of TGFα and MMP-9 mRNA levels following treatment of KRAS mutant *vs* WT NSCLC cells with FAK-TKIs. Mutant and WT KRAS NSCLC were treated for 24 hours with DMSO as a vehicle control or with different concentrations of FAK-TKI in a serum staved medium. RNA was collected using RNeasy Mini Kit and cDNA synthesis was carried out using M-MLV RT reagent. The qRT-PCR was run in a 7500 FAST thermocycler and the reaction used was in the following steps: hold at 50°C for 20 seconds, then another hold at 95°C for 10 minutes, followed by 40 cycles of 95°C for 15 seconds and 60°C for 1 minute for each cycle. TGFα mRNA levels assessed A) KRAS mutant A549, H460, A427 NSCLC cells and B) WT KRAS H1299, H1563 and Calu3 NSCLC cells. C) KRAS mutant (A549) and KRAS WT (H1299) MMP9 mRNA levels. Analysis was performed with the Applied Biosciences Software version 2.3 designed specifically for the 7500 FAST machines. Relative expression was determined via ΔΔCt method whereby the amount of RNA in each sample was normalized to β-actin levels within that sample and was then compared to the levels of the control DMSO treated sample. All data is collected from three independent biological experiments. All statistically significant differences were determined by ANOVA. Asterisks denote statistically significant differences (* = $p<0.05$, ** = $p<0.01$, *** = $p<0.001$). (ns) denotes statistically insignificant difference compared to DMSO control.

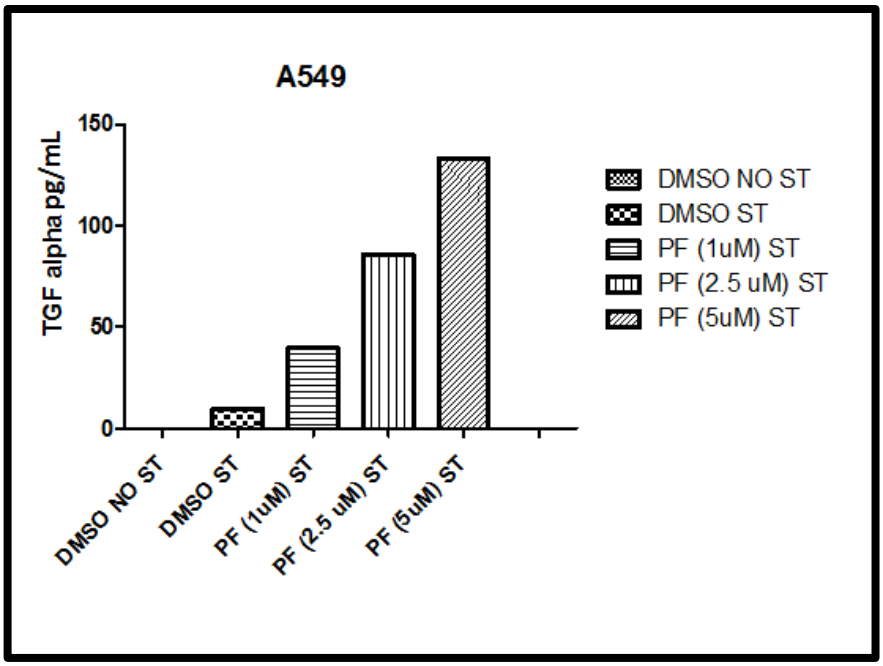

Figure 20. TGFα protein levels are elevated in A549 cells following treatment with FAK-TKIs. TGF-α levels (pg/mL) measured from A549 cell supernatant using Quantikine Elisa kit. Supernatant was collected from the KRAS mutant cell line A549 following serum starvation and treatment with DMSO as control, 1 µM, 2.5 µM, or 5 µM PF-271 for 24 hours. The presented data is an average of three biological replicates.

CHAPTER 4: DISCUSSION

Blocking the activity of EGFR has been a primary therapeutic target for NSCLC. Even though EGFR-TKIs have transformed treatment of NSCLC, most responses have not proved to be durable in many patients. Specifically, WT EGFR patients with KRAS mutant NSCLC show a reduced rate of survival post treatment with EGFR-TKIs as compared to KRAS WT patients (73,74). The acquired resistance to EGFR-TKIs puts a large number of patients in urgent need for additional therapeutic approaches for patients with WT EGFR. Thus, there is a demanding need for identifying other signalling pathways that can be additionally targeted.

Previous studies have shown that FAK is up-regulated in NSCLCs. Specifically, the data indicated a statistically significant correlation between FAK up-regulation and higher disease stages as well as aggression levels (75). This suggests that in addition to EGFR up-regulation, FAK up-regulation also contributes to lung cancer progression. Thus, dual blockade of FAK and EGFR may result in a more efficient cancer treatment. In support of this notion, it has been shown that dual inhibition of FAK and EGFR pathways cooperatively induces death receptor-mediated apoptosis in human breast cancer cells (76). More significantly, other studies have been investigating the enhanced tumor inhibition efficiency with the combination of FAK-TKIs and other existing therapeutic compounds such as the BCL-2/BCL-XL antagonist ABT-737, the multi-targeted receptor tyrosine kinase inhibitor Sunitinib and, most importantly, the EGFR-TKI Erlotinib (77, 78, 61).

A recent study performed by Dr. Addison's lab has provided evidence to demonstrate the effectiveness of combining the EGFR-TKI ERL and FAK-TKIs for use in known EGFR wild-type EGFR-TKI resistant cells (61). In NSCLC cells resistant to ERL, the addition of FAK-TKIs (PF-573,228 or PF-562,271) to ERL treatment inhibited tumor cell growth to a greater extent than either treatment alone, therefore indicating the contribution of FAK to EGFR-TKI resistance in NSCLC (61). In the study presented here however, a more clinically relevant irreversible EGFR-TKI, AFA, was used in combination with the FAK-TKI PF-271. Initial data from cell viability assays showed that the two cell lines, H4006 and H827, with a known EGFR mutation (a deletion in exon 19) that make them sensitive to EGFR-TKIs, are similarly sensitive to AFA as they are to ERL (Figure 3) (79). However, AFA seemed to be more potent than ERL in the two EGFR mutant cell lines. This could be an indicator that AFA in combination with FAK-TKIs could be a better potential combination therapy than ERL when combined with FAK-TKIs due to its potential increased potency as a single agent.

Furthermore, the IC_{50} values obtained from cell viability assays in mutant KRAS (A549, H460 and A427) compared to wild type KRAS (H1299, H1563 and Calu3) NSCLC cells following 48 hours treatment with AFA alone were all compared to each other's and to that of an NSCLC cell line that expressed a double mutated active EGFR as a control (H1975). (Figure 4, Table 1) For a patient with such a tumor profile, AFA would be the standard of care treatment (80). Our data confirmed, as previously seen, that KRAS mutant cells are slightly more resistant to AFA drug compared to KRAS WT cells (81). It has also been shown that mutant KRAS A549 is less sensitive than WT KRAS Calu3 and H1299 (81). On the other hand, the IC_{50} values we obtained from

cell viability assays 48 hours post-treatment with PF-271 show that KRAS mutant cells were more sensitive to FAK-TKI than KRAS wild-type NSCLC (Figure 5). This could mean that mutant KRAS cells are more dependent on FAK activity for tumor survival. If so, then this observation would be deemed novel as it has not been previously seen in the literature. However, a recent study showed that in mutant KRAS A549 there was an increased phosphorylation of FAK and FAK was implied to be a main player in A549 invasion (82). Their findings support our observation that mutant KRAS is dependent on FAK, which explains its sensitivity to FAK inhibition.

Our data also seems to confirm the results obtained from a study conducted on KRAS mutant and LKB1 mutant NSCLC; where LKB1 is a negative regulator of FAK (83). They were able to show that treatment of early, stage-matched tumors in KRAS and LKB1 mutant genetically engineered mouse models with a FAK-TKI monotherapy resulted in a striking inhibition of tumor progression, invasion, and tumor-associated collagen (83). They also showed that chronic treatment extended survival and hindered local lymph node spread. They also provided evidence to show that upregulated FAK and high levels of collagen caused collective invasion in KRAS and LKB1 co-mutated human lung adenocarcinoma patients; suggesting that patients with LKB1 mutant tumors should be treated with FAK-TKIs (83). The three mutant KRAS cell lines tested in our study (A549, H460, A427) also harbor a mutation in LKB1 (84). Altogether, this could mean that KRAS mutant cell lines are more dependent on FAK activity than KRAS WT. They would therefore be more likely to show effective tumor inhibition when exposed to EGFR and FAK-TKI combination treatment as compared to the KRAS WT due to this dependency on upregulated FAK.

Interestingly, in the recently published study from the Dr. Addison lab, LKB1 function was restored to WT A549 cells and were tested to see if restoring LKB1 would increase the sensitivity to the combination treatment of FAK and EGFR TKI (61). The data collected in the study, however, showed no increased sensitivity to the combination treatment. Thus, despite the data showed in the above study (83), while LKB1 may contribute to general FAK-TKI sensitivity, it is not responsible in KRAS mutant cell line for the increased sensitivity to the combination treatment of PF-271 and AFA.

The EGFR WT mutant KRAS cell lines A549, H460 and A427 cells, as predicted, seemed to be sensitive to the EGFR-TKI AFA when they were treated in combination with FAK-TKI PF-271 (Figure 6). WT KRAS cell lines H1299, H1563 and Calu3 seem to be affected by AFA alone, similar to the combination of both AFA and FAK-TKI. Moreover, our data suggests that treatment of NSCLC cells with AFA and FAK-TKI in combination also enhanced the growth reduction of mutant KRAS NSCLC cells in 3-dimensional assays (Figure 7). In WT KRAS, the combination treatment was as potent as AFA treatment on its own (Figure 8). Taken together, our data supports the notion whereby the addition of a FAK-TKI to existing treatment with AFA resulted in enhanced sensitivity in known AFA insensitive cells. Specifically, our results suggest that mutant – not WT – KRAS NSCLC, are more likely to show significantly enhanced effective tumor inhibition using this combination treatment. Moreover, the previous study conducted in Dr. Addison's lab (61) also shows that dual inhibition using ERL and FAK-TKIs seems to be more potent in KRAS mutant A549 vs KRAS WT H1299. Thus, the results obtained from this project, with AFA being the EGFR-TKI used instead of ERL, replicate the findings of the previous study. This

project however, presents the same behaviour observed from additional mutant and WT KRAS cell lines. This supports the notion that the observed sensitivity is indeed associated with the presence of KRAS mutations.

The reasons for this observed combination effect have not been previously studied. In addition to confirming that KRAS mutant NSCLC is more sensitive to drug combinations including an EGFR-TKI with a FAK-TKI, this project also investigated potential mechanisms of action. Our data suggests that the use of FAK-TKIs in combination with AFA inhibited mutant KRAS NSCLC tumor cell growth in both 2D and 3D. This was observed concomitant with an increased induction of apoptosis in combination treated cells (Figure 11). While more modest induction of apoptosis was observed in WT KRAS H1299 cells, apoptosis increased significantly in A549 cells treated with FAK-TKI and AFA combinations (Figure 12). This implies that the observed reductions in cell viability observed in 2D and 3D in KRAS mutant cells are due in part to increased cell death. It was noteworthy that both combination treated mutant and WT KRAS cell lines showed no significant difference when compared to cells treated with 5μM PF-271 alone. This could be explained by the fact that higher concentrations of PF-271 are associated with off target effect or that higher PF-271 concentrations has robust induction of apoptosis on its own, therefore making it difficult to get substantially more effect in combination (85).

Our data confirmed a previous study, where mutant KRAS cell line A549 does not show increased apoptosis post treatment with AFA on its own (86) (Figure 11). They also showed that similar results in H460, another mutant KRAS NSCLC. On the other hand, in the same study, they showed that AFA induces apoptosis in NSCLC

without EGFR mutations through the Elk-1/CIP2A/PP2A/Akt pathway. The apoptotic effect of AFA in sensitive cells was associated with down-regulation of CIP2A, promotion of PP2A activity and decrease in Akt phosphorylation. This finding also supports our observations regarding Akt phosphorylation; as both A549 and H460 cells lines do not see reduction in p-Akt with AFA drug treatment alone (Figure 10). However, the drug combination of FAK-TKI and AFA increased apoptosis and resulted in significant inhibition of p-Akt in A549 cells (Figure 10). This means that the co-treatment with both of FAK and EGFR-TKIs sensitized resistant A549 cells to AFA-induced apoptosis and p-Akt down-regulation. Similar effects on Akt phosphorylation have been observed following combination treatments of EGFR-TKI-resistant cell lines with AFA and forskolin, a cyclic AMP analog which has shown inhibitory effect of Akt phosphorylation (86, 87). Moreover, it has been shown before that integrin expression is linked to EGFR-TKI resistance in NSCLC cell lines that have reduced phosphorylation of ERK and Akt; therefore contributing to increased sensitivity to Gefitinib in cell lines depleted of β1-integrin (88). Previous evidence shows that integrin β1-FAK signaling directs the proliferation of metastatic lung cancer cells (89). FAK is also known to promote cell survival through enhancing the activity of Akt (49), and persistent Akt activation is associated with a lack of response to EGFR-TKIs (66) thus making regulation of Akt an important likely contributor to the decreased cell viability observed upon treatment with AFA and FAK-TKIs. Our data supports this concept, whereby the drug combination resulted in the most inhibition of cell viability and increased apoptosis concomitant with the highest reductions in Akt activity. This is an indicator that reduction of Akt activity may be a key in effective drug combinations for EGFR-

TKI-resistant cells (Figure 6, 10 & 11). To support the data presented in this project, another student in the Addison lab generated cell lines with differential KRAS status and tested the efficacy of drug combinations in this scenario. In this case, KRAS mutant A549 cells were transfected with a plasmid to allow overexpression of WT KRAS, and a plasmid encoding mutant KRAS (G12D, or G12C) was used to transfect H1299 WT KRAS cells. In addition to showing similar cell viability phenotypes with the drug combination, the phosphorylation of Akt post treatment with each of AFA and PF-271 alone or in combination was tested using western blots and is presented in Supplementary Figure 1. As predicted, the drug combination only significantly reduced p-Akt levels in cells in which mutant KRAS is expressed. Hence the 'reversal' of the cell phenotypes compared to the parental A549 and H1299 cell lines was observed (Supplementary Figure 1).

Activated FAK is also known to cross-talk with EGFR, and activates EGFR by FAK-Src complexes in a ligand independent manner (42, 43) (Figure 2). This activation plays a critical role in EGFR-induced cell growth and survival signaling (90). Therefore, we proposed that co-treatment with FAK and EGFR-TKIs is more effective than a single drug treatment because blocking the FAK-Src activation of EGFR somewhat sensitizes EGFR-TKI resistant cells to EGFR-TKI. Interestingly, a study showed that Src is activated in EGFR-TKI-resistant NSCLC with acquired T790M mutation, and dasatinib, a small molecule-inhibitor of Src-family protein-tyrosine kinases, together with EGFR-TKIs overcame drug resistance (91). Our data and proposed model would predict that a dasatinib and EGFR-TKIs combination would also reverse EGFR-TKI resistance in mutant KRAS NSCLC. This is predicted because

mutant KRAS cell lines show more FAK activation and dependence on FAK, so they are therefore more likely to be increasingly dependent on FAK-Src cross talk.

Another study demonstrated that AFA-resistant cells were more susceptible to the cytotoxic effects of dasatinib or Src knockdown; suggesting that SRC is a potent gene involved in the survival of AFA-resistant cells (92). In the same study, they showed that knockdown of Src inhibited the survival of AFA resistant sublines. It also showed that dasatinib inhibited cell growth and Akt phosphorylation more strongly in AFA resistant sublines than AFA sensitive cells; again suggesting that the survival of AFA resistant sublines is dependent on Src signaling (92). They also showed that blocking Src using dasatinib did not completely inhibit Akt phosphorylation in AFA resistant sublines. This suggests other unknown mechanisms of action, in addition to FAK-Src cross talk with EGFR, might be also involved in the cell survival of AFA resistant cell lines. Those studies and our study share a similar notion: that blocking Src sensitizes AFA resistant cells to AFA. Our study shows that inhibiting FAK would have the same effect. Thus, together those studies and our study promote the idea that FAK-Src complex interacts with EGFR and confers cell survival. Therefore, blocking either FAK or Src has a similar effect: sensitizing resistant cells to AFA.

Another different proposed mechanism of action that is possibly causing the resistance to EGFR-TKI compounds in KRAS mutant tumors is due to decreased EGFR activity. This is derived from the fact that, in colorectal tumors, KRAS mutations desensitize tumor cells not only to EGFR TKIs but also to the EGF ligand itself (68). The authors suggested this is in part due to reduced cell surface expression of EGFR. Interestingly, when we treated serum starved KRAS mutant cells with 5 μM FAK-TKI

we saw increased phosphorylation of EGFR, which was not observed in KRAS WT (Figure 14). To our knowledge, we are the first group to identify the upregulation of EGFR phosphorylation by FAK-TKIs. Given that our data suggested that FAK may block EGFR signaling in KRAS mutant but not in KRAS WT cells (Figure 13), and the work in colon cancer that suggested KRAS mutation blocks EGFR surface expression (68), we speculated that perhaps EGFR trafficking is affected by FAK in this context. This was also supported by the fact that FAK is known to regulate vesicle trafficking and receptor endocytosis (69). We therefore hypothesized that FAK activation, downstream of mutant KRAS, induces EGFR endocytosis and blocks recycling; thereby impairing EGFR signaling in mutant KRAS cells.

This idea was tested post-treatment with FAK-TKI in mutant and WT KRAS cell lines using flow cytometry. We were able to show that, after 2 hours in EGF-treated KRAS mutant cells (A549), EGFR levels increase on the cell surface following treatment with higher doses of FAK-TKI (Figure 16 & 18A). This behaviour was not significantly observed in WT KRAS cell line H1299 (Figure 17 & 18B). Interestingly, in Figure 17C the sample treated with 5μM of PF-271 and EGF stimulated for 2h show a second small population shifted to the right. This could be due to the fact that a higher drug concentration caused cells to burst allowing the EGFR antibody to break in and bind to internalized and surface EGFR.

Importantly, the obtained EGFR surface staining data following FAK inhibition is consistent with the notion of FAK as an important mediator of tumorigenesis in KRAS mutant NSCLC, suggests it may modulate EGFR endocytosis and disrupt receptor recycling in KRAS mutant settings. This data also supports the notion that

FAK-TKIs need to be used in combination with EGFR-TKIs in KRAS mutant NSCLC in order to overcome the 'reactivation' of EGFR signaling that is induced by FAK blockade.

The restored EGFR on the surface of mutant KRAS cells as a proposed explanation for the increased EGFR phosphorylation post-treatment with FAK-TKI in serum starved conditions was accompanied by a second proposed cause of action. A study conducted on A549 mutant KRAS NSCLC showed that gene expression of TGFA was significantly higher in tumor tissues as compared to adjacent normal tissue and high TGFA gene expression strongly correlated with poor survival in patients with lung adenocarcinoma (93). Additionally, they showed that treating A549 cells with TGF-α neutralizing antibody resulted in the suppression of cell proliferation and invasion (93). Therefore, we hypothesised that the results from our lab, shown in Figure 14, could be also due to the fact that inhibiting FAK allows an autocrine production of EGFR ligands in mutant KRAS which would, in turn, phosphorylate EGFR on the surface. Our data suggesting that EGFR phosphorylation is increased following treatment with FAK-TKI, in the absence of serum or exogenous ligands, supports the notion that the activation of EGFR is due to endogenous production or release of EGFR ligands. We focused our analysis on TGF-α as opposed to other EGFR ligands due to the previously reported effects on cell growth, as discussed above. However, it is also highly possible that other EGFR ligands could be modulated following treatment with FAK-TKI, and these additional ligands should also be investigated in future studies.

We tested this hypothesized mechanism of action using real time PCR and we were able to confirm in a mutant KRAS cell line (A549) that FAK inhibition caused a

dose-dependent increase in TGFα mRNA (Figure 19). Similar increases in TGFα mRNA levels were not observed in the control KRAS WT cell line (H1299) (Figure 19). This is consistent with our preliminary data where inhibiting FAK caused phosphorylation of EGFR in the absence of exogenous EGFR ligands in A549 but not in H1299 (Figure 14). Additionally, we looked at the mRNA levels of additional cell lines to see if they held the trend of KRAS mutant *vs* WT. This is despite the fact we did not test if FAK inhibition would cause increase in EGFR phosphorylation in these cells lines. Similarly to A549, other mutant KRAS cell lines (A427 and H460) seem to show significant increases in TGFα mRNA levels. The levels at least doubled post-treatment with FAK-TKI as compared to the control samples. Additional WT KRAS cell lines (H1563 and Calu3) show a similar trend to that observed in the mutant KRAS cell lines, particularly at high doses of PF-271 (5 μM). This data does not match the observed data we saw in H1299. However, we cannot make any conclusions based on these observations alone as not all mRNA get translated into protein. We speculate that these factors are possibly regulated by FAK at the transcriptional level. FAK has now been shown to traffic to the nucleus where it may influence transcription via mechanisms involving regulation of p53 activity (94). It has also been shown that FAK-TKIs such as PF-271 can induce FAK accumulation in the nucleus promoting its nuclear role (95). It has also been shown that, in primary human cells, FAK knockdown raised p53-p21 levels and slowed cell proliferation (96). Thus, nuclear FAK can regulate cell proliferation and survival by facilitating p53 turnover as nuclear-localized FAK contributes to chromatin remodeling and gene expression (97). It was also shown that p53 increases transcriptional activity of the TGF-α promoter by approximately 2.5-fold

(98). Furthermore, H1563 is a carrier for an INK4 mutation (99); a gene that coordinates a signalling network that depends on the activities of the retinoblastoma protein (RB) and the p53 transcription factor. Therefore, it is possible that inhibiting FAK restores the activity of p53 which increases TGFα production and thus promotes survival. Finally, in order to prove that up-regulation of TGF-α following treatment with FAK-TKI is responsible for the increased phosphorylation in EGFR we observed, we attempted to look at the protein level using an ELISA kit (Figure 20). However, we were only able to validate TGF-α increases at the protein level following treatment with FAK-TKI in one cell line, A549. This does not mean that the effect of FAK-TKI on TGF-α does not happen in other cell lines. It could simply mean that, the protein levels of other cell lines TGF-α were undetectable as they were below the threshold of sensitivity of the available assays systems. Future work could evaluate this by using a neutralizing anti-TGF-α antibody in mutant KRAS cells preceding treatment with FAK-TKI and then look at the phosphorylation of EGFR in serum starved conditions similar to the method used in (Figure 13) to confirm a role for TGF-α in this context. In such an experiment, we expect mutant KRAS NSCLC not to show FAK-TKI induced EGFR phosphorylation.

EGFR could also be phosphorylated post-binding to different ligands other than TGF-α such as: epidermal growth factor (EGF), heparin-binding EGF-like growth factor (HBEGF), amphiregulin (AREG), betacellulin (BTC), epiregulin (EREG), and epigen (EPGN). Therefore, using different primers and real time PCR to measure the expression levels of these other EGFR ligands post treatment with FAK-TKI will allow us to gain more perspective on the hypothesised theory of increased autocrine

production of EGFR ligands after treatment with FAK-TKI in mutant KRAS NSCLC as well as narrow down the scope of those to be confirmed at the protein level.

These two proposed mechanisms could be both contributing to the high expression of p-EGFR in the absence of ligand in KRAS mutant cells following inhibition of FAK with PF-271. More specifically, flow cytometry data in mutant KRAS A549 cells showed increased surface levels of EGFR post treatment with FAK-TKI. However, similarly treated WT KRAS H1299 cells did not show similar results. Also, the FAK-TKI dose dependent increase in mRNA expression of TGF-α was evident in mutant KRAS but not in WT KRAS. All together, we could conclude that the two proposed mechanisms possibly go hand in hand when contributing to the high expression of p-EGFR in the absence of ligand in KRAS mutant cells following inhibition of FAK with PF-271. As a whole, our results suggest that the co-treatment with both a FAK-TKI (PF-271) and a EGFR-TKI (AFA) is a very promising effective combination treatment specifically in mutant KRAS mutant NSCLC cells. Our findings that suggest that the use of FAK-TKIs as single agents in KRAS mutant NSCLC patients may result in re-activation of EGFR signaling, and that the blockade of EGFR is required in combination with FAK-TKIs for optimal therapeutic activity, is novel. In fact, a phase II study using the FAK-TKI defactinib (VS-6063) in KRAS mutant patients was conducted. The study results are still not published to date, and a subsequent Phase III has not been initiated. This suggests that defactinib may not have shown sufficient efficacy as single agent in this study, the reasons for which could be explained with the findings from our study (100).

Our study has also identified and tested unique and previously unrecognized potential mechanisms of action for this unexpected effect of FAK-TKI treatment's enhanced efficacy when used in combination with EGFR-TKIs. It would be of great interest to test tumor tissue from NSCLC patients treated with a FAK-TKI for levels of p-EGFR or TGF-α expression. This would confirm if our putative mechanisms are relevant in NSCLC patients. Finally, it would be important to test the efficacy of the combination treatment using in vivo xenograft models of NSCLC; which would then form the foundation for future clinical trials testing this combination in patients if found to be effective in preclinical models.

REFRENCES

1- Hoffman PC, Mauer AM, Vokes EE (2000) Lung cancer. Lancet 355: 479–485.

2- GLOBOCAN. (2012) Cancer incidence, mortality and prevalence worldwide Retrieved December 19, 2017from http://www-dep.iarc.fr/

3- Howlader NNA, Krapcho M et al.(2013) SEER Cancer Statistics Review, 1975–2010. Bethesda, MD: National Cancer Institute. Retrieved December 19, 2017 from http://seer.cancer.gov/

4- Thomas A, Chen Y, Yu T et al. (2015) Trends and characteristics of young non-small cell lung cancer patients in the United States. Front Oncol 5: 113.

5- Ferlay J, Shin HR, Bray F, Forman D, Mathers C, Parkin DM (2010) Estimates of worldwide burden of cancer in 2008: GLOBOCAN 2008. Int J Cancer 127: 2893–2917.

6- Lung Cancer (2017) Lung Cancer Canada, Retrieved December 19, 2017 from www.lungcancercanada.ca/lung-cancer.aspx.

7- Ozlu T, Bulbul Y: (2005) Smoking and lung cancer. Tuberk Toraks 53:200-209.

8- Canadian Cancer Society's Advisory Committee on Cancer Statistics. (2017). Canadian Cancer Statistics 2017. Toronto, ON: Canadian Cancer Society

9- Riihimaki M, Hemminki A, Fallah M, et al. (2014) Metastatic sites and survival in lung cancer. Lung Cancer ; 86: 78–84.

10- Tamura, T., Kurishima, K., Nakazawa, et all. (2015). Specific organ metastases and survival in metastatic non-small-cell lung cancer. Molecular and Clinical Oncology, 3, 217–221.

11- Zarogoulidis K, Zarogoulidis P, Darwiche K, et al. (2015) Treatment of non-small cell lung cancer (NSCLC). J Thorac Dis,5 Suppl 4:S 389–S96.

12- Riely GJ, Marks J, Pao W (2009): KRAS mutations in non-small cell lung cancer. Proc Am ThoracSoc, 6: 201–205.

13- Wieduwilt MJ, Moasser MM(2008). The epidermal growth factor receptor family: Biology driving targeted therapeutics. Cell Mol Life Sci, 65:1566–1584.

14- Dutta PR, Maity A: (2007). Cellular responses to EGFR inhibitors and their relevance to cancer therapy. Cancer Lett, 8;254(2):165-77.

15- Downward J, Parker P, Waterfield MD (1984). "Autophosphorylation sites on the epidermal growth factor receptor". Nature, 311 (5985): 483–5.

16- Scaltriti M, Baselga J Clin; (2006) The epidermal growth factor receptor pathway: a model for targeted therapy. Cancer , 12(18):5268-72.

17- Bethune G, Bethune D, Ridgway N, et al (2010). Epidermal growth factor receptor (EGFR) in lung cancer: an overview and update. J Thorac Dis. 2(1):48-51

18- Perez-Soler R (2004) The role of erlotinib (Tarceva, OSI 774) in the treatment of non-small cell lung cancer. Clin Cancer Res, 10:4238

19- Fukuoka M, Yano S, Giaccone G, et al. (2003) Multi-institutional randomized phase II trial of gefitinib for previously treated patients with advanced non-small-cell lung cancer. J Clin Oncol, 21:2237-2246

20- Chan BA, Hughes BG. (2015) Targeted therapy for non-small cell lung cancer: current standards and the promise of the future. Transl Lung Cancer Res,4(1):36–54.

21- Shepherd F.A., Rodrigues Pereira J., Ciuleanu T., et al. (2005) Erlotinib in previously treated non-small-cell lung cancer. N Engl J Med, 353: 123–13

22- Bareschino M, Casaluce F, Ciardiello F, et al: (2012) The role of EGFR tyrosine kinase inhibitors in the first-line treatment of advanced non small cell lung cancer patients harboring EGFR mutation, Curr. Med. Chem. 19(20): 3337-3352

23- Zhou F, Chen X, Zhou C (2014) Epidermal growth factor receptor–tyrosine kinase inhibitors in lung cancer patients with EGFR wild-type tumors: When there is a target, there is a targeted drug. J ClinOncol, 10.57.5449.

24- Yun, C.H. et al. (2008) The T790M mutation in EGFR kinase causes drug resistance by increasing the affinity for ATP. Proc. Natl Acad. Sci. USA 105, 2070–2075

25- Cobo M, Felip E, Goker et al: (2015) Afatinib vs. erlotinib as second-line treatment of patients with advanced squamous cell carcinoma of the lung (LUX-

Lung 8): An open-label randomised controlled phase 3 trial. Lancet Oncol. 16, 897–907.

26- J. R. Gomes and M. R. S. Cruz(2015) "Combination of afatinib with cetuximab in patients with EGFR-mutant non-small-cell lung cancer resistant to EGFR inhibitors," OncoTargets and Therapy, vol. 8, pp. 1137–1142

27- Morgillo F, Corte CMD, Fasano M, et al. (2016) Mechanisms of resistance to EGFR-targeted drugs: lung cancer. ESMO.

28- Zou Y, Ling YH, Sironi J, Schwartz EL, et al. (2013) The autophagy inhibitor chloroquine overcomes the innate resistance of wild-type EGFR non-small-cell lung cancer cells to erlotinib. J Thorac Oncol, 8: 693-702.

29- Ellis CA, Clark G: (2000) The importance of being K-Ras. Cell Signal, 12:425-34

30- Olson MF, Marais R: (2000) Ras protein signalling. SeminImmunol 12:63-73.

31- D'Arcangelo M, Cappuzzo, F. (2012) K-ras mutations in Non-Small-Cell Lung Cancer: Prognostic and Predictive Value. ISRN Molecular Biology,837306.

32- L. Bos, (1989). Ras oncogenes in human cancer: a review,Cancer Research, 49: 4682–4689.

33- G. J. Riely, M. G. Kris, J. L. Marks et al. (2008) Frequency and distinctive spectrum of KRAS mutations in never smokers with lung adenocarcinoma, Journal of Clinical Oncology, vol. 26

34- Reinersman JM, Johnson ML, Riely GJ, et al: (2011) Frequency of EGFR and KRAS mutations in lung adenocarcinomas in African Americans. J ThoracOncol 6:28-31

35- Ledford H. (2015). Cancer: the Ras renaissance. Nature, 520: 278-280.

36- Vo U., Vajpai N., Flavell L., et al. (2016). Monitoring Ras interactions with the nucleotide exchange factor son of Sevenless (Sos) using site-specific NMR reporter signals and intrinsic fluorescence. J. Biol. Chem. 291: 1703–1718.

37- Konstantinidou G, Ramadori G, Torti F, et al: (2013) RHOA-FAK is a required signaling axis for the maintenance of KRAS-driven lung adenocarcinomas. Cancer Discov, 3:444-57

38- Heasman SJ, Ridley AJ: (2008) Mammalian Rho GTPases: new insights into their functions from in vivo studies. Nat Rev Mol Cell Biol, 9:690-701.

39- Zent R., Pozzi A: (2009) Cell-extracellular matrix interactions in cancer,Springer.

40- McMillin DW, Negri JM, Mitsiades CS: (2013) The role of tumour-stromal interactions in modifying drug response: challenges and opportunities. Nat Rev Drug Discov. 12:217-28

41- Schlaepfer DD, Hauck CR, Sieg DJ: (1999) Signaling through focal adhesion kinase. ProgBiophysMolBiol, 71:435-78

42- Tomar A, Schlaepfer DD: (2010) A PAK-activated linker for EGFR and FAK. Dev Cell, 18(2):170–172

43- Cabodi S, Moro L, Bergatto E, et al: (2004) Integrin regulation of epidermal growth factor (EGF) receptor and of EGF-dependent responses. BiochemSoc Trans 32:438-42.

44- Weiwen Long,1 Ping Yi,1 Larbi Amazit, et. al (2010) SRC-3Δ4 mediates the interaction of EGFR with FAK to promote cell migration. Mol Cell ; 37(3): 321–332.

45- Lindfors HE1, Drijfhout JW, Ubbink M.(2012).The Src SH2 domain interacts dynamically with the focal adhesion kinase binding site as demonstrated by paramagnetic NMR spectroscopy.IUBMB Life, 64(6):538-44

46- Carelli S, Zadra G, Vaira V, et al: (2006) Up-regulation of focal adhesion kinase in non-small cell lung cancer. Lung Cancer, 53:263-71

47- Wang S, Basson MD. (2011) Akt directly regulates focal adhesion kinase through association and serine phosphorylation: Implication for pressure-induced colon cancer metastasis. Am. J. Physiol. Cell Physiol, 300:C657–C670.

48- Bill HM, Knudsen B, Moores SL, Muthuswamy SK, et. Al (2004) Epidermal growth factor receptor-dependent regulation of integrin-mediated signaling and cell cycle entry in epithelial cells. Molecular and Cellular Biology, 24: 8586–8599

49- Mitra SK, Schlaepfer DD (2006) Integrin-regulated FAK-Src signaling in normal and cancer cells. Curr Opin Cell Biol 18: 516–523.

50- Fumarola C, Bonelli MA, Petronini PG et al (2014) Targeting PI3K/AKT/mTOR pathway in non small cell lung cancer. Biochem Pharmacol. 90:197–207.

51- Sarbassov, D. D., Guertin, D. A., Ali, S. M. & Sabatini, D. M. (2005). Phosphorylation and regulation of Akt/PKB by the rictor-mTOR complex. Science, 307: 1098–1101

52- M. Andjelkovic, D. Alessi, R. Meier, A. et al. (1997).Role of translocation in the activation and function of protein kinase B. J. Biol. Chem, 272: 31515–31524

53- Guo Y, Du J, Kwiatkowski DJ. (2013) Molecular dissection of AKT activation in lung cancer cell lines. Mol Cancer Res,11: 282–293.

54- Luo, J., Manning, B. D. & Cantley, L. C. (2003).Targeting the PI3K-Akt pathway in human cancer: rationale and promise. Cancer Cell, 4: 257–62.

55- Pino MS, Shrader M, Baker CH, Cognetti F, Xiong HQ, Abbruzzese JL, et al. (2006) Transforming growth factor alpha expression drives constitutive epidermal growth factor receptor pathway activation and sensitivity to gefitinib (Iressa) in human pancreatic cancer cell lines. Cancer Res, 66: 3802–3812.

56- Lin, Y.; Wang, X.; Jin, H. (2014) EGFR-TKI resistance in NSCLC patients: Mechanisms and strategies. Am. J. Cancer Res, 4: 411–435

57- Yoeli-Lerner, M. et al.(2005) Akt blocks breast cancer cell motility and invasion through the transcription factor NFAT. Molecular cell, 20: 539–550.

58- Zhou, G. L. et al.(2006) Opposing roles for Akt1 and Akt2 in Rac/Pak signaling and cell migration. The Journal of biological chemistry, 281: 36443–36453.

59- Rao G, Pierobon M, Kim IK, Hsu WH, Deng J, (2017) Inhibition of AKT1 signaling promotes invasion and metastasis of non-small cell lung cancer cells with K-RAS or EGFR mutations. Sci Rep 7:7066.

60- Lara PN, Jr, Longmate J, Mack PC, et al. (2015) Phase II study of the AKT inhibitor MK-2206 plus erlotinib in patients with advanced non-small cell lung cancer who previously progressed on erlotinib. Clin Cancer Res, 21(19):4321–4326

61- Howe, G.A., Xiao, B., Zhao, H., et al. (2016). Focal adhesion kinase inhibitors in combination with erlotinib demonstrate enhanced anti-tumor activity in non-small cell lung cancer.

62- Gazdar AF (2009) Activating and resistance mutations of EGFR in non-small-cell lung cancer: role in clinical response to EGFR tyrosine kinase inhibitors. Oncogene 28 Suppl, 1: S24–31.

63- Balak MN, Gong Y, Riely GJ, et al. (2006) Novel D761Y and common secondary T790M mutations in epidermal growth factor receptor-mutant lung adenocarcinomas with acquired resistance to kinase inhibitors. Clin Cancer, Res 12: 6494–6501.

64- Roberts, W. G., Ung, E., Whalen, P., et al. (2008). Antitumor activity and pharmacology of a selective focal adhesion kinase inhibitor, PF-562,271. Cancer Research, 68: 1935–1944.

65- E. Cukierman, R. Pankov, D.R. Stevens, K.M. Yamada (2001) Taking cell-matrix adhesions to the third dimensionScience, 294: 1708-1712

66- Pino MS, Shrader M, Baker CH, et al (2006) Transforming growth factor alpha expression drives constitutive epidermal growth factor receptor pathway activation and sensitivity to gefitinib (Iressa) in human pancreatic cancer cell lines. Cancer Res 66:3802-12

67- Lee, M. J.Ye AS, Gardino AK et al. (2012) Sequential application of anticancer drugs enhances cell death by rewiring apoptotic signaling networks. Cell, 149: 780–794

68- VanHoudt WJ, Hoogwater FJ, de Bruijn MT, et al: (2010) Oncogenic KRAS desensitizes colorectal tumor cells to epidermal growth factor receptor inhibition and activation. Neoplasia, 12:443-52

69- Wang Y, Cao H, Chen J, et al (2012) A direct interaction between the large GTPase dynamin-2and FAK regulates focal adhesion dynamics in response to active Src. Mol Biol Cell, 22:1529-38.

70- Roepstorff K, Grandal MV, Henriksen L, et al. (2009) Differential effects of EGFR ligands on endocytic sorting of the receptor. Traffic, 10: 1115–1127.

71- Huang CL, Liu D, Ishikawa S, et al. (2008) Wnt1 overexpression promotes tumour progression in non-small cell lung cancer. Eur J Cancer, 44(17):2680–2688

72- Mitra S. K., Lim S.-T., Chi A., Schlaepfer D. D.(2006) Intrinsic focal adhesion kinase activity controls orthotopic breast carcinoma metastasis via the regulation of urokinase plasminogen activator expression in a syngeneic tumor model. Oncogene, 25(32):4429–4440.

73- Zhu CQ, da Cunha SG, Ding K, et al. (2008) Role of KRAS and EGFR as biomarkers of response to erlotinib in National Cancer Institute of Canada Clinical Trials Group Study BR.21. J Clin Oncol, 26:4268-4275

74- Wu S-G, Liu Y-N, Tsai M-F, C, et al. (2016) The mechanism of acquired resistance to irreversible EGFR tyrosine kinase inhibitor-afatinib in lung adenocarcinoma patients. Oncotarget, 7:12404–13.

75- Carelli, S., Zadra, G., Vaira, V, et al. (2006). Up-regulation of focal adhesion kinase in non-small cell lung cancer. Lung Cancer, 53: 263–271

76- Golubovskaya V, Beviglia L, Xu LH, et al. (2002).Dual inhibition of focal adhesion kinase and epidermal growth factor receptor pathways cooperatively induces death receptor-mediated apoptosis in human breast cancer cells. J. Biol. Chem, 277: 38978–38987

77- Yoon H, Choi YL, Song JY, et. al (2014) Targeted Inhibition of FAK, PYK2 and BCL-XL Synergistically Enhances Apoptosis in Ovarian Clear Cell Carcinoma Cell Lines. PLoS One, 9 (2)

78- Bagi CM, Christensen J, Cohen DP, et al.(2009) Sunitinib and PF-562,271 (FAK/Pyk2 inhibitor) effectively block growth and recovery of human hepatocellular carcinoma in a rat xenograft model. Cancer Biology and Therapy, 8(9):856–865

79- Amann J, Kalyankrishna S, Massion PP, et al. (2005) Aberrant epidermal growth factor receptor signaling and enhanced sensitivity to EGFR inhibitors in lung cancer. Cancer, Res 65: 226–235.

80- Booth L, Roberts JL, Tavallai M, et al. (2016) The afatinib resistance of in vivo generated H1975 lung cancer cell clones is mediated by SRC/ERBB3/c-KIT/c-MET compensatory survival signaling. Oncotarget, 19620–30.

81- Suzawa K, Toyooka S, Sakaguchi M, et. al (2016) Antitumor effect of afatinib, as a human epidermal growth factor receptor 2-targeted therapy, in lung cancers harboring HER2 oncogene alterations. Cancer Sci, 107:45–52.

82- Meng, X. Jin, Y. Yu, Y., et al. (2009). Characterisation of fibronectin-mediated FAK signalling pathways in lung cancer cell migration and invasion. British Journal of Cancer, 101(2): 327–334.

83- Gilbert-Ross,M. Konen, J. Koo,J. (2017)Targeting adhesion signaling in KRAS, LKB1 mutant lung adenocarcinoma. JCI Insight. 9; 2(5)

84- Koivunen, J. P. Kim J, Lee J, Rogers AM et al. (2008). Mutations in the LKB1 tumour suppressor are frequently detected in tumours from Caucasian but not Asian lung cancer patients. Br. J. Cancer, 99: 245–252

85- Roberts, W. G., Ung, E., Whalen, P.et al. (2008). Antitumor activity and pharmacology of a selective focal adhesion kinase inhibitor, PF-562,271. Cancer Research, 68: 1935–1944.

86- Chao TT, Wang CY, Chen YL (2015) Afatinib induces apoptosis in NSCLC without EGFR mutation through Elk-1-mediated suppression of CIP2A. Oncotarget. 6:2164–2179

87- Hayashi H, Sudo T (2009) Effects of the cAMP-elevating agents cilostamide, cilostazol and forskolin on the phosphorylation of Akt and GSK-3beta in platelets. Thromb Haemos, t 102:327–335

88- Ju L, Zhou C, Li W, Yan L (2010) Integrin beta1 over-expression associates with resistance to tyrosine kinase inhibitor gefitinib in non-small cell lung cancer. J Cell Biochem 111: 1565–1574

89- T. Shibue, R.A. Weinberg. (2009) Integrin beta1-focal adhesion kinase signaling directs the proliferation of metastatic cancer cells disseminated in the lungsProc. Natl. Acad. Sci, 106: 10290-10295

90- Wilson LK, Luttrell DK, Parsons JT, et. al (1989) pp60c-src tyrosine kinase, myristylation, and modulatory domains are required for enhanced mitogenic responsiveness to epidermal growth factor seen in cells overexpressing c-src. Mol Cell Biol, 9:1536–44.

91- Yoshida T, Zhang G, Smith MA, et al. (2014) Tyrosine phosphoproteomics identifies both codrivers and cotargeting strategies for T790M-related EGFR-TKI resistance in non-small cell lung cancer. Clin Cancer, Res. 20:4059–74

92- Murakami Y, Sonoda,K, Abe, H. et. al (2017) The activation of SRC family kinases and focal adhesion kinase with the loss of the amplified, mutated EGFR gene contributes to the resistance to afatinib, erlotinib and osimertinib in human lung cancer cells. Oncotarget, 8(41): 70736–70751.

93- Wu H, Liu Y, Shu XO, et al. (2016) MiR-374a suppresses lung adenocarcinoma cell proliferation and invasion by targeting TGFA gene expression. Carcinogenesis, 37(6):567–75.

94- Lim, S. T. (2013) Nuclear FAK: a new mode of gene regulation from cellular adhesions. Mol. Cells, 36: 1–6

95- Lim ST1, Miller NL, Chen XL, et al. (2012). Nuclear-localized focal adhesion kinase regulates inflammatory VCAM 1 expression. J. Cell Biol, 197: 907–919

96- Lim, S. T., Chen, X. L., Lim, Y., et al. (2008). Nuclear FAK promotes cell proliferation and survival through FERM-enhanced p53 degradation. Molecular Cell, 29: 9–22.

97- W. Luo, C. Zhang, B. Zhang, et al. (2009). Regulation of heterochromatin remodelling and myogenin expression during muscle differentiation by FAK interaction with MBD2. EMBO J. 28 :2568–2582.

98- Shin TH1, Paterson AJ, Kudlow JE (1995).p53 stimulates transcription from the human transforming growth factor alpha promoter: a potential growth-stimulatory role for p53.Mol Cell BioI, 15(9):4694-701.

99- Konstantinidou G, Ramadori G, Torti F, et al. (2013). RHOA-FAK is a required signaling axis for the maintenance of KRAS-driven lung adenocarcinomas. Cancer Discov. 3: 444–457

100- M. Keegan (2015). Virtual Library. Retrieved December 19, 2017, from https://library.iaslc.org/search-speaker?search_speaker=31384

APPENDIX

A)

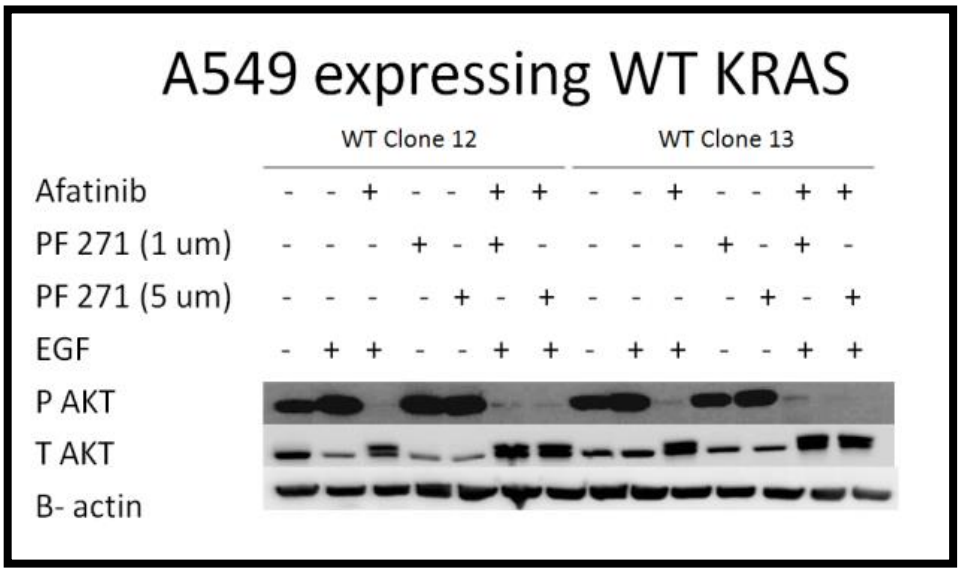
A549 expressing WT KRAS
WT Clone 12
WT Clone 13
Afatinib
PF 271 (1 um)
PF 271 (5 um)
EGF
P AKT
T AKT
B- actin

B)

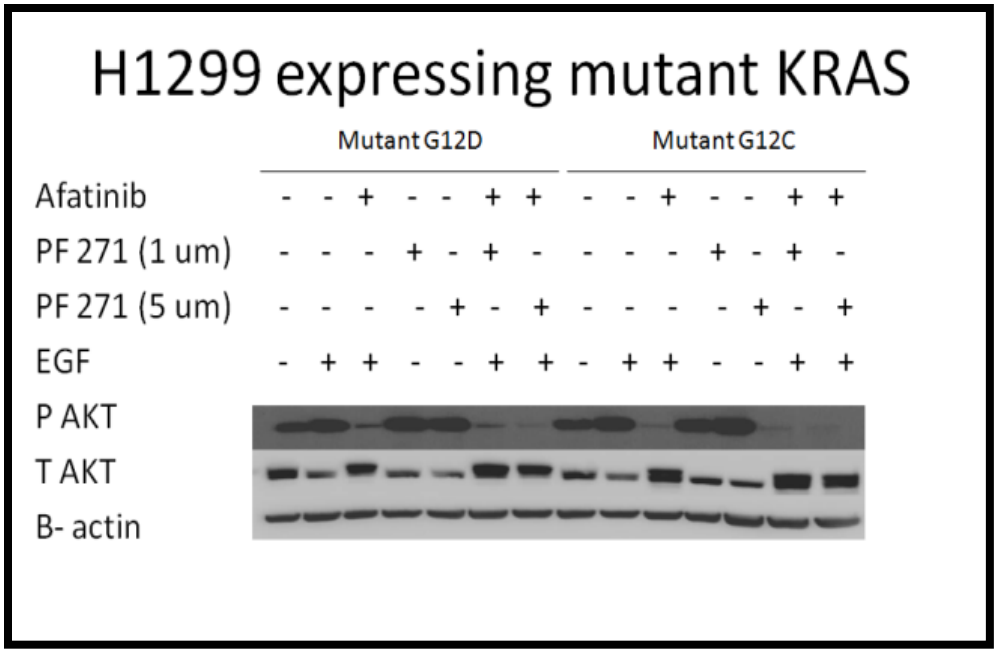
H1299 expressing mutant KRAS
Mutant G12D
Mutant G12C
Afatinib
PF 271 (1 um)
PF 271 (5 um)
EGF
P AKT
T AKT
B- actin

Supplementary Figure 1: Akt phosphorylation (S473) is reduced following treatment with both AFA and PF-271 in combination in WT KRAS expressing KRAS mutant but not in mutant KRAS expressing WT. A) A549 mutant KRAS NSCLC expressing WT KRAS B) H1299 WT KRAS NSCLC expressing a mutant KRAS. All cell lines were serum starved and were treated with: vehicle control (DMSO), AFA (10 μM), PF-271 (1 μM or 5 μM), or a combination of both AFA and PF-271 for 30 minutes prior to stimulation of cells with 100 ng/mL EGF. After 30 minutes of EGF stimulation, total cellular protein was isolated. Phosphorylated and total Akt were detected by western blotting. β-actin was used as loading control. Data presented is representative of results obtained from three independent experiments. This figure was done by Zeinab Moazin.